POLITECNICO DI MILANO
DEPARTMENT OF MECHANICAL ENGINEERING
DOCTORAL PROGRAMME IN
MECHANICAL ENGINEERING

Integrated Control of Active Vehicle Chassis Control Systems

Doctoral dissertation of
Arash Hosseinian Ahangarnjead

Supervisor
Prof. Stefano Melzi

Co-Supervisor
Prof. Federico Cheli

Tutor
Prof. Roberto Vigano

Chair of the Doctoral Program
Prof. Bianca M. Colosimo

2017 - Cycle XXX

Arash Hosseinian Ahangarnejad
Integrated Control of Active Vehicle Chassis Control Systems
Doctoral dissertation in Mechanical Engineering
Politecnico di Milano

To My family

Abstract

The principle of integrated vehicle dynamics is investigated in this thesis by proposing a new control scheme to coordinate active aerodynamics subsystems, active rear steering, and hydraulically interconnected suspension. A nonlinear vehicle model is utilized by employing VI-CarRealTime commercial software for this study, incorporating nonlinear tire model. This model consists of 14 degrees of freedom that include longitudinal, lateral and yaw motions of the vehicle and body roll, pitch and heave motions relative to the chassis about the roll, pitch and heave axis as well as the rotational dynamics of four wheels. The vehicle dynamics are analyzed for the entire handling region, and three distinct control objectives are defined, i.e., safety, performance, and comfort which correspond to yaw rate tracking, sideslip and roll motion bounding, respectively. In this thesis, different subsystems are developed in order to improve safety, performance, and comfort of the vehicle. Active Aerodynamics Control (AAC) subsystem is designed based on the response of vehicle in cornering maneuvers at high speeds. This control logic monitors the states of the vehicle to correct vehicle behavior by altering load distribution of the vehicle. Active Rear Steering (ARS) is utilized to track the yaw rate reference and bound the sideslip motion of the vehicle. Electronic Stability Control (ESC) is developed in order to increase the safety of the vehicle. Hydraulically Interconnected Suspension (HIS) is employed to reduce roll motion and lateral load transfer. Active Anti-Roll Bar (AARB) is designed to increase the comfort of the vehicle, reduce the lateral load transfer and enhance the safety and performance of the vehicle. Torque Vectoring system (TV) is used in high-performance vehicles in order to enhance traction and cornering ability. Active Suspension system (ASS) is employed to be able to change the longitudinal load distribution of the vehicle to overcome the understeer and oversteer situations in transient situations. The effectiveness of each standalone chassis control system is assessed for the different range of handling via various maneuvers. It is proved that each controller has a capability of improving vehicle handling in the certain range of handling where a passive ve-

hicle cannot. After analyzing and investigation, four subsystems are selected in order to develop integrated vehicle chassis control system. In the first part, three controllers (ARS, TV and HIS) are integrated based on two methods: an optimal control and a fuzzy logic approach. These proposed integrated control systems are evaluated by comparing passive, each subsystem and combined control. The second part is related to the integration of four controllers (AAC, ARS, TV and HIS) based on a fuzzy logic approach. The results demonstrate that the proposed integrated scheme can optimize the overall vehicle performance by minimizing the objective conflicts of the subsystems and increasing the functionalities of individual subsystems.

Acknowledgement

This work was conducted in the Department of Mechanical Engineering at Politecnico di Milano. The author gratefully acknowledges the support of the department and also wishes to thank them for their financial support throughout the Ph.D. study.

I would like to express my sincerest gratitude to my supervisor, Prof. Stefano Melzi, who has been instrumental to me throughout this thesis. He has forever changed my life, and I cannot begin to thank him enough for his help and support. This project would not have been possible without him. Also, I would like to thank him for kindly offering me the opportunity to cooperate with the research group of Virginia Tech. In addition, I would like to express my appreciation for the given opportunity to be a teaching assistant.

I feel very fortunate to have been given the opportunity to work closely with Prof. Mehdi Ahmadian at Virginia Tech in the laboratory of CVeSS who graciously granted me the privilege of a visiting scholar in Blacksburg during the first semester of 2016-2017. I enjoyed working with his research team, and the cooperation was very productive and fruitful under his supervision.

I would like to take this opportunity to pass my gratitude to Prof. Federico Cheli for his guidance at the beginning of my Ph.D. project and for providing me the opportunity to be involved in the Ferrari project.

I am also grateful to my tutor Prof. Roberto Vigano for his critical comments throughout Ph.D. study.

Also, I would like to thank my colleagues and friends in Department of Mechanical Engineering for providing a good working environment.

Finally, but by no means least, thanks go to mom, dad, and Mina for almost unbelievable support. They are the most important people in my world, and I dedicate this thesis to them.

Arash Hosseinian Ahangarnejad
November 2017
Milan, Italy

Contents

List of Figures

List of Tables

List of Symbols

A_l	Area of lower chamber in HIS
A_u	Area of upper chamber in HIS
a_x	Longitudinal acceleration
a_y	Lateral acceleration
B	Stiffness factor in magic formula
C	Shape factor in magic formula
C_α	Tire cornering stiffness
c_t	Tire damping
c_s	Damper coefficient of suspension
c_ϕ	Damping coefficient of anti-roll bar
D	Peak value of the curve in magic formula
d	Longitudinal distance of front spoiler to CoG
d_p	Pipeline diameter
E	Curvature factor in magic formula
e	Longitudinal distance of front spoiler to CoG
F_D	Drag force of spoiler

F_L	Lift/down force of spoiler
F_x	Longitudinal force
F_y	Lateral force
F_z	Vertical or normal force
h_{CoG}	Height of center of gravity
h_f	Height of front spoiler
h_r	Height of rear spoiler
h_P	Height of pitch center
h_R	Height of roll center
I_w	Moment of inertia of wheel
I_{xx}	Moment of inertia about x-axis
I_{xz}	Moment of inertia about x-z axis
I_{yy}	Moment of inertia about y-axis
I_{zz}	Moment of inertia about z-axis
k_s	Spring constant of suspension
k_t	Tire stiffness
k_{us}	Understeer coefficient
k_ϕ	Stiffness of anti-roll bar
L	Weighting constant
l_f	Distance between the front axle and the vehicle's center of mass
l_r	Distance between the front axle and the vehicle's center of mass

l	Distance between front and rear axles
m	Vehicle mass
m_s	Sprung mass
m_u	Unsprung mass
M_z	Aligning moment
M	Torque generated by spoiler
P	Actuator power requirement
P_a	Pressure of accumulator in HIS
P_l	Pressure of lower chamber in HIS
P_u	Pressure of upper chamber in HIS
q_l	Volumetric flow rate of accumulator in HIS
q_l	Volumetric flow rate of lower chamber in HIS
q_u	Volumetric flow rate of upper chamber in HIS
R	Radius of turn
R_t	Tire effective rolling radius
t_f	Vehicle front track
t_r	Vehicle rear track
u_s	Actuator force
V_a	Volume of accumulator in HIS
V_char	Characteristic speed
v_x	Longitudinal velocity

v_y	Lateral velocity
(W)	Weighting parameter
W_f	Static load on front axle
W_r	Static load on rear axle
x	Tire sideslip angle or longitudinal slip ratio in magic formula
y	longitudinal force, lateral force, or aligning moment value in magic formula
z_s	Vertical displacement of sprung mass
$\dot{z}_s$	Vertical velocity of sprung mass
$\ddot{z}_s$	Vertical acceleration of sprung mass
z_u	Vertical displacement of unsprung mass
$\dot{z}_u$	Vertical velocity of unsprung mass
$\ddot{z}_u$	Vertical acceleration of unsprung mass
ω	Wheel angular velocity
τ	acting driving torque on wheel
λ	Tire longitudinal slip
β	Vehicle sideslip angle
$\dot{\beta}$	Vehicle sideslip rate
β_{oil}	Bulk Modulus of oil
ρ_{vis}	Viscosity of oil
α_f	Front tire sideslip angle
α_r	Rear tire sideslip angle

γ	Camber angle
γ_f	Front tire velocity angle
μ	Road friction coefficient
ζ	Damping ratio
ε	the percentages of required yaw moment
ψ	Vehicle yaw angle
$\dot{\psi}$	Vehicle yaw rate
$\ddot{\psi}$	Vehicle yaw acceleration
δ_f	Front steering angle
δ_r	Rear steering angle
ϕ	Roll angle
$\dot{\phi}$	Roll rate
$\ddot{\phi}$	Roll acceleration
θ	Pitch angle
$\dot{\theta}$	Pitch rate
$\ddot{\theta}$	Pitch acceleration
ΔN_x	Longitudinal load transfer
ΔN_y	Lateral load transfer
ω_n	Natural frequency
ω_{BW}	Bandwidth frequency

List of Abbreviations

4WS Four-Wheel Steering

AAC Active Aerodynamics Control

AARB Active Anti-Roll Bar

ABC Active Body Control

ABS Anti-lock Braking System

ACU Airbag Control Unit

AFS Active Front Steering

ARB Anti-Roll Bar

ARC Active Roll Control

ARS Active Rear Steering

ASS Active Suspension System

AWD Active-Wheel Drive

AYC Active Yaw Control

BCM Body Control Module

CDC Continuous Damping Control

CoG Center of Gravity

DOF Degree of Freedom

DYC Direct Yaw Moment Control

ECS Electronically Controlled Suspension

ECU Electronic Control Unit

EKF Extended Kalman Filter

ESC Electronic Stability Control

ESP Electronic Stability Program

EPS Electronic Power Steering

FWD Front-Wheel Drive

HIS Hydraulically Interconnected Suspension

HMI Human Machine Interface

IVDC Integrated Vehicle Dynamics Control

LQR Linear Quadratic Regulator

PCM Power Control Module

PSCU Electronic Power Steering Control Unit

RMS Root Mean Square

RWD Rear-Wheel Drive

TCS Traction Control System

TV Torque Vectoring

Chapter 1

Introduction

Nowadays, high end vehicles are equipped with highly advanced user interfaces which respond to the driver requirements and choices. Addresses, directions and traffic information are supplied by these systems. Another object of the systems is to prevent collisions and enhance the vehicle's dynamics according to vehicle situations. Moreover, they can assist the driver to park the vehicle and to keep the lane and follow the correct speed limit. This thesis focuses on the intelligent control of the vehicle's lateral stability. A target is to enhance the vehicle performance in order to reduce the possibility of accidents and increase passengers' safety. In this chapter, the existence of electronic elements in modern vehicles will be introduced. Then, the controllers which is given in this thesis will be introduced.

1.1 Electronic control in modern vehicles

In the last three decades, the automotive manufacturers have been focused on car mobile computers which are known as Electronic Control Units (ECUs). In the 1980s, radio and engine controllers were the main electronic devices and the main criteria to buy a car were engine power, car speed, and body design [51]. However, nowadays automotive manufactures utilize more electronics to enhance the comfort, safety, fuel consumption and extra luxury option. Therefore, these arising options affect customers choice. Bosch [10] pointed out that a modern upper-class car would have likely 70 ECUs. Some examples of ECUs which can be found in today's car are shown in Table 1.1. It is interesting to point out that the expense of ECUs present which is the ratio between the cost of an electronic embedded system to the cost of the car was one percent during the 1980s and boosted to twenty percent during 2005 and raised up to forty percent in 2015 [167].

Table 1.1: Examples of Electronic Control Units (ECUs) [54]

ECU	Description
Active Steering systems	adds a steering correction value to improve the car handling and stability
Airbag Control Unit (ACU)	the control unit responsible of the deployment of the airbag
Anti-lock Braking System (ABS)	a braking control system that prevents the wheels from locking up (ceasing rotation) and avoids uncontrolled skidding
Battery Management systems	in electric and hybrid vehicles
Body Control Module (BCM)	monitors and controls various car electronic accessories like; power windows, power mirrors, airconditioning, immobilizer system, central locking, etc
Electric Power Steering Control Unit (PSCU)	responsible for the managing of the power assisted steering
Electronic Stability Control (ESC)	a braking control system that detects and prevents skids, by varying the braking moment in different wheels
Electronically Controlled Suspension (ECS)	including control systems of active and semiactive suspensions
Engine Control Unit (ECU)	monitors and controls internal combustion engine to ensure its optimum running
Human Machine Interface (HMI)	responsible for the high level interactions between the car users and the car control units
Navigation systems	including GPSs, speed control units, radar based brake assist(BAS), park assist, lane keep assist, collision prevention assist, trafic sign assist, etc
Powertrain Control Module (PCM)	Sometimes the functions of the Engine Control Unit and Transmission Control Unit are combined into a single unit called the Powertrain Control Module
Radio system	including radios, music players, speakers and amplifiers
Transmission Control Unit	controls modern electronic automatic transmissions to calculate how and when to change gears in the vehicle for optimum performance, fuel economy and shift quality

1.2 Active Chassis Control

Several active control systems have been developed for enhancing vehicle performance and active safety by utilizing different concepts or advanced control methodologies. The most of the active control systems by consideration of improving passenger comfort and vehicle ride handling can be classified into three groups based on control objects (see Figure 1.1):
1. Longitudinal control
2. Lateral control
3. Vertical control

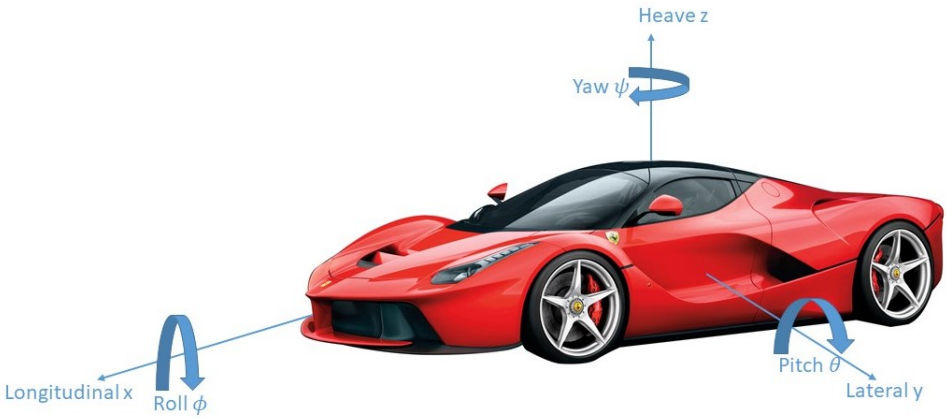

Figure 1.1: Chassis Dynamics Variables Using ISO Coordinates

Longitudinal control systems consist of Anti-lock Braking System (ABS) and Traction Control System (TCS) by modifying the braking or tractive force for the enhancement of braking or traction performance of the vehicle. Lateral control systems act cornering maneuvers to control the vehicle stability and avoid the vehicle from oversteering and understeering conditions, such as Active Four-wheel Steering (4WS), Torque Vectoring (TV) and Direct Yaw Moment Control (DYC). Vertical control systems intervene to control the vertical movement of the vehicle on uneven, such as active and semi-active suspensions, Hydraulically Interconnected Suspension (HIS), Active Roll Control (ARC) and Active Anti-Roll Bar (AARB). This thesis mainly focuses on lateral control systems which will be discussed in the next chapters.

1.2.1 Driver, controller and vehicle dynamics interactions

The vehicle dynamics can be controlled by a driver in three ways which are the control of vehicle throttle, the braking pedal, and the steering wheel. Vehicle throttle and braking pedal are related to vehicle's longitudinal motion while the steering wheel controls the lateral motion. As mentioned before, this thesis concentrates in the control of lateral motion, so that the driver steering input is of utmost importance of vehicle lateral control. Path following which is normal direction task and vehicle stabilization which is the action of an attempt to compensate for any undesired maneuver or lateral instability are the main aspects which affect the driver steering input. The both of the tasks are accomplished by the driver by monitoring the feedback of vehicle motion (see Figure 1.2). The second task which is not favored by driver leads to reduce the feeling of safety and ride comfort.

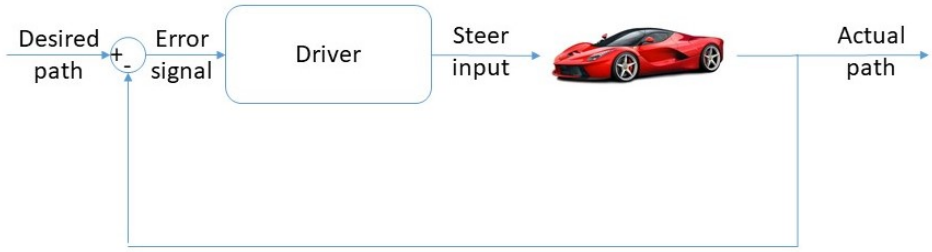

Figure 1.2: Block diagram of the driver-vehicle interaction

The second task influenced by the driver's response time, driving expertise and the possibility of overacting to the situation. Also, the risk of the vehicle lateral instability increase when the vehicle faces stressful situations such as driving at high speed or on slippery road surfaces or severe maneuvers, and this makes harder for the driver to control. Therefore, vehicle dynamics control system evolve into a very valuable system to prevent the probability of human-error through avoiding and recovering from any unwanted road disturbance. The control systems monitor the feedback information from the vehicle motion through sensors and observers to obtain the desired response. During this process, the controller decides and acts the control action by comparison of the vehicle dynamics states and the desired ones as shown in Figure 1.3 which is related to the block diagram of the general concept of control systems.

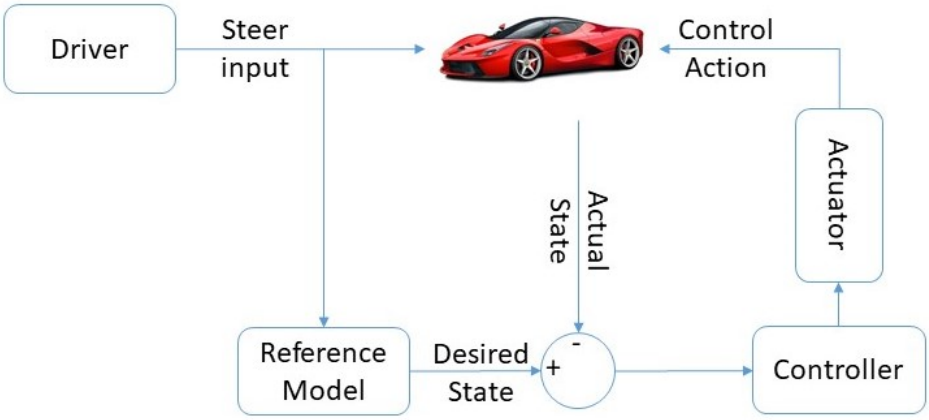

Figure 1.3: Block diagram of the driver-vehicle-controller interactions

1.2.2 Standalone Chassis Controllers

As mentioned above, nowadays automotive are equipped with numerous active chassis control systems. These controllers are working on their own without collaboration or network system between them. The primary purpose of the controllers is to control the vehicle handling dynamics actively. Each controller has its effective region and a principal function and can be classified concerning tire forces they target as follows:

- Longitudinal force: Electronic stability Control (ESC), Torque Vectoring (TV)
- Lateral force: Active Front Steering (AFS), Active Rear Steering (ARS) and Active Four Wheel Steering (4WS)
- Normal force: Active suspension, Active Anti-roll Bar (AARB), Hydraulically Interconnected Suspension (HIS), Active Aerodynamics Control (AAC)

The first group of controllers perform directly on the differential longitudinal tire forces between the right and left tires with respect to the condition of the vehicle in order to generate a counter yaw moment to stabilize the vehicle. The advantage of these controllers is that they are also effective when the vehicle reaches its handling limits of adhesion. However, the drawback of them is actively influencing the longitudinal dynamics of the vehicle in normal driving conditions. The second group which influences the lateral tire forces is useful in the linear handling region. In this region, the lateral tire forces are proportional to the

corresponding tire sideslip angle. But when the vehicle reaches to its handling limit, it is not very efficient. The third group aims to change the load distribution of vehicle between front and rear or between right and left sides of the vehicle. Each controller in this group has its effective region, and the way of performing is different. For instance, Active Aerodynamics Control is changing the load distribution of vehicle from front to rear and vice versa concerning the understeering or oversteering situation of the vehicle. This system is effective when the vehicle is traveling at high speeds. Active Anti-Roll Bar (AARB) is altering the roll moment distribution between front and rear suspensions during cornering, so the modification of the normal forces of the front and rear axles regulates the vehicle handling behavior. This system is efficient when the vehicle subjects to high levels of lateral acceleration situations [165].

1.2.3 Integrated Chassis Control

Each of the aforementioned standalone chassis control system has its advantage and disadvantage as can be seen in the previous section. Therefore, the combination of the standalone controllers is suggested to be able to overcome the weakness point of each controller. However, the combination of these systems is not an easy task due to the probability of a conflict between these subsystems or an overcorrection behavior. Therefore, a precise and careful the system of integration should be developed corresponding to the behavior of each of subsystems which the integration system has the characteristics of modularity, scalability and robustness [195]. Another benefit of the integration system is reducing the complexity of the controlling system and cost because of sharing sensors and actuators between different subsystems. Also, the integration system can enhance the flexibility of the control system design. In other words, the integration system can handle the control target in case of a broken subsystem [76, 68]. A detailed study of the previously mentioned active control systems will be discussed in Chapter 2 and these chassis control systems will be developed in Chapter 5. In this thesis, an integration system of Active Rear Steering (ARS), Torque Vectoring (TV), Active Aerodynamics Control (AAC) and Hydraulically Interconnected Suspension (HIS) will be addressed in Chapter 6 along with the explanation of reasons for choosing these subsystems in particular.

1.3 Thesis Outline

In this thesis, the arranging of the next chapters will be as follows:
Chapter 2 Introduces the review of the state of arts of several standalone chassis control systems. The chapter details the different standalone chassis controllers, and it explains the commercial and academic attention which these systems have received.
Chapter 3 describes the various methods for integration and the concepts integration technique. Emphasizing on the significance of integrated systems and the challenges faced while integrating different systems.
Chapter 4 starts by describing tire modeling and various models of the vehicle dynamics for the aim of using. Then it continues with explanation of the vehicle cornering dynamics and the characteristics of the vehicle stability state.
Chapter 5 depicts the simulation results obtained by several standalone chassis control system in comparison to a passive vehicle. Different maneuvers and various road surfaces are tested in order to evaluate the robustness and effective handling range of the controller.
Chapter 6 proposes a novel integrated vehicle dynamics control system. An integrated vehicle dynamics system control of the two subsystems, Active Rear Steering (ARS) and Torque Vectoring (TV), is first developed based on optimal control and fuzzy logic for further integration analysis. Then, integrated vehicle dynamics system based on four subsystems by utilizing fuzzy logic method is proposed. The proposed integrated control system is compared with the combined control system for various maneuvers. Simulation results for this approach are presented, and the improvements in overall vehicle handling performance are analyzed.
In Chapter 7, the conclusions and the contributions of this thesis are presented. Besides, the possible future steps to continue the work done in this project are mentioned.

1.4 Objectives

1.4.1 Problem Statement

Undesired or higher level of lateral acceleration leads the vehicle to be unstable and uncontrollable from driver's point of view when a vehicle is turning at high speeds. In other words, an undesired vehicle behavior such as understeer or oversteer causes the vehicle to leave intended path or rollover. Also, the lateral vehicle in leading severe deadly accident is verified by statistical studies. For overcoming this problem,

researchers introduced various control system to generate a reverse action to be able to bring back to its desired path. Therefore, control systems aim to change the tire force for making compensation forces to stabilize the vehicle's lateral motion. Each control system introduces a distinct control strategy; some targets are to directly influence longitudinal forces to create a yaw moment around the vertical axis of the vehicle, others affect and alter the vertical load distribution between the tires and others adjusts the tire steering angle to generate lateral forces. Therefore, the capabilities of control systems are entirely different to each other due to the different characteristic of each system. Consequently, some control systems are more efficient at moderate instability conditions, others are more efficient when the vehicle reaches its handling limits, and others are more efficient when the lateral acceleration of vehicle surpasses a definite value. On that account, the utilizing of several control systems can ve advantage due to the distinct controlling concepts. However, the combination of several standalone vehicle control systems is a complex and challenging task due to the conflict between control systems or overlapping the objectives of control systems. Besides, the combination of active controllers can reduce the cost because of the possible repetition of sensors, actuators, and signal connecting cables and systems. Therefore, For coordination of several chassis control systems Integrated Vehicle Dynamics Control (IVDC) has been introduced. Integrated Vehicle Dynamics System can remove the conflict between different active chassis control systems and provide a better performance compared with standalone control systems. As mentioned before, by integrating various chassis control system, the cost and complexity of the system can be decreased because of the possible use of sensors, actuators, cables and control units in shared with others. Nowadays, the IVDC has attracted more and more attention by automotive manufacturers and researchers. The different combination of active chassis control systems and various control strategies have been proposed. In addition, in past years utilizing different vehicle chassis control systems individually, which all chassis control systems are working in parallel, has been common. The working principle of this kind of chassis control is that each chassis control system has its hardware and controllers do not share information. Therefore, target overlapping between controllers can occur.

1.4.2 Objectives

The primary goal of this thesis is to overcome the problems faced and introduce a reliable, robust and predictable Integrated Vehicle Dynamics Control in order to improve vehicle handling, maneuverability, and

stability of the vehicle in all range of vehicle handling through optimum using the actuators in a coordinated manner. Therefore, the aim of the proposed IVDC is to act in the best way possible over a wide range of handling in a wide range of road conditions. To obtain the goal, a work breakdown of aims should be defined:

- Detailed review of state of the art and literature review for the each of standalone chassis control and presenting the pros and cons of each controller
- Describing and analyzing linear and non-linear full vehicle model with respect to the Degrees of Freedom and complexity
- Detailed review for state of the art of integrated Vehicle Dynamics System strategies
- Introducing several standalone vehicle chassis controllers where each one covers the part of handling range
- Evaluating standalone vehicle chassis control systems by comparing with the passive vehicle in various maneuvers and velocities and road conditions in order to illustrate the improvement regarding vehicle handling
- Selecting the proper standalone active chassis control system for Integrated Vehicle Dynamics Control with consideration of compliment the uncovered zones of handling, complexity, cost, market availability
- Definition of two methods for integration and comparing to each other
- Introducing two types of driving mode on Integrated Vehicle Dynamics System for driver for different situation and conditions
- Exploiting the maximum advantages of standalone chassis vehicle control system by employing Integrated Vehicle Dynamics System
- Comparing the results of Integrated Vehicle Dynamics System and standalone chassis controllers

Chapter 2

Literature Review

2.1 Introduction

This chapter presents a detailed investigation of literature available in the field of standalone chassis control.

2.2 Major Strategies for Vehicle Dynamics and Control

- Suspension system
- Active aerodynamics control
- Active four-wheel steering
- Hydraulically interconnected suspension
- Active Anti-roll bar system
- Anti-lock braking system
- Electronic stability program
- Torque vectoring control

The following sections will describe these strategies in detail and review the research literature available in those fields.

2.3 Suspension System

In this section, an outline on the essential theoretical basis for vehicle suspension will be described.

2.3.1 Quarter-car model

The heave, roll and pitch movements of chassis are the primary degrees of freedom in vertical dynamics of a vehicle. Various models exist in the literature to explain dynamic behavior. These models are: quarter car model which represents only the heave motions of a corresponding sprung mass and one wheel, half car model for the evaluation of pitch and roll movements, and full car model that consider the dynamic behavior of complete vehicle [118]. A quarter-car model is a proper model in the frequency range of interest (i.e., 0-25 Hz) to control suspension under an assumption that the motion of four wheels is decoupled [157].

Figure 2.1 demonstrates the quarter car model for various types of suspensions, which will be described in more detail in this section. Generally, a quarter car model includes unsprung mass m_u (tire, wheel, brake and suspension system are included in this part), sprung mass m_s (a quarter of the mass of the chassis including passengers and loading is involved) and suspension system represented by a parallel spring and damper configuration which connects the two masses and a tire model. Semi-active suspension adjusts damping $c_s(t)$ while active suspension generates a force $u_s(t)$ by an actuator between sprung and unsprung mass. For the evaluation of vertical dynamic behavior, a quarter car model is suitable because of simple structure and acceptable accuracy in case the consideration of nonlinear suspension [57, 81, 89, 100, 168].

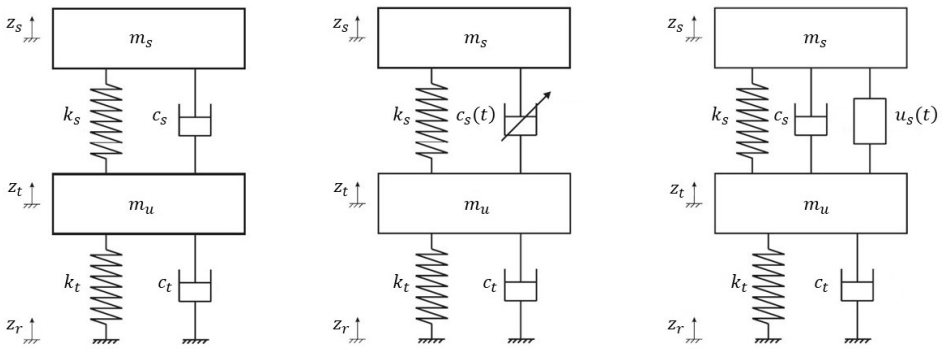

Figure 2.1: Quarter car models of a passive, semi-active and fully active suspension system

2.3.2 System requirements and performance evaluation

Ride comfort

The minimization of root mean square (RMS) value of the vertical chassis acceleration is described as ride comfort. A suspension system isolates chassis from vibration which is caused by road in order to improve ride comfort. Accordingly, in terms of vertical translatory vibrations, ride comfort can be evaluated by the acceleration of the chassis mass in case of neglect of the suspension of the seat. However, human sensitivity for vibrations which the most sensitive frequency range is 4-8Hz [59, 118] must be taken into account for the evaluation of ride comfort. This reality is considered in the design of suspension setups because the mass proportion of sprung and unsprung mass and additionally the stiffness of spring and tire are selected in order that the frequency interval is situated between the natural frequencies of sprung and unsprung mass.

Safety requirements

Ride safety as far as the behavior of vertical vehicle dynamic is given by the suspension if forces can be transferred between tire and road. This characteristic provides a more freedom to a driver to authorize over steering, braking and throttle actions. A clear rule to ensure ride safety is that the dynamic wheel load must not surpass the static wheel load, which can be accomplished if the dynamic wheel load is limited.

Requirements on suspension deflection

For preventing of peak-like chassis accelerations and wear of components, the deflection of suspension must be constructionally kept within given limits. In addition, the behavior of the suspension can be predictable for the driver by following the suspension limits. So, the suspension deflection must restrict between its lower and upper bound. A violation of compression limit (lower bound) is more critical than a violation of rebound limit (upper bound); for instance, the base value of the damper can be damaged by hitting the compression end stop. Moreover, the transferred energy may be higher so the compression end stop must dissipate the heavier sprung mass.

Normal load distribution control

In ordinary driving, longitudinal load transfer is a consequence of the longitudinal acceleration of the vehicle. Active suspensions can gener-

ate a system of internal forces inside the vehicle to control the heave, pitch and roll motion of chassis. In principle, a longitudinal load transfer can be obtained with a proper combination of vertical and pitch accelerations produced through active suspensions.

Actuator power demand

An active suspension system should work with a minimum amount of power. For classification of actuator power demand, the RMS value of actuator power ||P|| is taken into account as calculated in the following:

$$\begin{aligned} ||P|| &= \sqrt{\frac{1}{T}\int_0^T P^2 \tau d\tau} \\ P(t) &= \begin{cases} u(t)\Delta\dot{x}_{act}(t), & \text{for } u(t)\Delta\dot{x}_{act}(t) > 0 \\ 0, & \text{else} \end{cases} \end{aligned} \tag{2.1}$$

where
$\Delta\dot{x}_{act}(t)$ = the relative velocity of the actuator rod
u(t) = actuator force

Furthermore, For analyzing of total power demand in a more realistic way, the efficiency of actuator system (e.g., hydraulic/electrical) and additionally potential recuperation effects should be considered. In the design of actuator, low actuator friction, compact packaging, low weight and cost, less moving part for minimizing wear and low maintenance effort have to be considered.

2.3.3 Mechatronic suspension systems: State of the art

Mechatronic suspension system can be categorized concerning their actuator bandwidth, the power demand of actuators and range of their controllability [157]. Correspondingly, mechatronic suspension system can be classified as follows [157]:

- **Automatic level control systems** act quasi-statically and the distance between chassis and road is consistently kept for compensation in different loading levels of the vehicle [77]. A level control system can found on air springs and compressors. Therefore, soft, comfort adapted suspension configuration with sufficient suspension travel can be independently recognized from the vehicle's load level. The range of requirement of power is 100-200 W [157].
- **Adaptive suspension systems** have a slow variation of spring and damper characteristics. The working principle of this system

is changing the height of vehicle's center of gravity according to vehicle velocity in order to ensure a more sportive road holding. This system was utilized in Porsche Panamera 2009 by using air spring [78]. An adaptive suspension system named hydractive suspension was introduced by Citroen in 1989. The operating area of this system is to adjust air spring and damper characteristics [144]. Their power requirement relies on the demand energy to change spring stiffness.

- **Semi-active suspensions** generate force based on the direction of relative motion of the element. Semi-active dampers can alter the level of energy dissipation, but energy is not applied to the system. Correspondingly, the power requirement is about 20-40 KW per damper. The bandwidth of the system can be altered from 0 to 40 Hz [157]. Currently, Audi R8, BMW 7 series, Porsche 911 and Mercedes Benz E-class use a semi-active damper.

- **Slow active systems** use an additional actuator (e.g., a linear electrical motor or hydraulic cylinder), which is integrated into series to the suspension. Suspension forces are applied which are independent of the relative motion of chassis and wheel. The bandwidth of the system is 5 Hz. The energy demand of slow active suspension is in the range of 1-5 KW [157].

- **fully active systems** utilize an actuator with a bandwidth of 20 Hz or higher which is replaced or supplemented with a passive damper [157]. The main disadvantage is that fully active suspension requires high energy which ranges from 4-20 KW [77].

The primary classifications of a mechatronic suspension system are summarized in Figure 2.2 Semi-active and fully active suspension systems are explained in more detail in the following section.

Semi-active suspension systems

Semi-active suspension systems are able to adapt the damper characteristics of the shock absorber swiftly [90]. Three principles of operation are listed below:

- **Hydraulic damper** dissipate energy with entering hydraulic oil between chambers inside the damper. The system utilizes valves to vary the cross-section of opening between the chambers so that the level of dissipation is modified [72].

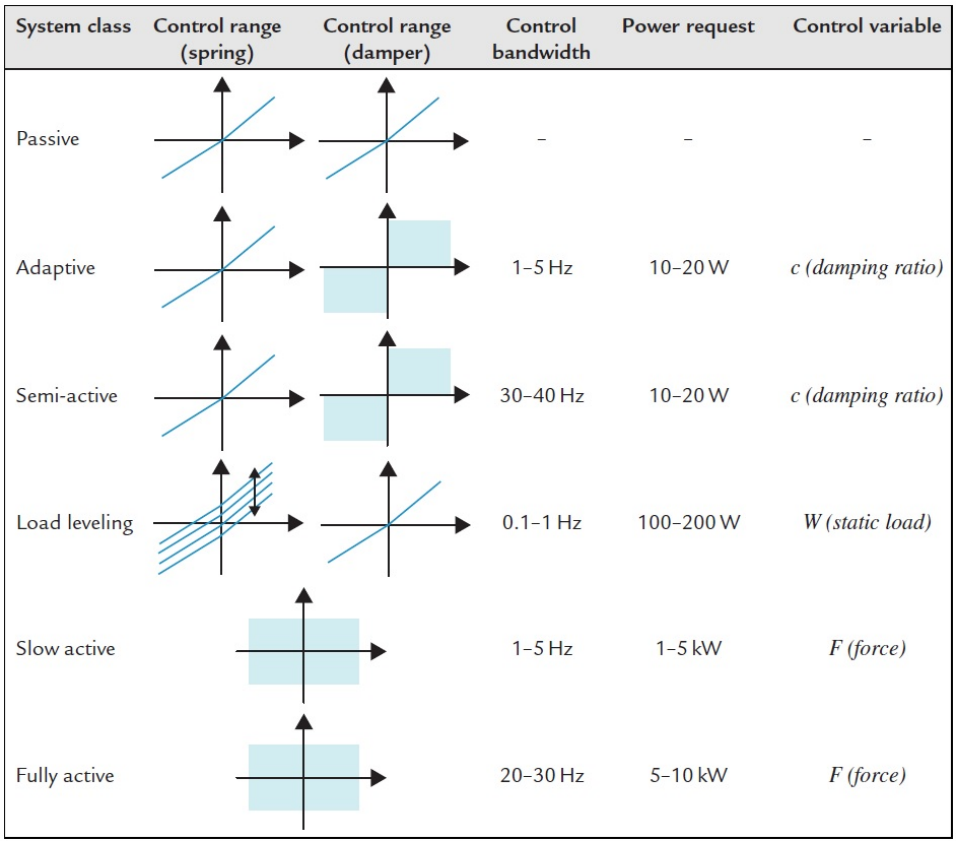

Figure 2.2: Classification of suspension systems [157]

- **Magnetorheological damper** alters the viscosity of a magnetorheological fluid by employing a magnetic field, which makes magnetic particles in the fluid to arrange chains [157, 61].

- **Electrorheological damper** performs according to the variation of flow properties of the contained electrorheological fluids. Besides, an electrical field is utilized to form particle chains in the fluid [40]. The durability of the seals is better compared to magnetorheological damper since the particles in the fluids are not wearing.

Since semi-active cannot provide energy to the suspension system, the damper is described as a passive element. Because of low power consumption, low cost and simple structure, a semi-active damper is more popular than active systems among automotive manufacturers.

Active suspension systems

Fully active and slow active systems are classified as active suspension systems as described in the previous section. A company which has been working on a fully active suspension system since 1980 is BOSE [88]. In the system mentioned above, linear electrical motors replace a conventional passive damper; additionally, torsion bar suspends static load of the vehicle as demonstrated in Figure 2.3. For the reduction of the resonance peak at the natural frequency of the unsprung mass, each wheel attaches to a reaction mass absorber as shown without transmission to the chassis (see Figure 2.3 right). Even though a fully active suspension system can recover energy by driving linear motor in generator mode, and BOSE company claimed that the power consumption of their system is less than 1/3 of the power requirement which is used by air condition of the car [88]. However, the BOSE system has not been used in automotive manufactures because of packaging aspects, costs, and power requirement.

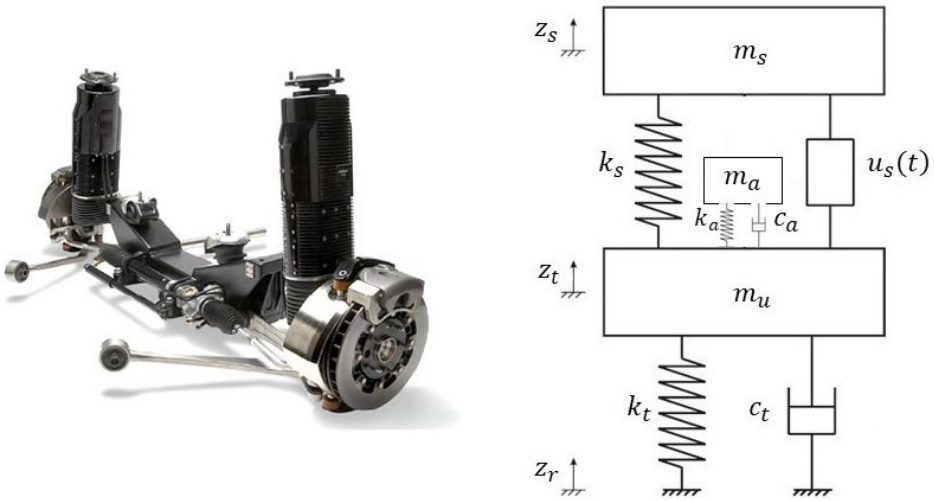

Figure 2.3: High bandwidth active suspension concept by BOSE [88] (left) and its quartercar model (right)

Active Body Control (ABC) which was introduced in 1999 by Mercedes Benz in the Mercedes Benz S-class, the coupe CL-class and the SL roadster [144] by employing a low bandwidth active suspension as shown in Figure 2.4. A hydraulic cylinder is used and integrated into the suspension in series to the primary suspension (see Figure 2.4 right) and the control bandwidth of it is 5 Hz. The system can damp the

vertical movements additionally pitch and roll motions as well [183]. However, a passive damper is employed to damp the unsprung mass. An improved version of ABC system was introduced in 2008 in the concept car Mercedes Benz F700 where lidar scanners were employed in the vehicle's headlights to scan the road profile in the front of the car. By using this information, the control algorithm can prevent road induced in advance [199, 182].

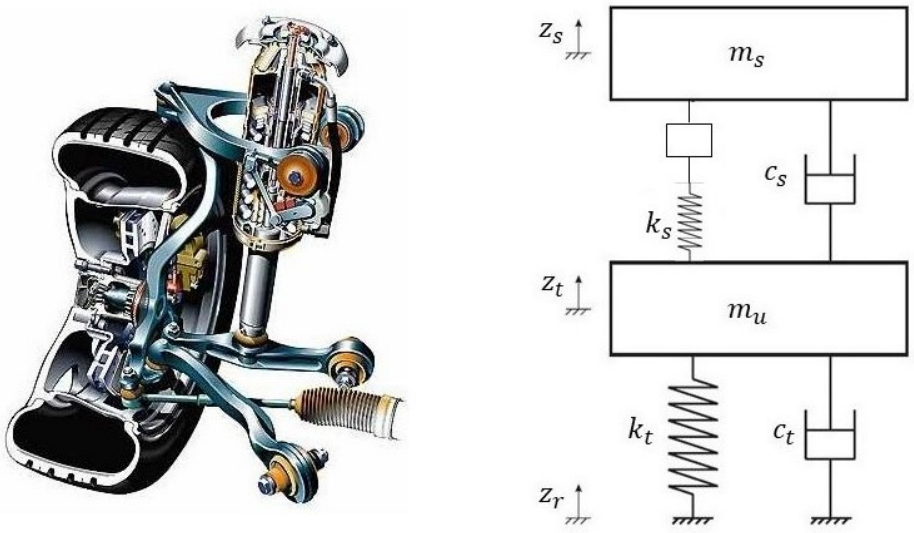

Figure 2.4: Active Body Control (ABC) low bandwidth active suspension system by Mercedes Benz [144] (left) and its quarter-car model (right).

Munster et al. [124] introduced a prototype of an electromechanical slow active suspension system which is integrated with series to the spring of suspension. This system is based on a spindle motor and it is pointed out that the power consumption of the system is much lower than the hydraulic ABC system by up to 0.6 $\frac{litres}{100km}$. But still, it is not integrated into a production vehicle. In addition, a concept of an active suspension named ASCA which is based on rotary actuators to generate a force between chassis and wheel mass was introduced in [53]. An advantage of the system is low power consumption because of parallel placement of the efficient actuators to air springs [77, 207]. The design of electromagnetic actuators for active suspension system are described in [112, 113] and for semi-active suspension in [140]. Furthermore, several types of research have been done about recovering energy for low bandwidth suspension actuators, and semi-active suspension where energy is recovering can be up to 50% by using proper

electronics which can be found in [70, 52]. Another utilization of slow active suspension system is to damp or decrease roll motion which is available in production cars. Also, integration of semi-active damper and active anti-roll bars is feasible to attenuate roll motion [78].

Advantages and disadvantages of active suspension are listed below:

Advantages

- Low static deflection
- Low natural frequencies Passenger comfort
- Consistent characteristics with varying loads
- High bandwidth

Disadvantages

- Potentially high cost
- Complexity in servicing
- Concerns over reliability due to complexity
- heavy weight

2.4 Hydraulically Interconnected Suspension

Vehicle posture, ride comfort, road holding and vehicle agility are influenced by suspension [194]. Therefore the accuracy of suspension's model is crucial for predicting the properties of the vehicle. Advanced models of suspension such as semi-active suspension, active suspension and various models of shock absorber have been proposed and developed by researchers in recent years [82, 184]. This kind of suspensions have some drawbacks such as increased cost, uncertain reliability, power consumption requirement and inherent complexity [206]. Recently, researchers introduced advanced suspensions to overcome the drawbacks of above controllable suspensions. Interconnected suspension system between the individual wheel stations has been introduced to overcome the ride-handling performance compromise [179]. The working principle of interconnected suspension is that a displacement at one wheel station can give rise to forces at other wheel stations. Interconnected suspensions between wheel stations have been conducted by mechanical [141], hydraulic [215], air [18, 91], or hydro-pneumatic (hydro gas) [107] systems. The interconnected suspension has an advantage concerning

conventional suspension regarding ride comfort and handling performance. Interconnected suspension enables the designer to focus on controlling the stiffness and damping of each suspension mode, rather than entirely relying on single-wheel stiffness and damping to implicitly define the suspension's modal characteristics. Moreover, the Interconnected suspension can individually uncouple the four modes of wheels with respect to the vehicle movements [179]. The advantages of an interconnected suspension to an active-type suspension are: low price, simplicity, reliability and easily fabricated. Nowadays, the hydraulically interconnected suspension has attracted more and more attention because of many advantages of a conventional suspension. Not only it has a functionality of traditional suspension, but also it improves stiff stiffness in a pitch and roll modes and soft stiffness in the bounce and wrap modes. Dynamic interactions between the hydraulic circuits and mechanical motions characterize hydraulically interconnected suspension system. Therefore, the hydraulically interconnected suspension is a mechanical and hydraulic coupled system, in which the conventional damper is replaced by single-acting or double-acting hydraulic cylinders, the cylinder chambers are interconnected via hydraulic circuits, and the accumulators are incorporated in these circuits to provide additional stiffness for suspension. The relative motion between the sprung and unsprung masses forces in HIS depends on pressure which means that the hydraulic fluids in the high-pressure cylinder chambers to flow into the low-pressure ones in the circuit. Consequently, the accumulators are compressed or expanded because of existing flow-volume deviation caused by the difference between the inflow and outflow volumes in this circuit. This causes a pressure change in the circuit and subsequently results in a new suspension strut force applied to the sprung and unsprung masses. Meanwhile, the vibration of sprung and unsprung mass is reduced due to damping forces. The research papers [28, 215, 190] demonstrate that damping coefficient can be independently tuned in different motions. Smith et al. [215, 180] developed the mathematical model of HIS where assumed that damper valves had a linear characteristic. Oritz [135] introduced integrated mechanical/hydraulic schematic for supplying separate spring and damping to two-mode combined motion, pitch/bounce and roll/wrap. The new concept of an interconnected suspension was proposed by Fontdecaba [25] for implementing a complete model of decoupling by independently adjusting roll stiffness and damping levels via the central suspension unit. Mace [108] investigated a theoretical study for a HIS systems utilizing network theory and system synthesis methodologies with consideration of ideal interconnections. The investigation of the properties

and dynamic characteristics of interconnected hydro-pneumatic suspension has been done by Cao et al. [27, 29]. The study has been done in roll and pitch planes with consideration of the pressure loss of hydraulic circuit and damper valves. The results of investigation demonstrated that there was an enhancement in stiffness and damping of roll and pitch mode, as well as the ride and handling performances, even though there were not any improvement in soft bounce and wrap modes.

2.5 Active Antri-Roll Bar (AARB)

Two most important aspects of the vehicle are ride and handling which have a strong relation to the customer perception of satisfaction. Unfortunately, there are trade-offs between these aspects, and it is a challenge for an automotive engineer to make a vehicle with decent ride and handling at the same time. Many studies have been done for tackling these trade-offs. Some researchers prefer to develop active suspension while others prefer to develop an anti-roll bar. However, the cost is the critical factor in tackling these trade-off from manufacturer's point of view. Therefore, anti-roll bar has an advantage to active suspension in terms of cost for finding a solution at this compromise. The benefit of the anti-roll bar is reducing body roll acceleration and roll angle during single wheel lifting or cornering maneuvers for improving driving safety and handling stability [39]. Besides, anti-roll bar controls the distribution of lateral load transfer which leads to increase understeer behavior. The working principle of the anti-roll bar is transferring vertical forces from one side of suspension to the other side and it generates moment against lateral one during cornering maneuvers. When a vehicle is going on straight line, ride comfort can be deteriorated due to road irregularities which have the same effect of cornering maneuvers. Therefore, for tackling these kinds of problems an active anti-roll bar is developed. Besides, it improves the disadvantages of a passive anti-roll bar. And also it has advantages with respect to active suspension concerning lower cost and power consumption. For compromising the trade-off between ride and handling, various solutions have been proposed. Passive suspension systems, semi-active suspension systems, active suspension systems, and anti-roll bar are included in the solutions. Among the solutions, anti-roll bar has become more popular these days for researchers to tackle the trade-off between ride and handling. The effect of active anti-roll bar on ride and handling for off-road vehicles has been investigated by Cronjé and Els [45]. They also studied the potential of active anti-roll bar to enhance handling of

an off-road vehicle without sacrificing ride comfort. The design of an active anti-roll bar for increasing vehicle stability and passenger comfort has been done by Gosselin-Brisson et al. [69]. For verifying the performance of active anti-roll bar, it was tested in benchmark with a conventional suspension with and without Anti-roll bar. There are two types of active anti-roll bar which are listed as follows:

2.5.1 Hydraulic anti-roll bars

In 1995, Citroen utilized the first application of hydraulic ARB in Xantia Activa. Since then, hydraulic ARB has been developed based on several rotary and linear actuator systems. Because of some drawbacks and disadvantages [30] which are following, utilization of hydraulic ARB has been limited:

- Requirement for dedicated hydraulic components like supply lines, control unit, valves, etc. and their associated cost
- Additional power requirements for hydraulic pump and impact on fuel efficiency
- Relatively poor frequency response
- Maintenance requirements on the hydraulic components

2.5.2 Electromechanical anti-roll bars

The working principle of electromechanical ARB is similar to passive ARB. The difference is that any torque can be requested at any time by utilizing electromechanical ARB instead letting the torsion dictate the produced torque by ARB. Electromechanical ARB consists of two halves of passive ARB connected to each other by way of an electric motor and a gearbox. A motor which rules the torque of ARB is received a signal from a controller to set an output torque. In addition, a controller determines the output torque by consideration of disturbance to be able to have a desired value. Figure 2.5 shows the working concept of electromechanical ARBs. In 2005, Toyota and Aisin Seiki Co. introduced the first application of electromechanical ARB in Lexus G430 [43]. Recently, electromechanical ARB has gained popularity among automotive manufacturers for their premium cars such as: Bentley [17], Porsche [142], Audi [12] and BMW [71].

The aim of most studies od developing an anti-roll bar system is to control roll motion. However, Kim et al. [98] proposed Active Roll Control (ARC) and made a distinction regarding actuator types and

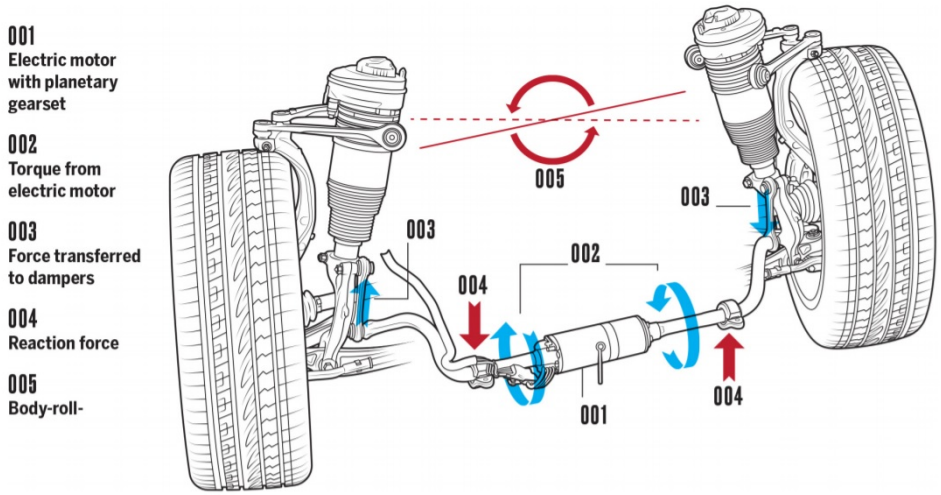

Figure 2.5: Concept behind electromechanical AARB [191]

the actuator locations. A hydro-pneumatic and hydraulic system is the most popular actuator in ARC and especially in ARB. However, the disadvantages of these actuators are manufacturing cost, power consumption and their slow responses to various roads and steering inputs. Kim and Lee have conducted an ARC system [97] by utilizing lateral acceleration and roll rate feedback in an electrical actuating system. Moreover, they suggested a hybrid roll control system for enhancement of controller performance in a transient region by taking advantage of the variable damper and also Shuuichi developed an electric active stabilizer suspension system as a technology for controlling vehicle body roll [176]. Besides, they demonstrated that the possibility of saving energy could be done by adopting a strain wave gearing mechanism for reducing gear and utilizing its hysteresis property in an electric actuation system. The active stabilizer actuators consist of electric motors and reduction gears for controlling roll and various sensors for detecting vehicle's states. BMW introduced Dynamic Drive which includes an active anti-roll bar system [181]. This system consists of a hydraulic valve block with integrated sensors, a hydraulic pump coupled to the power steering pump, a lateral acceleration sensor, a control unit, several hydraulic lines, and two active anti-roll bars with rotating hydraulic actuators. This system is capable of reducing roll angle during cornering maneuvers significantly. Advantages and disadvantages of active anti-roll bar are listed below:

Advantages

- Improving stability and handling without decreasing comfort
- Providing solution to ride and handling trade-off with lower cost compared to active suspension
- Minimizing rollover accidents

Disadvantages

- High cost
- Power demand

2.6 Active Aerodynamics Control

Vehicle aerodynamic field describes the forces acting on a vehicle when moving through a fluid. When stationary, the exterior of surfaces of an automotive (upper, lower, front and rear surfaces) are subjected to an atmospheric pressure and the sum of all forces acting on an automobile is equal to zero. The acting pressure on the exterior surface of vehicle alters proportional to the square of velocity when the vehicle starts to travel. The change of the pressures generates forces which act on the surface of the vehicle, and this slow downs the performance of the vehicle. Therefore, many researchers work on this topic to minimize these forces and in some cases utilized them to enhance performance and safety of the vehicle. Two main forces which are acting on the vehicle are lift and drag forces. The lift force is determined along the z-axis. Lift vector in the positive z-direction is named as a lift; meanwhile, the vector in the opposite direction is known as downforce. The drag force is determined along the y-axis, and it is in the negative direction of the y-axis. The controlling of these forces is essential regarding the performance and safety of the vehicle, therefore the usage of these forces can be different which depends on the logic of the controller. For example, automotive companies are seeking to minimize the drag for in order to reduce fuel consumption. Meanwhile, they utilize these forces for increasing the performance of the vehicle in terms of safety and handling. The tire behavior and forces are important factors which influence the dynamic behavior of vehicle [46]. This directly impacts longitudinal dynamic which is related to longitudinal forces generated by tires. Therefore, the acceleration and top speed of the car can become better by raising longitudinal forces. Similarly, the lateral dynamics can be affected by aerodynamic effects. So, this system can enhance of lateral dynamics as well. Generating force in a pneumatic tire is strongly related to normal tire force and the friction

coefficient between tire and road. The longitudinal acceleration of a vehicle is a function of friction, gravity and downforce [116, 14, 47]. Therefore, the vertical load of the tire should be taken into account as an essential factor that can enhance vehicle dynamics. The downforce of the vehicle is strongly related to the location of the center of gravity. The location of the center of gravity could be altered in various maneuvers because of lateral and longitudinal load transfers. So this influences the behavior of vehicle dynamics, and by adjusting of tire downward force vehicle handling and dynamics, capabilities can be improved. Wings and spoilers are utilized in order to increase total down forces. A spoiler can generate downforce, lift force and drag force. The magnitude of forces is related to the angle of attack of spoiler and the square of longitudinal vehicle velocity [93].

In a nutshell, various application of aerodynamic forces in the automotive industry is as follows:

- Increasing normal loads
- Distribution of normal loads
- drag reduction

Nowadays, the capabilities of spoilers for various applications have been studied in automotive industry [160, 115]. Active spoiler system known as an Active aerodynamic system as well can be employed to adjust downforce of the front and rear axles. The working principle of active aerodynamics control is to change the angle of attack to generate downforce, lift force and drag force. Corno et al. [42] presented a paper for enhancement of vehicle's comfort at high speeds and also investigated the effects of Active Aerodynamics Control (AAC) on semi-active suspensions. Savkoor et al. [159] presented the design of the aerofoil for the pitch control of trucks where a detailed model of fluid dynamics is employed, and a Linear Quadratic Regulator (LQR) controller is designed. The primary focus of the research is to improve the pitch dynamics without consideration of trade-off performance. The paper proposed by Savkoor and Happel [158] further proves the utility of AAC. This paper proposes a comparison of several AAC control strategies to improve vehicle handling (yaw and roll dynamics). In [160], authors investigate the potential of active aerodynamics to improve roll and yaw stability by using Linear Quadratic Regulator (LQR). However, this logic works when the magnitude and rate of steering input are small. Doniselli et al. [50] investigate the effects of aerodynamic forces on ride comfort and road holding by using sky-hook suspension. Numerical simulations and experimental tests have

been carried out to evaluate the effects of aerodynamic forces on ride comfort and road holding of the vehicle in high speed on various road profiles. Mohrfeld-Halterman, J.A. and Uddin, M. [120] develop a high fidelity quasi-steady-state aerodynamic model for pitch moment degree of a race car. They decrease the complexity of quasi-static model while maintaining the accuracy. In [119], authors implement high fidelity quasi-static model and conventional quasi-static model independently in multi-body quasi-steady-state simulations to determine the effects of the high fidelity aerodynamic model on race vehicle performance. Other studies were focused on aerodynamic drag reduction: in [22], drag reduction through active separation control is analyzed both experimentally and numerically; Fasel, H. et al. [55] analyzed a motor vehicle with an outer contour to reduce the air resistance. A research paper which explains the significance of the aerodynamic downforce and the improvement of performance of race car has been conducted by Katz [92]. A study for the reduction of drag and lift of automobile by utilizing front and rear spoilers have been investigated by Schenkel [163]. Brzustowicz et al. [23] analyzed the complex flow field of aerodynamic of NASCAR Dodge Intrepid R/T by utilizing scale wind tunnel models and Computational Fluid Dynamics (CFD). Zhang¤ and Zerihan [216] investigated the effect of a cambered, double-element, high-lift wing for aerodynamic performance and off-surface flow-field characteristics. It is pointed out that most of the downforce can be generated by the primary element when flow moves in three dimensional toward the airfoil but retains quasi-two-dimensional features near the center of the wing. Also, they found that at considerable heights downforce increases asymptotically with a reduction in height. Johansson and Katz [216] tested the aerodynamic characteristics of a sprint car in a small-scale wind tunnel. Side force, rolling moment, downforce and drag forces were measured during rapid cornering of race cars. They focused on conditions when the vehicle was subjected to considerable sideslip angle. The results were demonstrated that driver visibility could improve by reducing endplate size of the main wing without significant loss of aerodynamic downforce. Dimitriou and Garry [48] investigated boundary layer measurements above a full-width moving belt for identifying its side-edge effects in racing cars. The results showed a strong interaction between the side-belt edges and the fixed ground. Also, they proved that application of suction between the fixed and the moving ground is very efficient for removing this boundary layer and increasing the measurement accuracy. Advantages and disadvantages of active aerodynamics control are listed below:
Advantages

- Enhancement of safety and performance of vehicle at high speeds

Disadvantages

- works only at high speeds

2.7 Active Steering

Active steering systems affect vehicle handling behavior through directly modulating the generation of lateral tire forces. In this section three existing steering schemes, Active Rear Steering (ARS), Active Front Steering (AFS) and Active Four Wheel Steering (4WS) will be examined, respectively.

2.7.1 Active Rear Steering (ARS)

The most important control task for Active Rear Steering is to minimize the sideslip angle of the vehicle to follow the given path. Active rear steering was developed, and it was commercially used in 1980's. Shibahata et al. [172] and Takiguchi et al. [188] for Mazda suggested the so-called speed sensing Active rear steering. The working principle of this systems is that at low speeds the rear wheels are steered in the opposite direction to the front wheels for improving maneuverability, and at high speeds, the rear wheels are steered in the same direction to enhance stability. Sano et al. [153, 152] proposed ARS system such that when the steering wheel is turned at a small angle, the rear wheels steer in the same direction, but for large steering wheel angles the front and rear wheels steering in the opposite direction. [153, 152] assumed that large steering angle inputs are not used at high speeds. Another ARS system has been proposed by Fukui et al. [60]. The method is based on the fact that the rear wheels should be steered in the same direction to the front in case of wheels quick turning of the steering wheel; on the other hand in the case of slow turning the rear wheels would be steered in the opposite direction of the front ones. This logic aims to minimize sideslip angle in both steady and transient states.

Yaw rate feedback ARS has been proposed by Sato et al. [154, 155, 205, 210, 209] with consideration of external disturbances such as crosswinds or split-μ braking in order to improve vehicle handling. The control law of Active Rear Steering (ARS) is derived from an inverse model of vehicle bicycle model. The control logic is a combination of feed-forward of front wheel steer angle and feedback of yaw rate for making the vehicle sideslip angle to be zero continuously. The effectiveness of the proposed control strategy has been tested through

numerical simulations, especially when the vehicle is subject to external distributes. But, the robustness of the proposed control strategy according to vehicle velocity and the variations of friction coefficient is questionable. An adaptive sideslip angle ARS has been introduced by Wakamatsu et al. [200] in order to minimize the vehicle sideslip angle even on split-μ road surfaces. The proposed control strategy consists of feedforward compensation, yaw rate feedback and an estimator of μ. Moreover, intelligent control techniques fuzzy logic control has been utilized in ARS as well. A feedforward fuzzy logic ARS controller has been applied in [185] to minimize vehicle sideslip angle. The proposed control strategy utilizes front wheel steer angle and vehicle velocity as an input and fuzzy logic control determines rear wheel steer angle. Numerical simulations approve the effectiveness of the control logic at high speeds; however, there is no consideration of low speeds in the control strategy. Another drawback of this research is that the proposed method is not robust to environmental conditions. Senger et al. [166] introduced sideslip angle minimization ARS in order to improve regarding quicker steering response and better stability by comparison with the conventional 2WS. Whitehead [205] and Nalecz et al. [128] introduced ARS to improve vehicle handling at high speeds and only correspond to high-frequency excitation at high speeds. [172] reports that rear wheels steering in the opposite direction to the angle of front wheels at a large angle are not efficient in improving low-speed maneuverability since this causes the rear end of the vehicle stick out further toward the outside of a curve. Another control strategy to zeroing vehicle sideslip angle, a combination of feedforward part which is derived from an inverse model of the desired dynamics and utilized to compensate for steady-state response and a feedback part which is computed based on μ-synthesis and to compensate for the transient dynamics has been proposed by Hirano et al. [79] in order to make the vehicle to follow the desired yaw rate and sideslip angle. Meanwhile, another application of active steering is to avoid obstacle during an emergency and critical states which are out of the scope of this research.

2.7.2 Active Front Steering (AFS)

Nowadays, the active front steering has gained popularity in vehicle engineering because it is a useful method to improve vehicle handling. This control strategy applies an additional steer angle to the driver's steer command. A pole-assignment self-tuning adaptive control algorithm and a least square parameter identification method have been utilized in [202] to track the reference of yaw rate and lateral acceleration. An AFS controller based on a robust model matching algorithm

has been proposed by Tagawa et al. [186] for achieving robustness according to parameter variations and disturbances such as varying speed and friction coefficient of road surfaces. The realization of closed-loop frequency between the driver's steer input and vehicle yaw rate has been used in the proposed control strategy. Computer simulations in both frequency and time domains are carried out to show the effectiveness of developed controller. A new way of investigation and analyzing of vehicle stability by utilizing bifurcation theory has been introduced by Ono et al. [133] [132]. Ono proposed H_∞ controller based on the model following structure and demonstrated that the proposed control strategy could efficiently stabilize a vehicle through identifying the peak cornering force of a tire and limiting the steering wheel angle so that all tires work in the unsaturated regions on the slip-force curve. The development of the robust model for decreasing yaw disturbance by making yaw rate unobservable from lateral acceleration has been introduced by Ackermann [7, 4, 3, 177, 201]. Both computer simulations and road tests are carried out and explicitly indicate the effect of a robust controller on disturbance rejection. Mammar et al. [109, 110] developed H_∞ controller to track yaw rate reference and reject disturbances. Maintaining optimal lateral tire forces during steering by an AFS system has been conducted by Huh and Kim [83]. In this research, estimation of lateral tire forces by using Extended Kalman Filter (EKF) and development of a fuzzy logic controller to compensate for the lack of lateral tire forces on low-μ surfaces have been designed. The verification of the method is verified by using a steering Hardware-In-the-Loop system under different road surface conditions. Güvenc et al. [73] conduct an AFS system based on two degrees of freedom control structure to enhance yaw dynamics by tracking of reference and rejection of disturbance.

2.7.3 Four Wheel Steering (4WS)

This section will consider the Four Wheel Steering (4WS) systems in which both front and rear wheels can be actively steered in order to control the balance of lateral tire forces on the front and rear axles. Such systems are designed by multi-input-multi-output control techniques. Nagai et al. [125] developed 4WS by utilizing an LQR controller to track the reference yaw rate and sideslip angle. Feedforward and feedback control laws are formulated to steer front and rear wheel cooperatively actively. Numerical and road tests demonstrated a higher stability in transient regime. Aga et al. [9] proposed a linear control law based on bicycle vehicle model to track the references of yaw rate and sideslip angle. The numerical results indicated that the proposed

control theory is more stable against external disturbances. An active rear steering based on active four-wheel steering has been conducted by Lin [106] to minimize vehicle sideslip angle and at the same time maintain a constant steering. The proposed method refines the yaw rate feedback ARS by adding an extra yaw rate feedback control to the front wheels for overcoming the oversteer tendency at low speed and extreme understeer at high speeds. The theoretical and comparative studies of the design of robust active steering have been introduced by Ackermann and colleagues [5, 8, 6]. An AFS control law to decouple the yaw mode from the lateral mode of the front axle to assist a driver to track a given path by yaw rate feedback to the front wheels has been introduced in the first study. A second research developed a controller to make independent of vehicle velocity through yaw rate feedback to rear wheel steering in order to overcome the drawback of degraded yaw damping by AFS controller. Simulation results show that the control algorithm can reject disturbances but there is no description of an appropriate vehicle model, and it fails to show enhancement in vehicle handling in the nonlinear regime. Gianone et al. [64] introduced control strategy which is the combination of LQR and H_∞ controllers for ARS and 4WS. In this study, optimal robust controllers can reject disturbances and adapt to parameters variation. An active robust Active Four-wheel Steering controller has been investigated by Horiuchi et al. [80] by using a two DoF control structure in which a feedforward controller is developed based on an inverse linear model for tracking yaw rate reference and lateral acceleration reference and a feedback H_∞ controller is designed to reject uncertainty and external disturbances and add an extra robustness to the system.

Advantages and disadvantages of active steering are listed below:

Advantages

- Ultimate cornering ability
- Smallest turning circle possible
- Better stability of the vehicle
- The intensity of four wheel steering can be adjusted by the driver according to personal preference

Disadvantages

- The linkages are extremely complicated
- Chances of overturning increases

- More components means more weight of the vehicle
- There is a high rate of failure to incorporate the four wheel steering just yet

2.8 Anti-lock Braking System (ABS)

Anti-lock braking system (ABS) is one of the most important system in vehicle's safety by preventing from locking wheels which helps to keep a vehicle steerable and stable during hard braking. Longitudinal slip of wheels increases during severe braking on a slippery road surfaces which causes instability in vehicle. The aim of ABS is to modify wheel slip in order to obtain maximum friction coefficient for reducing stopping distance. Typical ABS components include: vehicle's physical brake, wheel speed sensor (encoder), an electronic control unit (ECU), brake master cylinder, a hydraulic modulator unit with pump and valves [203]. There are six methods for ABS algorithm which are classical control, optimal control, nonlinear control, robust control, adaptive control and intelligent control. So many research papers have been done by researchers for developing and improving ABS performance and controller. And some of them have been developed and implemented. Jiang and Gao [87] suggested a non-linear PID controller which assisted robust performance and alleviation of tuning. Chen and Huang [33] proposed adaptive PID controller. In this method a fuzzy logic was employed to tune PID gains to help robustness of controller on different conditions. Yu et al [212] and Zhang et al. [214] utilized a fuzzy logic to optimize slip ratio on different road surfaces. Alleyne [11] investigated about a sliding mode controller in order to improve ABS performance and robustness based on vehicle parameters and actuator dynamics.

2.9 Electronic Stability Control (ESC)

Electronic stability control is an active vehicle control system that improves the stability of a vehicle. In general yaw rate and side slip angle are the two-vehicle state parameters used to define whether a vehicle is stable or not. The magnitudes and the trends of these two parameters are highly complex and nonlinear processes which are generally controlled by many vehicle parameters, such as vehicle's inertial properties, its ability to generate the lateral forces and the rate at which it can generate the lateral forces, the amount of steering input, the speed at which a vehicle operates etc. The strategy of controlling vehicle stability or influencing a vehicle's dynamic behavior by generating either

a supporting or an opposing yaw torque is called active yaw control. In today's modern ESC system both the brake and drive torque can be applied for this purpose. For this thesis, an ESC system that is based only on brake torque is considered. Abe et al. [2] developed sideslip controller in electronic stability control to stabilize the lateral dynamics of the vehicle. It was also demonstrated that the controller as mentioned above had a better capability in stabilizing vehicle compared with 4WS. Tondel and Johansen [193] developed a nonlinear controller for yaw stabilization of vehicle. This controller calculates the required moments to stabilize the vehicle, and it distributes brakes to wheels based on this calculation. Park et al. [139] proposed feedforward and feedback controller alongside with a sideslip angle estimator to stabilize lateral dynamics. 14 DoF vehicle and brush tire model are used in this research and simulation results indicate that the proposed control algorithm has a good capability to improve lateral vehicle dynamic properties. Bang [13] developed a robust sliding mode controller based on a quarter car model to increase yaw dynamics performance. The simulation results demonstrate that the controller has a good performance in tracking reference slip ratio regardless of modeling errors and disturbances. On the other hand, when longitudinal motion combines with lateral motion, the performance of tracking reference slip ratio in braking is not satisfactory. Buckholts [24] investigated a fuzzy logic based on control of yaw rate by setting the desired wheel slip for every wheel to calculate brake torque. In [24], the fuzzy logic strategy was utilized based on a yaw rate and sideslip angle for enhancing the stability of the vehicle. In this paper, the effect of the limitation of sideslip angle by supervision of fuzzy control logic was investigated. The results proved the capability of the method in yaw stabilization of the vehicle. Another research related to the fuzzy logic controller to improve the stability of vehicle under severe maneuver was conducted by Khajavi et al. [94]. Their strategy was to apply brakes on inner or outer tires based on the deviation of the path from the desired one. The results confirm that the proposed algorithm improves stability control compared with passive vehicle. Booada et al. [19] proposed fuzzy control to produce a decent yaw moment based on the difference of brake forces between front wheels where 8 DoF vehicle was employed to test the proposed algorithm. The simulation results demonstrated the effectiveness of the controller in different cornering maneuvers.

Advantages and disadvantages of electronic stability control are listed below:

Advantages

- Correcting impending oversteering or understeering
- Stabilizing the car during sudden evasive maneuvers
- Improved rapid lane-changing maneuvers
- Smaller turning radius
- Cornering stability

Disadvantages

- Decreasing the velocity of vehicle due to braking

2.10 Torque Vectoring Control

Recently, another chassis control system was introduced for active safety named torque vectoring system. Torque vectoring control has been widely utilized in high-performance vehicles to improve traction and cornering ability. The working principle of torque vectoring is to generate force-mentioned torque moment by the calculation of corrective yaw moment of the vehicle. The benefit of torque vectoring is to prohibit a vehicle's understeer and oversteer for maintaining vehicle stability. Another advantage of torque vectoring is to reduce the acceleration loss and enhance lateral vehicle stability. Academic research on the topic was carried out in recent years. Shibahata and Shimada [173, 174] proposed torque vectoring based on yaw control by the decent distribution of traction and braking force on the wheels in order to improve vehicle maneuverability. Sawase et al. [161, 162] investigated an in-depth analysis of different TV configurations as applied to the Front-wheel drive (FWD), Rear-wheel drive (RWD) and Active-wheel drive (AWD) vehicles. Another research has been don by Motoyama et al. [122] to control traction force distribution to wheels. The effect of lateral traction force distribution has been demonstrated in this research. The direct yaw control system by using lateral braking force difference has been proposed by Inagaki et al. [84] in order to stabilize a vehicle in critical cornering maneuvers. The first application of the method as mentioned earlier commercially was introduced by Mercedes Benz in S series [123].

Also, the description of two types of differentials, which enable to implement the torque vectoring system on a vehicle, is in the following:

2.10.1 Semi-active differential

The semi-active differential has a capability to only transfer torque from the fastest to the lowest wheel by braking one of the half shafts. This system consists of hydraulically operated clutches and friction plate between the output shaft and differential box. The working principle of the semi-active differential is to transfer the torque from one wheel to another by the intervention of the clutches according to the information that receives from sensors. Electro-hydraulic actuator activates friction plate for locking differential in a wide operating range. The first application of semi-active differential as an E-Diff was introduced by Ferrari in F430 model [31, 147, 150]. Figure 2.6 shows the scheme of the semi-active differential.

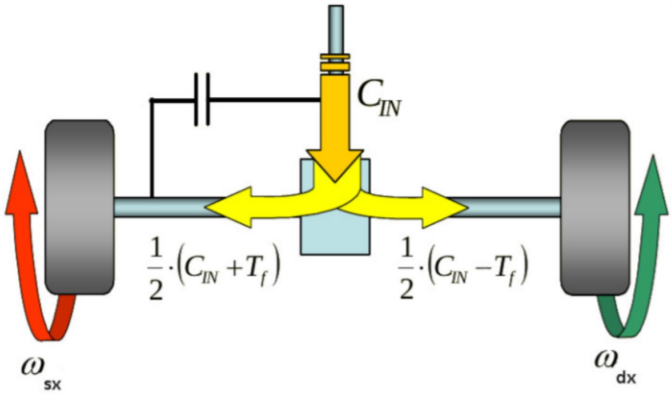

Figure 2.6: Semi-active differential scheme [198]

where
C_IN = input torque to the differential
$\omega_{dx,sx}$ = angular velocity of output shafts

2.10.2 Active differential

The active differential has been developed to overcome the drawbacks of the semi-active differential which is able to transfer torque from fast to slow and vice versa and also it can regulate the amount of torque transfer. This helps to generate a yaw moment in order to stabilize the vehicle. By increasing the driving torque of one wheel, braking torque can be applied at the same time to the other wheel. However, the drawback of the active differential is that implementing the system can be highly expensive. Figure 2.7 illustrates the scheme of active differential.

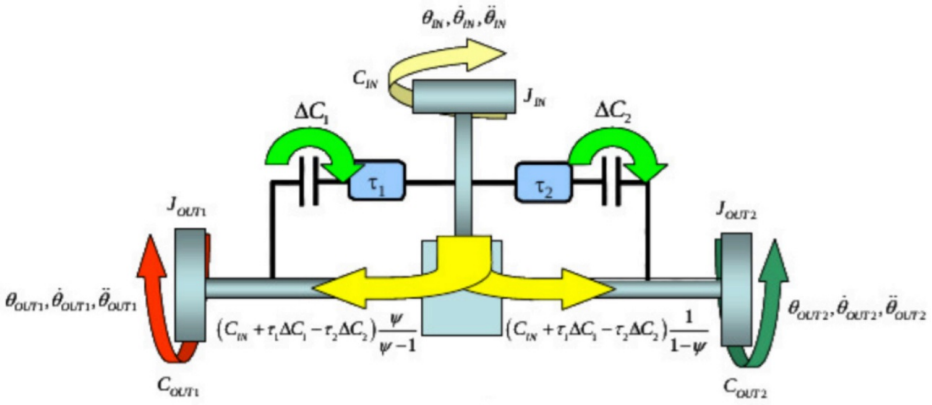

Figure 2.7: :Active differential scheme [198]

Advantages and disadvantages of torque vectoring system are listed below:

Advantages

- The enhancement of vehicle traction and stability
- Regulation of the individual wheel speeds to keep each tire operating in its optimal longitudinal slip range for the best traction
- Enhancement of the vehicle handling response by generating a corrective yaw moment to influence the vehicle yaw behavior

Disadvantages

- Implementing of the system can be highly expensive

2.11 Summary

This chapter explains the investigation of literature available in the field of active chassis control with a definition of the seven significant strategies utilized to control the vehicle handling dynamics actively. The advantages and disadvantages of each controller are described. Finally, a brief review of aims and objectives of each controller is presented as follows:

Active rear steering improves the safety and performance of the vehicle by adjusting the angles of rear wheels. While torque vectoring system enhances the safety and performance of the vehicle by altering the distribution of driving torque between the left and right wheels. The hydraulically interconnected suspension is improving the comfort

of the vehicle by sending fluid to the opposite side of the car to control roll motion of the vehicle. The active anti-roll bar is enhancing the comfort, safety, and performance of the vehicle through a dynamic variation of the roll stiffness distribution between the two axles of the car. Active aerodynamics control improves the performance and safety of the vehicle through changing the angle of attack of the spoilers to modify the normal load distribution between the front and rear axles. However, electronic stability control enhances the safety of the vehicle through the differential braking in order to generate the corrective yaw moment. When it comes to the active suspension system, the latter can enhance comfort, safety, and performance of the vehicle by changing the distribution of normal loads.

Table 2.1: Brief description of active chassis control systems

	ARS	TV	HIS	AARB	AAC	ESC	ASS
Comfort			F_z	F_z			F_z
Safety	F_y	F_x		F_z	F_z	F_x	F_z
Performance	F_y	F_x		F_z	F_z		F_z

Chapter 3

Integrated Controllers

3.1 Introduction and Background

This section begins with a depiction of the three major strategies used to control the vehicle handling dynamics actively. This involves the literature review on active vehicle dynamics systems used for this research. Then the need for integration of active vehicle dynamics control systems is investigated followed by a detailed review of state of the art in integrated vehicle dynamics and control.

Chapter 2 has focused on the stand-alone vehicle dynamics control systems to affect vehicle handling by utilizing different aspects of vehicle dynamics. For overcoming the drawbacks of individuals systems, coordination and integration of standalone systems have been suggested in order to improve overall vehicle performance. Moreover, these systems also have financial benefits such as cost reduction, hardware, and space-saving through sharing sensor information and coordinating subsystems. On the other hand, avoiding the integration of these subsystems' intervention is the most significant challenge for enhancement of overall vehicle dynamics performance. Various active control systems such as ABS, 4WS, ESP and different types of suspensions, etc. were installed in vehicles for improving vehicle performance in terms of safety and comfort. Many problems could occur when these systems work together because the coupling of vehicle dynamics inherently exist. So, the research on integrated vehicle dynamics control has become a focus on solving this kind of problems. Two main issues of integrated vehicle dynamics control are:

- Complication in the design of software and hardware because of increases in the number of sensors and signal cables
- Possible function overlapping among this system and their conflicts of control objectives and actions

If without coordination, the dynamic performance of this system could be worse than that of individual systems or even worse than a passive system without any active control. Therefore, the two critical problems of integrated vehicle dynamics control to be solved are:

- Preventing the conflicts and interventions among different subsystems
- Create synergies from standalone active controls by communication and coordination among them

Despite the fact that many important kinds of research have been published in recent years, the definition of Integrated Vehicle Dynamics Control is not very definitive and accurate. However, attributes are explicit, i.e., coordination of subsystems is needed to control objectives and actions concerning software and hardware, rather than merely put the subsystems altogether. Besides the obvious benefits of Integrated Vehicle Dynamics Control, including reducing the number of sensors and actuators, reduction of mounting space and weight, improve overall vehicle dynamics performance can be done by utilizing Integrated Vehicle Dynamics Control.

3.2 Development of Integrated Vehicle Dynamics Control

The beginning period of Integrated Vehicle Dynamics Control (IVDC) is between the 1980s and 1990s. Nissan introduced its concept ARC-X in 1985 Tokyo International Auto Exhibition. In this concept car, the subsystems were able to obtain integrated function by communication and coordination [192]. Toyota presented integrated of active air suspensions, 4WS, engine control, gearbox ratio control, 4WD and ABS in the concept car FXV-II in 1987 [99]. Moreover, Toyota introduced another model named Sorare in 1991 which coordinated 4WS, ABS and TCS [156, 189]. In [149] indicated that an integration control of vehicle systems should be in three parts: the integration of hardware, the integration of function and the integration of research. Fast developing period of IVDC happened since ESP was developed (the mid-1990s). Researchers have achieved spectacular success both in academic and industry field. GM has introduced the stability system based on braking and continuous adjustable-damper in its Cadillac Seville model in 2002. The name of the integration model is Delphi's Integrated Chassis Control System.

Continental [217, 148] proposed Active Front Steering to its second generation ESP besides its first differential braking and engine interventions to improve handling performance in emergency cases by sacrificing ride comfort. In 2006, Toyota introduced safety concept on its Lexus 460. In hardware feature, its control units are categorized into four functional groups which are power transmission control, safety control, body control and multimedia control. In software feature, integrated vehicle dynamics control is utilized to control anti-lock braking system, traction control, active braking intervention, and steering system harmoniously.

3.3 Integrated Control Structure

Two methods are used in literature for integrated control which is: bottom-up and top-down methods. A decentralized control structure is shown in Figure 3.1 is used in the bottom-up method; however, a centralized method is utilized in the top-down method. For more complicated integrated control system, a multi-layer control structure has been introduced to deal with the coordination and distribution of subsystems.

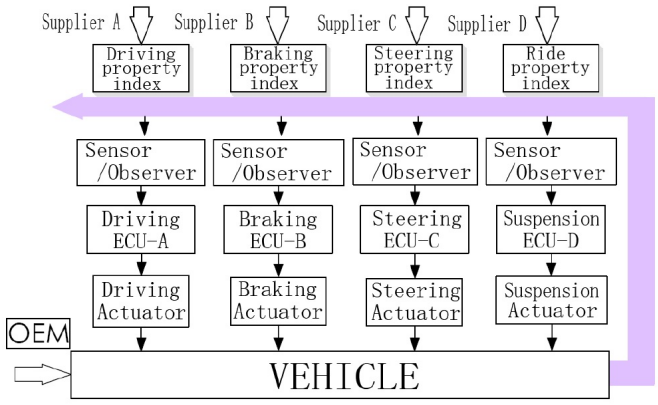

Figure 3.1: Decentralized control structure [213]

3.3.1 Decentralized Control Structure

In this structure, each standalone system is working independently as shown in Figure 3.1, meantime it can go along with other standalone systems in case of need to have desire manner. Because of the integration of sensors and related hardware, this integration method is very

limited. Furthermore, original equipment manufacturer (OEM) and automotive suppliers developed such integration systems in case of need to supply corresponding interfaces necessary to subsystems. Gorden et al. [68] investigated about this structure, and he mentioned that this kind of structure is not suitable for vehicle integration system. However, this structure was utilized and adopted in most early researches on integrated vehicle dynamic control. For example, Mitsubishi and Toyota used the decentralized method [117, 156]. Moreover, the primary aim of suspension systems is to enhance ride comfort while it can indirectly affect the handling performance in comparison to braking and steering system. This can be a reason to utilize a decentralize structure by researchers [35, 34] to integrate suspension system with other subsystems.

3.3.2 Centralized Control Structure

In centralized control structure, a global controller provides control inputs to all standalone control systems as demonstrated in Figure 3.2. A centralized control structure can only be developed by OEM and

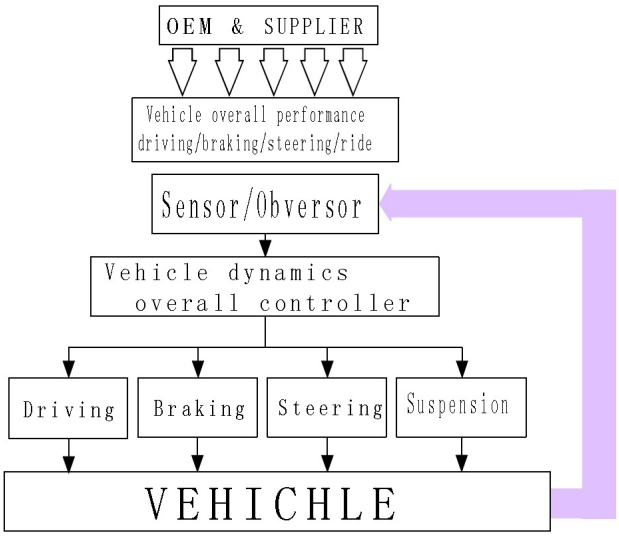

Figure 3.2: Fully centralized control structure [213]

suppliers. By taking the whole system into account, integrated vehicle dynamics control can be designed more comprehensively to have a better performance due to top-down strategy. This structure requires much more powerful ECU due to controller's computing load. Furthermore, centralized control structure may evolve into less adaptable since when another subsystem is added, it is unavoidable to redesign

the system. Consequently, centralized control structure might not be accessible for integrated vehicle dynamics control up until now, in any case, it is a decent choice for those subsystems that are firmly related and coupled.

3.3.3 Multi-layer Control Structure

A multi-layer control structure is a suitable structure scheme which has full advantages regarding both hardware and software as demonstrated in Figure 3.3. When utilizing this structure, suppliers are still accountable for the design of subsystems, while OEMs are in charge of the integration. Coordination controller has two primary functions. The first of it is to determine desires control forces and moments according to the dynamic state of the vehicle and then distributes them to the desired state values of every subsystem. At that point, the controller supplies actuation layer controllers with these desired control forces and moments to track or regulate. The second of it is an ability to shift subsystems to work in different modes (e.g., to switch the suspension system between tire holding or ride comfort strategy).

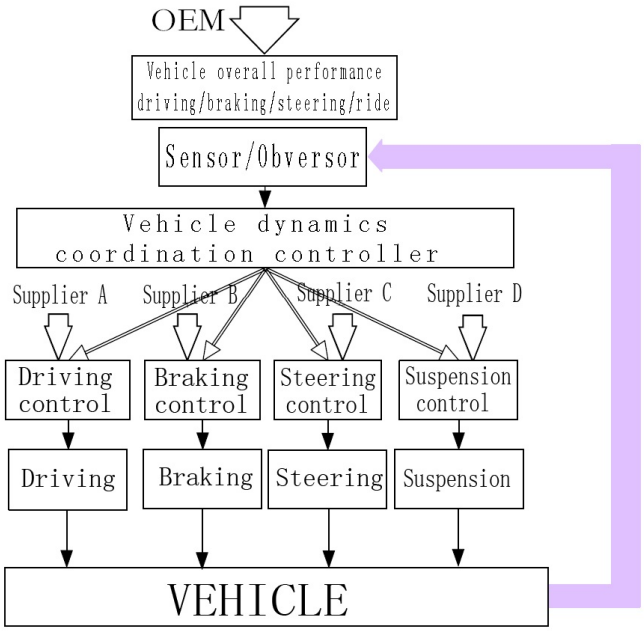

Figure 3.3: Multi-layer control structure [213]

3.4 Coordination and Integration Strategy

To control systems integration strategy and how to distribute and coordinate several actuators in a decent manner and make them work cooperatively are challenging tasks. Longitudinal and lateral control system integration and suspension system integration will be discussed in this section.

3.4.1 Longitudinal and Lateral System Integration

The real frameworks of longitudinal and lateral dynamics control are the braking/traction and steering systems, mainly alluding to the integration of ABS, ESP, and AFS/ARS/4WS. Longitudinal and lateral control systems have advantages of both control effect and intervention smoothness. First, steering system (e.g., 4WS, ARS, and AFS) can achieve excellent handling performance when the lateral acceleration is small therefore the side slip angle is small within the linear region. However, non-linear tire characteristics will display in crisis situations. Steering control is not able to achieve the desired control effect solely, while Dynamics Yaw Control (e.g., ESP based on braking system and AYC based on traction forces distribution) can significantly improve the handling performance. Second, with respect to intervention smoothness, when the control system applies a braking intervention, ESP could cause a sudden longitudinal speed variety and hence decreases the comfort performance. On the other hand, AYC redistributes the traction forces on the two sides (the left and right), guaranteeing the aggregate longitudinal force uninfluenced; thus the intervention of the control system turns out to be more smooth. Active steering can enhance the vehicle yaw performance with less interruption to the driver when the lateral acceleration is small. Some typical works of literature related to different approaches to integration and control structures will be reviewed in the following.

Decentralized Structure:to coordinate steering and braking/ traction subsystems by information interaction

Tire lateral force has been considered in the design of ABS controller which was proposed by Taheri and Law [187]. In steering/braking conditions, by altering front wheel steering angle and the desired tire slip ratio and diminishing rear wheels desired slip ratio, such design can enhance lateral forces margin. Yausi [211] proposed IVDC where electronic steering power (ESP) and electronic stability control (ESC) were coordinated as follows: tire lateral adhesion limits were firstly

estimated from the data acquired by ESC, and after that the estimated information was sent to ESP controller to prevent tire force saturation sent by decreasing tire longitudinal force when the tire characteristics entered the non-linear region.

Multi-layer Structure:firstly generate an active yaw moment then allocate it to subsystems

Two steps exist in multi-layer control structure for vehicle lateral stability control. The first one is to calculate the desired vehicle stability control force/moment by utilizing feedback controller. The second one is to distribute the control force/moment to each subsystem accordingly. As discussed above, ESP's intervention can bring about the deceleration of the vehicle, which can make an immediate undesirable effect the driver. On the other hand, the response of active steering is moderately smooth, hence the energy consumed by the controller can be lower. So, the general strategies in the design of vehicle lateral stability control between active steering and differential braking are 1) to give priority to adopt active steering (front/rear wheel). 2) when active steering is not able to create the desired stability yaw moment, to utilize the intervention of ESP or co-intervention of ESP and active steering [16, 26, 67]. It is better to determine the effective working area of each subsystem based on body sideslip angle β [138] or lateral acceleration [67] to regulate the active steering and ESP working areas, then distribute the desired yaw moment based on empirical rules (e.g., fuzzy logic [67]).

Centralized Structure:comprehensive consideration based on multivariable control method

A centralized structure has been utilized in the integration of braking/steering control based on literature review and can easily enhance performance. However, it needs powerful hardware controller due to high computational demand. A linear optimization control [127, 114, 151, 126, 175], optimization control [38], theory of μ-synthesis [134] have been used. Other research papers utilized robust theory controller based on linearizing of nonlinear vehicle model [151, 134]. This strategy managed the nonlinear factors as uncertainties before modeling by presetting the control gain to balance the undesired impact on the closed loop system imposed by the uncertainties. The integration of active steering and DYC has been proposed by Nagai and Colleagues [127, 126, 175] by utilizing the combination of feedforward control and LQR-based feedback control. Utilizing robust control [37], fuzzy logic

control [20] and robust eigenvalue assignment [38] have been developed by researchers based on feedback control law. The research about the distribution of tire forces by optimization has been done by Abe [121] and Hattori [75]. Shen et al. [170, 105, 171, 104, 169] proposed strategy which utilized two control loops in the controllers and considers tire as a force generator and places it into the servo loop to be managed it. This method optimally distributes tire forces by using unconstrained and constrained optimization with consideration of road adhesion, limits of actuators, etc.

3.4.2 Suspension Integration

The main aim of suspension control is to improve the ride comfort. Due to the coupling of tire force, the suspension system also couples the longitudinal and lateral control systems. The primary target of suspension may decrease the intervention of lateral and longitudinal systems when coordinating suspension into dynamic control. However, it is essential to sacrifice the ride comfort to guarantee the performance of ESP, AFS, and so on in emergency cases. Consequently, the strategies of integration control including suspension system can be partitioned into 1) Utilizing suspension to control vertical tire loads in order to guarantee tire grip and fully usage of road adhesion; 2) to determine vertical tire forces and indirectly create stability yaw moment by controlling suspension (e.g. active suspension, Continuous Damping Control (CDC) shock absorber or active stabilizer bar, etc.). Like this, the intervention of active braking and the sudden altering of longitudinal speed by braking can be reduced. The relevant works of literature are summarized as below.

Enhance tire grip by active suspension to assist longitudinal and lateral control system

The main principle of these researches [130, 56, 196, 146, 111], is to design two methods for active and semi-active suspensions. Under general conditions, ride comfort technique is embraced to enhance vertical dynamics; but in crisis situations, the dynamic suspension law will be changed to tire grip strategy by a supervisor controller, temporarily sacrificing ride comfort to guarantee the braking and stability performance of ABS and ESP. The tire grip control law of active suspension has been investigated by Feng et al. [56] to reach the maximum value of tire load and slip ratio for making full use of the road adhesion coefficient. Active front wheel steering and suspension controller have

been introduced by March and Shim [111] for controlling roll moment in order to enhance tire lateral performance.

Active suspension intervene yaw moment control

The integration of active suspension and active braking has been conducted by Smakman [178] by utilizing the similar strategy for active steering and ESP integration to control vertical load by active suspension for generating yaw moment and in case of insufficient of yaw moment active braking is enabled. Hac [74], Kou [101] developed the integration of CDC damper and ESP system, and declared that the acting time of active braking could be decreased by utilizing CDC suspension to create yaw moment. A vehicle understeering characteristics can be indirectly altered by utilizing active anti-roll bar or active roll torque distribution control. The working principle of this method is to change the lateral transfer magnitude of tire load between front and rear axles. Cooper and Crolla [41] introduced a central differential controller in order to assign more traction moment to the wheels with a larger vertical load by integration of active roll moment and active traction moment distribution. Moreover, authors declared that roll moment distribution between front and rear axles could affect understeering characteristic slightly. The contribution of active suspension to yaw stability is restricted because when the lateral acceleration is small, the total load transfer is relatively low. While other researchers tried to enhance vehicle vertical dynamics performance, the objective of works of relevant research which are mentioned above is to developed longitudinal and lateral dynamics by further integrating suspension control. The integration of Inverse steering of the rear wheel and increased front axle suspension damper has been proposed by Lee [102] in order to increase the anti-roll moment under large lateral acceleration circumstance to avoid the rollover. Chen and Wang [35, 34] developed the integration of active suspension and steering control system based on the output feedback random sub-optimal control to enhance steering quality and ride comfort.

3.5 Summary

A detailed investigation of literature available in the field of integrated chassis control was presented with a description of the three primary strategies used to actively control the vehicle handling dynamics. These strategies are listed below:
1. Centralized Structure: The centralized approach is allowed to utilize

all control inputs.
2. Decentralized Structure: The decentralized integration approaches aim to coordinate the control commands of the sub-control systems, which were separately designed for their objectives.
3. Multi-layer Structure: The application of the proposed multilayer coordinating control system is able to improve the overall vehicle dynamics in the three directions including lateral, longitudinal, and vertical and, hence, enhance the overall vehicle performance including handling stability, ride comfort, and braking performance.
Then a detailed review about the state of art of each strategy was presented.

Chapter 4

Vehicle Dynamics

4.1 Vehicle and tire modeling

4.1.1 Introduction

For designing dynamics control system, evaluating control performance and simulating handling performance of vehicle during various maneuvers, vehicle handling models must be developed. For a particular application, a vehicle handling model should be defined in the way of necessary complexity for a given application. For example, a simple linear vehicle model with many simplifying assumptions is sufficient for normal handling. However, a more complicated vehicle model is required for severe handling maneuvers. Consequently, it is better to model vehicle considering the degrees of freedom which include relevant and significant nonlinearities concerning the complexity of maneuvers and scenarios. In this study, we classified a vehicle handling model into two categories: 1) a linear model which will be used for controller design and creating the reference 2) a nonlinear vehicle model to control system evaluations through computer/numerical simulations. Therefore, to be able to study the vehicle handling behavior from the linear region in typical driving situations to the limit performance region during the emergency and severe maneuvers, various types of vehicle models will be developed.

4.1.2 Tire Dynamics

Tires are significant components of vehicles; the reduction the impact from the ground and supporting the weight of car are the primary roles of tires. Meanwhile, forces and torques through the interaction of tire and ground which influence the vehicle's motion are generated. The forces and torques consist of tractive force, braking force, and aligning

moment. Vehicle's handling, ride comfort, traction and braking performance are strongly related to the dynamic behavior of tires. The accuracy of dynamic performance analysis and the achievement of the chassis control system design depend intensely on the precision of the vehicle dynamics model and the tire dynamic model. The relationships between forces, deformation, and motion are highly nonlinear due to complex viscoelastic structures. Therefore, it is a challenging task to set up a precise numerical and mathematical model. Since 1930s many researchers have researched on tire modeling. In the following section, experimental tire model will be described.

Terminology and Concepts

1. Tire axis system and six-component wheel force

Three forces and three moments acting on the tire by the road can also be shown in this axis system. They are also known as the tire 6-component wheel forces, shown in Figure 4.1.

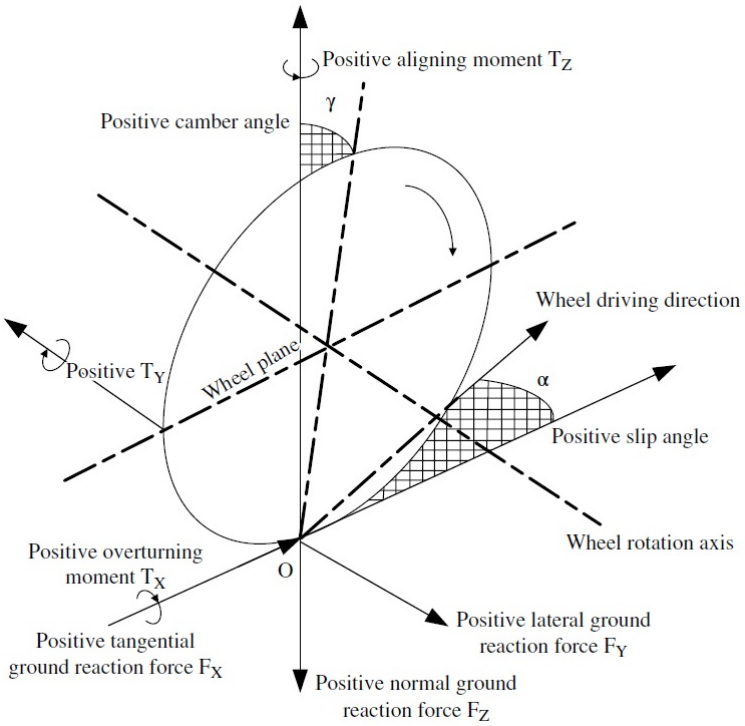

Figure 4.1: Tire coordinate system with forces and moments on the tire [36]

The origin of the coordinate system is the center of the tire-road contact path. The line of intersection of the wheel plane and the road

plane is described as X-axis which a positive direction is being forward. And the perpendicular to the X-axis is defined as Y-axis which is parallel to the pivot of the wheel where the positive direction is being to the right. Perpendicular to the road plane is recognized as a Z-axis with its positive direction pointing downwards. The longitudinal force F_x, the lateral force F_y, and the normal force F_z are categorized as the forces of tire. Forces in the X, Y, Z directions are defined as longitudinal, lateral, and normal forces. The positive directions of these forces are demonstrated in Figure 4.1. Moreover, the moments of tire in X,Y and Z direction are: the overturning moment M_x, the rolling resistance moment M_y, and the aligning moment M_z. Meanwhile, their positive directions are shown in Figure 4.1.

2.Slip ratio

Generally, a rolling wheel on a ground slides. The concept of slip ratio is presented for quantifying the proportion of sliding to wheel rolling movement. Slip ratio is described as follows

$$\lambda = \begin{cases} \dfrac{v_x - R_t\omega}{R_t\omega}, & \text{if } R_t\omega \geq v_x(acceleration) \\ \dfrac{v_x - R_t\omega}{v_x}, & \text{if } R_t\omega \leq v_x(braking) \end{cases} \tag{4.1}$$

where
R_t = tire effective rolling radius
v_x = traveling speed of the wheel
ω = angular velocity of the wheel
λ = slip ratio

3. Tire slip angle

An angle between the actual traveling direction of a rolling wheel and the direction toward is defined as a tire slip angle. The definition of tire side slip angle is in the following:

$$\alpha = arctan(\frac{v_y}{v_x}) \tag{4.2}$$

where
v_x = wheel travel speed
v_y = lateral velocity

4.1.3 Tire model

Tires are modeled as an arrangement of mathematical explanations which define the relationship between tire's 6-component forces and wheel parameters. Slip ratio, slip angle, radial deformation, camber angle, wheel speed, and yaw angle are included as an output of these models. The relationship between the inputs and the outputs is highly nonlinear.

Magic Formula Tire Model

Magic Formula tire model has been extensively utilized for the study of vehicle dynamics and control systems. The Magic Formula tire model was introduced by Pacejka [136]. For fitting tire experimental data, a combination of trigonometric functions was utilized. Longitudinal force, lateral force and aligning moment can be derived and calculated by the formula which is shown below:[36]

$$y = Dsin(Carctan[Bx - E(Bx - arctanBx)]) \tag{4.3}$$

where
y = longitudinal force, lateral force, or aligning moment
x = the tire slip angle or longitudinal slip ratio
D = the peak value which represents the maximum value of the curve
C = the shape factor (lateral force, longitudinal force, or aligning moment)
B = the stiffness factor
E = the curvature factor which represents the shape of the curve near the peak value

Under driving or braking conditions, longitudinal forces, lateral forces, and aligning moments on the tire can be described as follows [36]

1. Lateral force

$$F_y = (Dsin(Carctan(BX_1 - E(BX_1 - arctan(BX_1))))) + S_v \tag{4.4}$$

where
$X_1 = \alpha + S_h$
$D = a_1F_z^2 + a_2F_z^2$
$C = a_0$
$BCD = a_3sin(a_4arctant(a_5F_z))(1 - a_6\gamma)$
$B = \dfrac{BCD}{CD}$

$E = a_7 F_z^2 + a_8 F_z + a_9$
S_v = curve shift in the vertical direction
$S_v = (a_{10} F_z^2 + a_{11} F_z)\gamma$
S_h = curve shift in the horizontal direction
$S_h = a_{12}\gamma$
F_z = vertical load
γ = camber angle

2. Longitudinal force

$$F_x = (Dsin(Carctan(BX_1 - E(BX_1 - arctan(BX_1))))) + S_v \quad (4.5)$$

where
$X_1 = s + S_h$
$D = b_1 F_z^2 + b_2 F_z$
$C = b_0$
$BCD = (b_3 F_z^2 + b_4 F_z) e^{b_5 F_z}$
$B = BCD/BC$
$E = b_6 F_z^2 + b_7 F_z^2 + b_8$
$S_h = b_9 F_z + b_{10}$
$S_v = 0$ S = longitudinal slip ratio

3. Aligning moment

$$M_z = (Dsin(Carctan(BX_1 - E(BX_1 - arctan(BX_1))))) + S_v \quad (4.6)$$

where
$X_1 = \alpha + S_h$
$D = c_1 F_z^2 + c_2 F_z$
$C = c_0$
$BCD = (c_3 F_z^2 + c_4 F_z)(1 - c_5|\gamma|) e^{c_5 F_z}$
$B = \frac{BCD}{CD}$
$E = (c_7 F_z^2 + c_8 F_z + c_9)(1 - c_{10}|\gamma|)$
$S_v = (c_{11} F_z^2 + c_{12} F_z)\gamma + c_{13} F_z + c_{14}$
$S_h = c_{15}\gamma + c_{16} F_z + c_{17}$

4.1.4 Vehicle Modeling

This section describes various mathematical models of a vehicle which are widely utilized for replacing the physical vehicle in an analytical

study. These models are being used in order to analyze the handling behavior of a vehicle. The description of the chapter begins with the simplest vehicle model (bicycle vehicle model) and move towards complex vehicle model. As mentioned before, both linear and nonlinear vehicle models will be developed in this thesis; the linear one is to create the reference inputs to control purpose, and nonlinear one is to consider the vehicle-controller interaction. The coordinate system of a vehicle will be introduced which is utilized to explain vehicle motion.

Coordinate System

Generally, two coordinate systems are of utmost importance to analyze vehicle dynamics. These coordinate systems are inertial or earth-fixed coordinate system (X, Y, Z) and the body-fixed coordinate system (x,y,z). The orientation and location of the vehicle are defined by the inertial reference system which is fixed to the earth, while the body-fixed coordinate system is set to the vehicle's center of gravity and moves along with the vehicle which assists to determine the motion of the vehicle and analyze the forces acting on the vehicle.

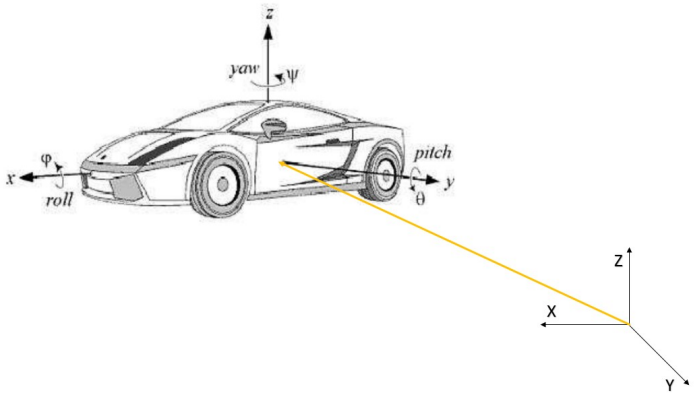

Figure 4.2: ISO coordinate system

In this thesis, the ISO coordinate system has been chosen to define the direction of forces and moments for earth-fixed coordinate system and the body-fixed coordinate system. The positive directions of forces and moments are demonstrated in Figure 4.2. The motions about x, y and z axes are defined as roll (ϕ), pitch (θ) and yaw (ψ) respectively.

Two degrees of freedom model (Bicycle model)

Two degrees of freedom vehicle model which defined as a bicycle model is vehicle's lateral and yaw motion [65, 208, 145]. This model is defined based on the following assumptions, which are accurate and precise when the vehicle is going under simple maneuvers within the primary handling regime.

- the vehicle is moving with a constant longitudinal speed (u =constant) on a flat surface.
- the steering input to front tires and the corresponding slip angles are small.
- the vehicle structure, including the suspension system, is rigid.
- the track width is small comparing to the radius of turn.
- there is no lateral weight transfer.
- aerodynamic forces are negligible.

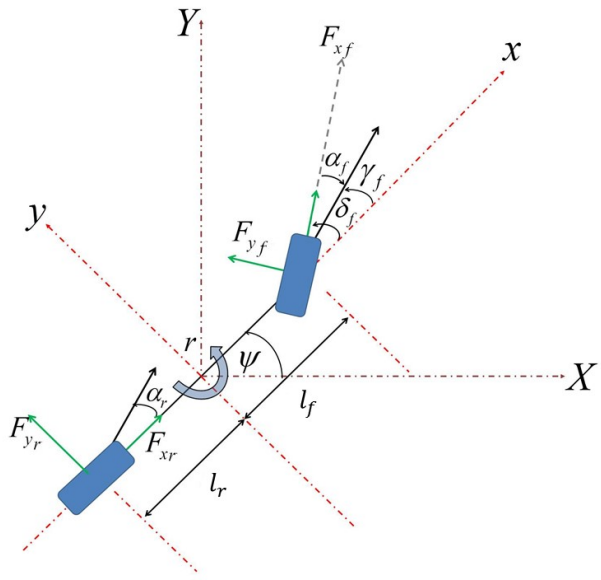

Figure 4.3: Two degrees of freedom bicycle model

Front and rear two tires can be produced by a single wheel under consideration of aforementioned assumptions as demonstrated in the 4.3. Motions such as heave, roll, and pitch have been ignored in order to decrease the complexity of the model. Despite the fact that the vehicle

is moving in the forwarding direction, the assumption of constant speed eliminates this degree of freedom. The symbols utilized in Figure 4.3 shows the following parameters and states.
l_f = distance between the front axle and the vehicle's center of mass.
l_r = distance between the rear axle and the vehicle's center of mass.
ψ, $\dot{\psi}$ = yaw angle and yaw rate of the vehicle respectively.
δ_f = front steering angle.
γ_f = front tire velocity angle.
F_{x_f}, F_{x_r} = longitudinal tire forces at front and rear respectively.
F_{y_f}, F_{y_r} = lateral tire forces at front and rear respectively.
α_f, α_r = Front and rear tire slip angles respectively.
Now applying the Newton's second law of motion, the equations for lateral and yaw motions can be written as:

$$\begin{aligned} ma_y &= \Sigma F_y \\ I_z\ddot{\psi} &= \Sigma M_z \end{aligned} \tag{4.7}$$

where
m = mass of the vehicle.
a_y = inertial acceleration of the vehicle in y-direction.
ΣF_y = sum of forces acting on the vehicle in y-direction.
I_{zz} = moment of inertia about z-axis.
ΣM_z = sum of moments acting on the vehicle about z-axis.
It can be observed from 4.3 that the total force in y-direction and total moment about the z-axis can be written as follows:

$$\begin{aligned} \Sigma F_y &= F_{y_f} cos\delta_f + F_{y_r} \\ \Sigma M_z &= F_{y_f} cos\delta_f l_f - F_{y_r} l_r \end{aligned} \tag{4.8}$$

The inertial acceleration of the vehicle consists of lateral acceleration $\dot{v}_y$ because of the motion of the vehicle along y-axis and multiplication of longitudinal velocity and yaw rate $v_x\dot{\psi}$; thus $a_y = \dot{v_y} + v_x\dot{\psi}$. By substitution of these values in Equation 4.7, the equation for vehicle's translational motion in lateral direction can be written as

$$m(\dot{v_y} + v_x\dot{\psi}) = F_{y_f} cos\delta_f + F_{y_r} \tag{4.9}$$

and the equation for rotational motion about z-axis as

$$I_{zz}\ddot{\psi} = F_{y_f} cos\delta_f l_f - F_{y_r} l_r \tag{4.10}$$

Due to the assumption of small steering angle, in the above equation, the term $cos\delta_f$ can be taken as 1. Tire behaves in the linear region

because of small tire sideslip angle. The following equation which is valid within in linear region is tire lateral force: $F_y = C_\alpha \alpha$

The above lateral force is substituted in Equation 4.9 and 4.10 which C_α is the cornering stiffness of the tire described below:

$$m(\dot{v_y} + v_x\dot{\psi}) = 2C_{\alpha_f}\alpha_f + 2C_{\alpha_r}\alpha_r \tag{4.11}$$

and

$$I_{zz}\ddot{\psi} = 2C_{\alpha_f}\alpha_f l_f + 2C_{\alpha_r}\alpha_r l_r \tag{4.12}$$

In the both of the above equations, terms f and r are utilized to represent the force generated by front and rear tires. Front and rear sideslip angle can be described as follows which is shown in Figure 4.3 [145]:

$$\begin{aligned} \alpha_f &= \delta_f - \frac{v_y + l_f\dot{\psi}}{v_x} \\ \alpha_r &= -\frac{v_y - l_r\dot{\psi}}{v_x} \end{aligned} \tag{4.13}$$

This tire sideslip angle is substituted in Equations 4.11 and 4.12 and then equations are readjusted to describe the system in a state space as follows:

$$\begin{aligned} \dot{x} &= Ax + Bu \\ y &= Cx + De \end{aligned} \tag{4.14}$$

where x is a 2×1 state vector having v_y and $\dot{\psi}$ as the state variable, e is a scalar representing the input, which is δ_f in this case. y is a scalar representing the system output. The matrices A (2 × 2), B (2 × 1) and C (1 × 2) define the relationship between the state, input and output variables. The matrices A and B for the bicycle model are given as:

$$A = \begin{bmatrix} \dfrac{-(C_{\alpha_f} + C_{\alpha_r})}{mv_x} & \dfrac{C_{\alpha_r} l_r - C_{\alpha_f} l_f}{mv_x} - v_x \\ \dfrac{(C_{\alpha_r} l_r - C_{\alpha_f} l_f)}{I_{zz} v_x} & \dfrac{-(C_{\alpha_f} l_f^2 + C_{\alpha_r} l_r^2)}{I_{zz} v_x} \end{bmatrix}$$
$$B = \begin{bmatrix} \dfrac{C_{\alpha_f}}{m} \\ \dfrac{C_{\alpha_f} l_f}{I_{zz}} \end{bmatrix} \tag{4.15}$$

whereas the matrices C and D are dependent on the desired output.

Non-linear vehicle model with 14 DOF

A 14-Do0F full vehicle dynamic models as shown in Figure 4.4 which consists of the vehicle longitudinal, lateral, vertical dynamics and the rotation of the wheels with taking into account of steering, braking, and suspension systems.

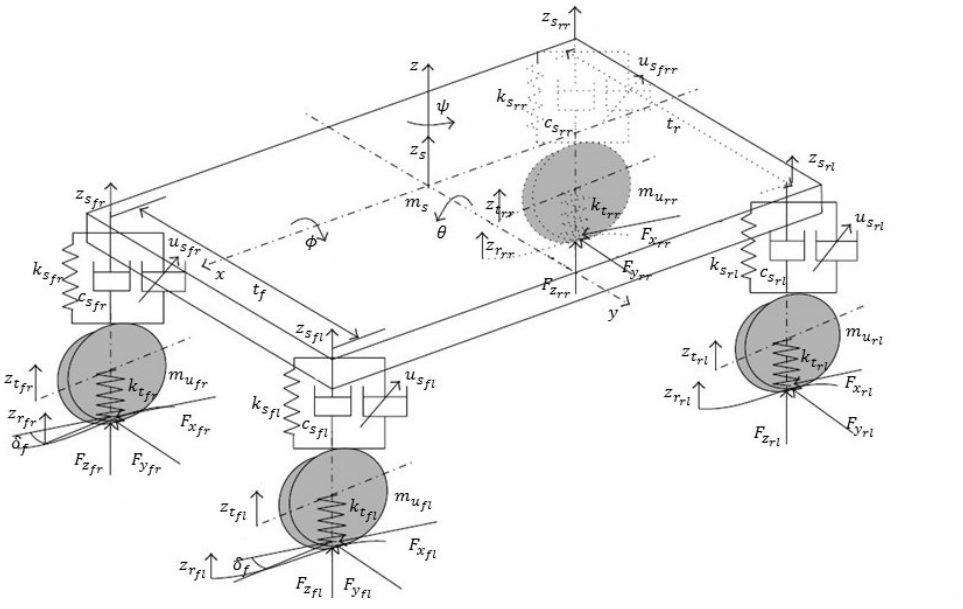

Figure 4.4: 14-DoF vehicle dynamic model

According to Newton's second law, the vehicle nonlinear dynamics

equations are obtained [95] by the combination of force analysis of Figures 4.5, 4.6, 4.7 and 4.8.

The sum of forces in longitudinal and lateral direction and the corresponding moments as demonstrated in Figure 4.5 can be expressed as:

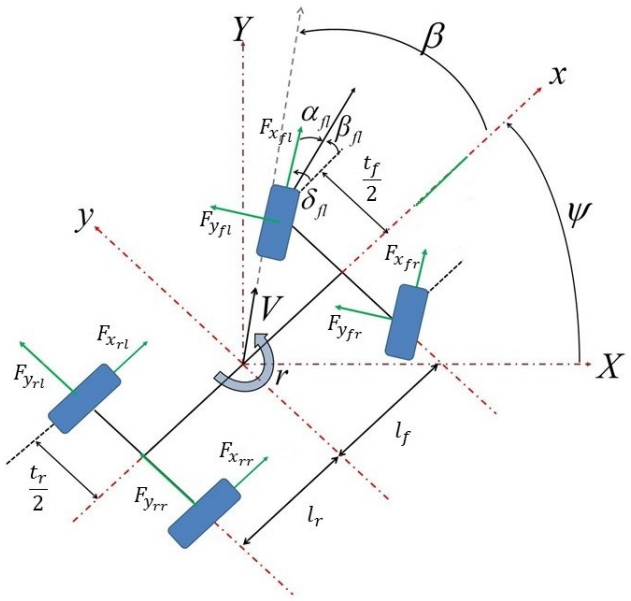

Figure 4.5: Planar vehicle model

$$\begin{aligned} ma_x = m(\dot{v}_x - v_y r) = \Sigma F_x = \{&F_{x_{fl}} cos\delta_{fl} - F_{y_{fl}} sin\delta_{fl} \\ &+ F_{x_{fr}} cos\delta_{fr} - F_{y_{fr}} sin\delta_{fr} \\ &+ F_{x_{rl}} + F_{x_{rr}} - F_d\} \end{aligned} \tag{4.16}$$

$$\begin{aligned} ma_y = m(\dot{v}_y + v_x\dot{\psi}) = \Sigma F_y = \{&F_{x_{fl}} sin\delta_{fl} + F_{y_{fl}} cos\delta_{fl} \\ &+ F_{x_{fr}} cos\delta_{fr} + F_{y_{fr}} cos\delta_{fr} \\ &+ F_{y_{rl}} + F_{y_{rr}}\} \end{aligned} \tag{4.17}$$

$$\begin{aligned} I_{zz}\ddot{\psi} = \Sigma M_z = \{&(F_{x_{fl}} sin\delta_{fl} + F_{y_{fl}} cos\delta_{fl} + F_{x_{fr}} cos\delta_{fr} \\ &+ F_{y_{fr}} cos\delta_{fr}) l_f - (F_{x_{fl}} cos\delta_{fl} - F_{y_{fl}} sin\delta_{fl} \\ &- F_{x_{fr}} cos\delta_{fr} + F_{y_{fr}} sin\delta_{fr}) \frac{t_f}{2} \\ &- (F_{y_{rl}} + F_{y_{rr}}) l_r - (F_{x_{rl}} - F_{x_{rr}}) \frac{t_r}{2}\} \end{aligned} \tag{4.18}$$

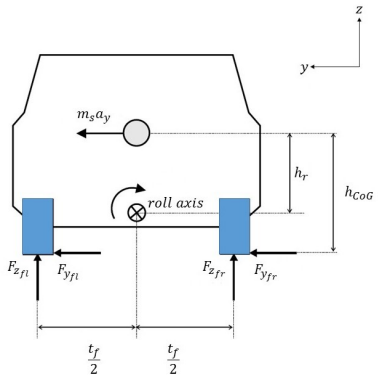

Figure 4.6: Torque balance at the roll axis

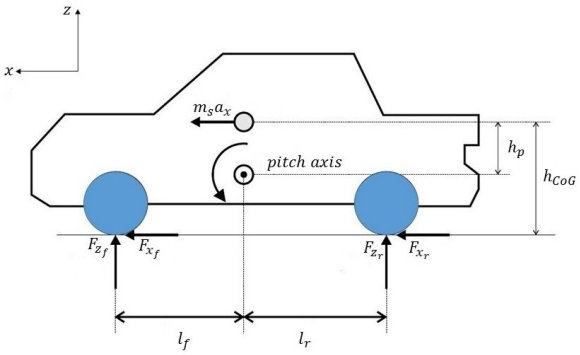

Figure 4.7: Torque balance at the pitch axis

According to Figures 4.6 and 4.7, torque equations about the roll and pitch axis can be derived as follows:

$$\begin{aligned} I_{xx}\ddot{\phi} = \Sigma M_x = \{&(F_{z_{fl}} - F_{z_{fr}})\frac{t_f}{2} + (F_{z_{rl}} - F_{z_{rr}})\frac{t_r}{2} \\ &+ (F_{y_{fl}} + F_{y_{fr}} + F_{y_{rl}} + F_{y_{rl}})(h_{CoG} - h_R) \\ &+ m_s a_y h_R\} \end{aligned} \tag{4.19}$$

$$\begin{aligned} I_{yy}\ddot{\theta} = \Sigma M_y = \{&-(F_{z_{fl}} - F_{z_{fr}})l_f + (F_{z_{rl}} - F_{z_{rr}})l_r \\ &+ (F_{y_{fl}} + F_{y_{fr}} + F_{y_{rl}} + F_{y_{rl}})(h_{CoG} - h_P) \\ &- m_s a_x h_P\} \end{aligned} \tag{4.20}$$

where
m_s = mass of the car body or sprung mass (kg)
I_{xx}=moment of inertia about x-axis (kgm^2)
I_{yy}=moment of inertia about y-axis (kgm^2)
h_R=height of roll center (m)
h_P=height of pitch center (m)
a_x=acceleration along the x-direction (m/s^2)
a_y=acceleration along the y-direction (m/s^2)

In Figure 4.4, a connection between sprung mass to the four unsprung mass which is front-left, front-right, rear-left, and rear-right wheels is suspension system. The suspension systems are free to have a bounce motion with respect to the sprung mass. Mathematical model of full vehicle suspension model is written as follows [96]:

For bouncing of the sprung mass

$$\begin{aligned} m_s\ddot{z}_s = \{&-c_{s_{fl}}(\dot{z}_{s_{fl}} - \dot{z}_{u_{fl}}) - c_{s_{fr}}(\dot{z}_{s_{fr}} - \dot{z}_{u_{fl}}) \\ &- c_{s_{rl}}(\dot{z}_{s_{rl}} - \dot{z}_{u_{fl}}) - c_{s_{rr}}(\dot{z}_{s_{rr}} - \dot{z}_{u_{fl}}) \\ &- k_{s_{fl}}(z_{s_{fl}} - z_{u_{fl}}) - k_{s_{fr}}(z_{s_{fr}} - z_{u_{fr}}) \\ &- k_{s_{rl}}(z_{s_{rl}} - z_{u_{rl}}) - k_{s_{rr}}(z_{s_{rr}} - z_{u_{rr}})\} \end{aligned} \tag{4.21}$$

and also for wheel motion in vertical direction

$$m_{u_i}\ddot{z}_u = c_{s_i}(\dot{z}_{s_i} - \dot{z}_{u_i}) + k_{s_i}(z_{s_i} - z_{u_i}) - k_{t_i}z_{u_i} + k_{t_i}z_{ri} \tag{4.22}$$

where

$$\begin{aligned} z_{s_{fl}} &= z_s + t_f\phi + l_f\theta \\ \dot{z}_{s_{fl}} &= \dot{z}_s + t_f\dot{\phi} + l_f\dot{\theta} \\ z_{s_{fr}} &= z_s - t_f\phi + l_f\theta \\ \dot{z}_{s_{fr}} &= \dot{z}_s - t_f\dot{\phi} + l_f\dot{\theta} \\ z_{s_{rl}} &= z_s + t_r\phi - l_r\theta \\ \dot{z}_{s_{rl}} &= \dot{z}_s + t_r\dot{\phi} - l_r\dot{\theta} \\ z_{s_{rr}} &= z_s - t_r\phi - l_r\theta \\ \dot{z}_{s_{rr}} &= \dot{z}_s - t_r\dot{\phi} - l_r\dot{\theta} \end{aligned} \tag{4.23}$$

where
m_{u_i} = mass of the wheel or unsprung mass (kg)
z_s = car body displacement (m)
z_{s_i} = car body displacement for each corner (m)
z_{u_i}= wheel displacement (m)
c_{s_i} = damper coefficient (Nm/s)
k_{s_i}= spring stiffness (N/m)
k_{t_i} = tire stiffness (N/m)

In above equations, other force components are tire forces which are dependent on the tire sideslip angle as explained in detail in the previous section. The sideslip angle for each tire can be written as:

$$
\begin{aligned}
\alpha_{fl} &= arctan(\frac{v_y + l_f\dot{\psi}}{v_x - \frac{t_f}{2}\dot{\psi}}) - \delta_{fl} \\
\alpha_{fr} &= arctan(\frac{v_y + l_f\dot{\psi}}{v_x + \frac{t_f}{2}\dot{\psi}}) - \delta_{fr} \\
\alpha_{rl} &= arctan(\frac{v_y - l_r\dot{\psi}}{v_x + \frac{t_r}{2}\dot{\psi}}) \\
\alpha_{rr} &= arctan(\frac{v_y - l_r\dot{\psi}}{v_x - \frac{t_r}{2}\dot{\psi}})
\end{aligned}
\tag{4.24}
$$

In above equations, tire sideslip angles depends on the corresponding velocities of each tire which are discussed in detail in [116] and Genta [63]. The terms t_f and t_r are described as the track widths at front and rear respectively which are shown in Figure 4.5. In addition, these equations include arctan since small angle approximation is no more valid for this vehicle model.

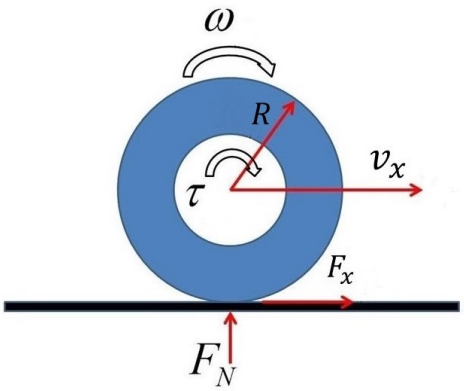

Figure 4.8: Longitudinal wheel model

Longitudinal motion of the wheel is demonstrated in Figure 4.8 where R_t represents the effective radius of the wheel and F_x is the longitudinal tire force. The wheel is traveling in the forward direction with an angular velocity ω due to the acting driving torque τ on it.

The rotational equation of motion for the wheel can be expressed as:

$$I_w\dot{\omega} = \tau - R_t F_x$$

$$\dot{\omega}_i = \frac{1}{I_{w_i}}(\tau_i - R_i F_{x_i}) \tag{4.25}$$

I_{w_i} and ω_i in the above equation represent the wheel's moment of inertia and its angular velocity respectively.

4.2 Vehicle lateral dynamics

The review of concepts of vehicle lateral dynamics will be discussed in this section because vehicle handling in this thesis mainly refers to the lateral vehicle dynamics.

4.2.1 Steady-state handling characteristics

When the vehicle is traveling at a constant speed and steering angle, which results in a steady radius turn, is called steady-state handling. Figure 4.9 shows the center of turn of a vehicle bicycle model at low and high speeds. As seen in the Figure 4.9, center of turn lies on the projection of the rear axle when the vehicle is turning at low speeds, therefore the tire's direction of heading and direction of travel are the equal because the tires do not develop lateral force so in this case sideslip angle of tires does not exist [66, 49]. Following equation represents the relation of the radius of turn and steering angle which is known as Ackerman Angle:

$$\delta = \frac{l}{R} \tag{4.26}$$

where l is the distance of front and rear axles and R is the radius of turn.

On the other hand, during cornering at high speeds lateral acceleration will be introduced. The sideslip angle of tires and lateral acceleration increase for counteracting the inertia force which is induced by lateral acceleration so that tire's direction will deviate from the path of the vehicle. The sideslip angle of the vehicle is positive when the lateral acceleration is negligible. However, sideslip angle of the vehicle becomes negative at high speeds due to the presence of negative sideslip angle at rear wheels. The relations of yaw rate and lateral acceleration with the radius of circular trajectory under the condition of steady state cornering are in the following:

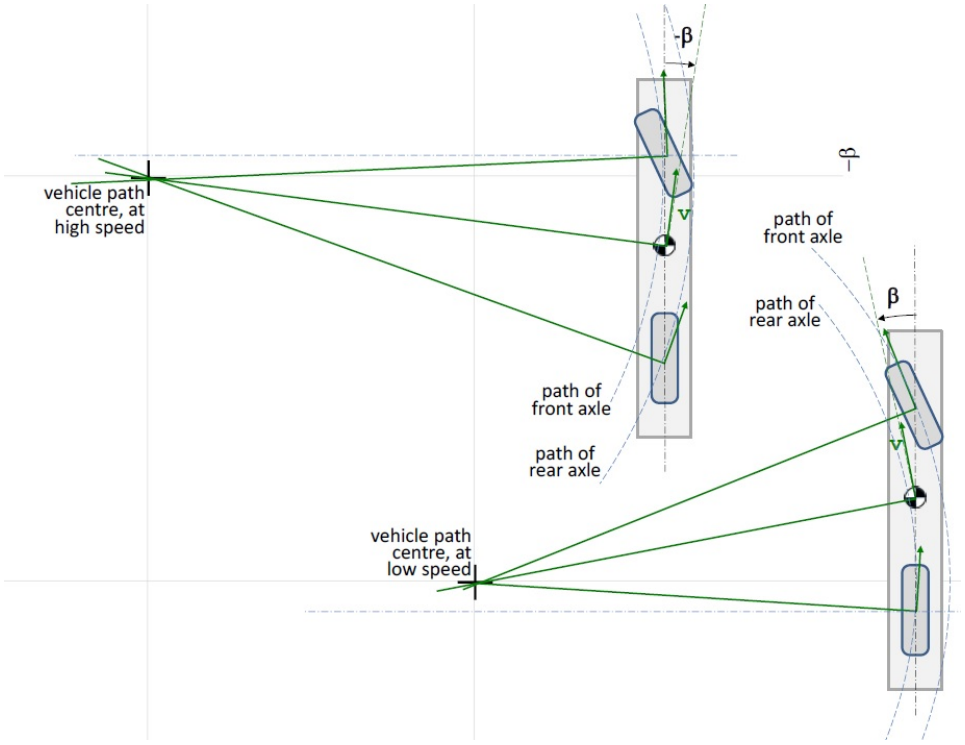

Figure 4.9: Vehicle sideslip angle for low and high speed steady state curves [85]

$$\begin{aligned} \dot{\psi} &= \frac{v_x}{R} \\ a_y &= \frac{v_x^2}{R} \end{aligned} \tag{4.27}$$

4.2.2 Oversteering and Understeering

Oversteering and understeering are two terms that extensively utilized throughout this thesis since the primary targets of the thesis is to amend the vehicle behaviors. These two expressions are extensively used throughout this thesis since the main objective of the thesis is to correct these undesired vehicle behaviors. Figure 4.10 shows understeering, oversteering and neutral condition of the vehicle during same cornering maneuver. A vehicle can be designed in a way that the general tendency of the vehicle is oversteering and understeering.

Under the consideration of lateral acceleration, the steering angle can be described as follows:

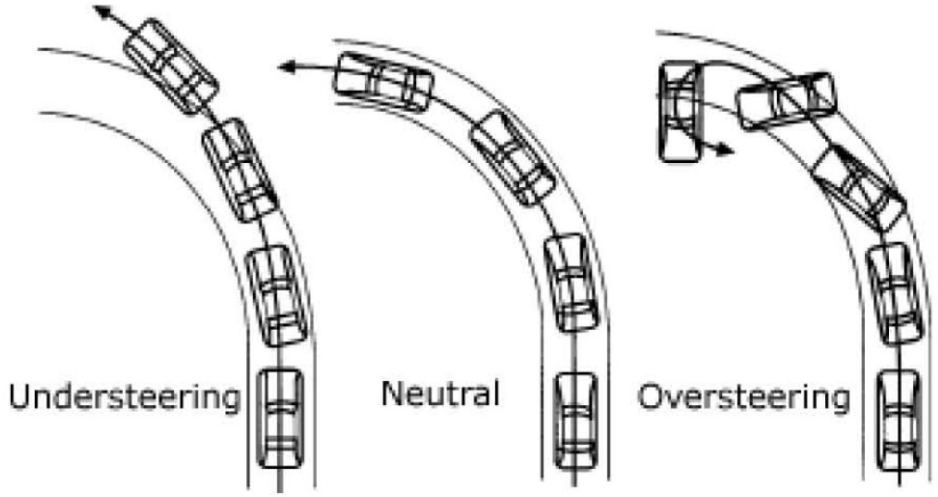

Figure 4.10: Neutral-, over- and under-steering conditions [62]

$$\delta = \frac{l}{R} + (\frac{ml_r}{C_{\alpha_f} l} - \frac{ml_f}{C_{\alpha_r} l})\frac{V^2}{R} \tag{4.28}$$

where $(\frac{ml_r}{C_{\alpha_f} l} - \frac{ml_f}{C_{\alpha_r} l})$ is defined as understeer gradient k_{us}, therefore the equation 4.28 can be rewritten as:

$$\delta = \frac{l}{R} + k_{us}\frac{V^2}{R} \tag{4.29}$$

k_us measures the handling performance of the vehicle in steady state condition. Three cases can occur during steady state maneuvers:
1. Understeer: $K_{us}>0$ which means that rear wheels have the large directional factor. In other words, the steering angle needs to be increased with speed;
2. Neutral steer: $k_{us}=0$, which means that the front and rear wheels have the same directional ability. In other words, the steering angle remains constant as the speed changes;
3. Oversteer: $k_{us}<0$, which means that front wheels have the large directional factor. In other words, the steering angle needs to decreases with speed.

Figure 4.11 depicts that how variations of speed affect the behavior of steering angle on a constant radius turn until the vehicle comes to its critical or characteristic speed. Therefore, the speed of vehicle plays a crucial role in displaying the effect of the vehicle's steering

behavior. As seen from the figure, Ackerman Angle (equation 4.26) can be used in a neutral condition. However, it is not feasible to utilize the Ackerman Angle in understeer and oversteer conditions because the relation between the steering angle and vehicle speed changes which are twice of Ackerman angle until the speed of the vehicle is less than the characteristic speed.

$$\delta = \frac{2l}{R} \tag{4.30}$$

and characteristic speed can be written as:

$$V_{char} = \sqrt{\frac{l}{k_{us}}} \tag{4.31}$$

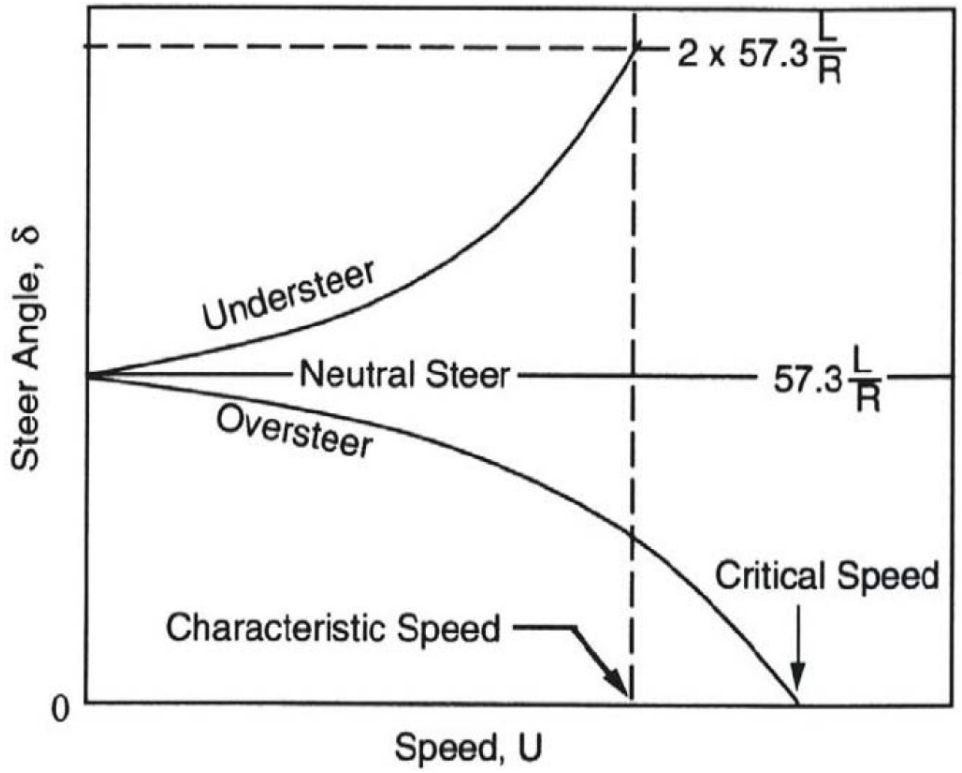

Figure 4.11: The effect of speed on the steering angle [65]

One can realize that the steering angle decreases with the square of the speed and becomes zero at critical speed in the case of oversteering. This means that the vehicle is going to be unstable and it is hard to control. It is also noteworthy to mention that lateral load transfer,

split-μ situations, and low friction coefficient toad significantly affect the understeer gradient which this leads to decrease the stability of the vehicle.

4.2.3 Vehicle behavior at the handling limit

Lateral tire forces, which are generated by the interaction of road and tire, dominate lateral vehicle dynamics. At low lateral accelerations, the relation of vehicle response and driver steer is linear because the behavior of tire is linear in this region. By increasing lateral acceleration, the behavior of tire is going to be highly nonlinear especially close to the handling limit. Therefore, the lateral vehicle dynamics demonstrates unexpected behavior in response to driver steer inputs because of inherent saturation characteristic of the lateral force in terms of tire sideslip angle. Two cases can happen during the handling limit [76]:
1. If the lateral tire forces of the rear axle pass the saturation point before those of the front axle, the further increase in sideslip motion and then in tire slip angle will increase front tire forces and decrease in rear tire forces. The resulting yaw moment will, therefore, accelerate the yaw motion and lead to vehicle instability and spin. 2. If the lateral forces of front tires exceed the saturation point before the lateral forces of rear tires, the opposite status will happen and yaw moment which is generated by lateral forces to balance between the front and rear axles will counteract the yaw motion. In other words, the vehicle is going to understeer condition. In other words, the driver is not able to control the direction of the vehicle through the turning the steering wheel due to the insufficiency of tires lateral forces which leads to decrease the authority of front axle in controlling the directional behavior of the vehicle.

4.2.4 Lateral vehicle dynamics regimes

As discussed in Chapter 2, each subsystem has its fundamental function and effective region over the entire range of vehicle handling regimes. Consequently, three distinct areas corresponding to the level of lateral acceleration of the vehicle can be described for formulating the control tasks for standalone and integrated control systems.

Low the range of lateral acceleration is from 0 to 0.3g which depicts normal cornering

Mid the range of lateral acceleration is from 0.3g to 0.6g which demonstrates moderate to vigorous cornering

High the range of lateral acceleration is from 0.6 to limit, which shows severe cornering approaching handling limit

The first region described as low lateral acceleration region is distinguished by low vehicle sideslip angle and the different phase of lateral acceleration and yaw rate is small. The moderate cornering region occurs with rapid driver steer inputs which leads to increase vehicle sideslip angle and lateral acceleration. Large and rapid steering inputs and a quick transition from throttle to brake lead to severe cornering (High range of lateral acceleration region).

Basically, low lateral acceleration region can be categorized as the linear regime, while the mid and high can be classified as nonlinear handling regime. It is noteworthy to point out that the selection of boundaries between regions is flexible and it can be affected by conditions of road surface (μ) [44].

4.2.5 Control targets

In order to design controller, the first step is to clearly define the control objectives for individual control algorithms. In this thesis, the control objectives are relevant to various aspects of the vehicle handling behavior to be enhanced. After analyzing lateral vehicle dynamics, three aspects are identified as:

- Safety
- Performance
- Comfort

Safety

The stability of the vehicle can be in danger when the vehicle is close to handling limit. Consequently, the vehicle should be stabilized at all conditions in terms of active safety point of view. Therefore, the task of the controller is to keep vehicle stability under the wide range of driving situations, especially in critical situations.

Performance

The performance of the vehicle depends on several factors such as lateral acceleration, understeer gradient, and yaw rate. Increasing the performance of the vehicle means:

- Having higher lateral acceleration

- Decreasing the $k_u s$ as much as possible and the ideal one is becoming zero or negative
- Extending the linear region of understeer coefficient as far as possible
- The higher limits of handling with more lateral acceleration in order to increase response time and change trajectory

Comfort

In this thesis, the third control target is the reduction of the roll angle of the vehicle body during cornering maneuvers. This target improves the comfort feeling transmitted by the vehicle to the passengers. In addition, it decreases the variation of the characteristic angles, particularly camber angle, between the tires and the road plane during vehicle turning.

4.3 Summary

This chapter discussed the development of various vehicle dynamics models. It began by describing the development of tire model for simulation purposes. Then a detailed discussion about the development of basic theory of vehicle dynamics followed by various vehicle dynamics models with increasing complexity has been conducted. On the other hand, description of lateral vehicle dynamics has been introduced. This section included steady state and transient vehicle handling behavior, definition of oversteer and understeer conditions, lateral vehicle dynamics regime and control objectives.

Chapter 5

Design of Dynamic Stability Subsystem Controllers

5.1 Introduction

Nowadays, car manufacturers develop automotive as a combination of passive systems. Operation of these vehicles under various situations such as dry and smooth roads at moderate speeds is acceptable. Dynamic behaviors to driver inputs are predictable in these conditions such as steering, acceleration, and braking. As mentioned in **??**, this part of a region of driving is named as the linear operating or driving region. When the vehicle is in the linear region driver takes pleasure of driving. However, the dynamic behavior of the vehicle to the driver's input is less under severe situations such as slippery, uneven road or at high speeds or in harsh maneuvers. The name of this region of driving is nonlinear driving region. Driver, occupants, and pedestrian are in danger as long as the vehicle is inside the nonlinear region. For tackling the drawbacks of a passive vehicle, the active chassis system is introduced in order to increase predictability of behavior of dynamic under severe conditions [58]. Also, active chassis control systems are able to enhance the comfort and response of vehicle in various maneuvers.
Therefore, for tackling the problems of the passive vehicle, various active chassis control systems are developed to improve the different aspect of vehicle handling which is listed below:

- Normal load control by active suspension
- Active aerodynamics control
- Active four-wheel steering
- Hydraulically interconnected suspension

- Active Anti-roll bar system
- Electronic stability control
- Torque vectoring control

All active control systems were modeled and tested numerically. The vehicle model used for numerical simulation was developed in Matlab/Simulink environment. A 14 DoF model derived from the commercial software VI-CarRealTime was imported in Simulink and interfaced with models for the actuators and the control logic. The parameters of the vehicle are reported in Table 5.1. The performance of the controlled vehicle was eventually evaluated and compared to that of the passive one in a series of open-loop handling maneuvers.

Models of active control subsystems are in some cases simplified with respect to the state of art of such systems implemented on board. The goal of the modeling is to provide a reasonable estimate of control's response and its effect on vehicle's dynamics. In this way, it will be possible to enable the performance of each controller alone and to develop a logic for their interaction.

5.2 Normal load control by active suspension

5.2.1 Introduction

Most of the research papers on active suspension are focused on controlling body movement, (heave, pitch, and roll) for improving comfort or increasing road holding. However, it is suggested to enhance vehicle's stability by controlling the body acceleration through active suspension; In particular, vertical and pitch accelerations are generated by the suspension system so that the resulting inertial forces can alter the normal load's distribution. The idea of control logic is to exploit active suspensions to produce a longitudinal load transfer (the front to the rear axle or vice versa) in order to stabilize the vehicle during fast transients. Longitudinal load transfer is a simple technique used by the experienced driver for controlling oversteer or understeer: deceleration caused by braking increases normal loads on front wheels thus reducing understeer. Oversteer can be controlled with a moderate acceleration causing the normal load on the rear axle to increase.
In ordinary driving, longitudinal load transfer is a consequence of the longitudinal acceleration of the vehicle. Active suspensions can generate a system of internal forces inside the vehicle in order to control the heave, pitch and roll motion of chassis. In principle, a longitudinal

Table 5.1: Vehicle model in Simulink environment

Vehilce parameters	Values
m (vehicle mass)	1302 kg
m_s (sprung mass)	1148 kg/rad
l (wheelbase)	2.920 m
l_f (didstance of CoG to front axle)	1.56 m
l_r (distance of CoG to rear axle)	1.35 m
t_f (front track width)	1.76 m
t_r (rear track width)	1.74 m
h_{CoG} (height of CoG)	0.41 m
steering gear ratio	22.29
C_{α_f} (cornering stiffness for front)	75,784 N/rad
C_{α_r} (cornering stiffness for rear)	84,160 N/rad
I_{xx} (moment of inertia about x-axis)	kgm^2
I_{yy} (moment of inertia about y-axis)	722.902 kgm^2
I_{yy} (moment of inertia about y-axis)	kgm^2

load transfer can be obtained with a proper combination of vertical and pitch accelerations produced through active suspensions. The stroke of actuators used in active suspensions is usually in the order of ±0.1 m. As a consequence, this kind of control can be utilized only for small periods of time, resulting in suitable for an emergency control during fast transients.

5.2.2 Active longitudinal load transfer control

Effect of longitudinal load transfer on understeer coefficient

Experienced drivers use longitudinal load transfer to alter the response of the vehicle in terms of oversteer or understeer. The normal load has a direct influence on tires cornering stiffness; therefore, longitudinal load transfer produced by deceleration can increase the cornering stiffness of front axle while reducing the cornering stiffness of the rear axle. The opposite effect can be obtained by accelerating the vehicle. To quantify the effect of longitudinal load transfer in affecting the vehicle response, it is possible to evaluate the understeer coefficient for the vehicle used in numerical simulations.
The following analysis does not aim at evaluating the vehicle's response to critical conditions; its goal is just to provide an idea of the potential of longitudinal load transfer in affecting understeer/oversteer behavior. The understeer coefficient k_{us} can be defined as [208].

$$k_{us} = \frac{W_f}{C_{\alpha_f}} - \frac{W_r}{C_{\alpha_r}} \tag{5.1}$$

where W_f and W_r represent the static load on individual front and rear tires, respectively, and C_{α_f} and C_{α_r} are the cornering stiffness of front and rear axle. Tire–road contact forces in the vehicle model used in the numerical analysis are described in section 4.1.3. According to equation 5.1 dependence of cornering stiffness on normal load is non-linear and can be estimated according to MF-tire model as follows:

$$C_\alpha = P_{Ky1} F_{z_0} sin(2arctan(\frac{F_z}{P_{Ky2} F_{z_0} \lambda_{F_{z_0}}}))\lambda_{F_{z_0}} \lambda_{K_y}(1 - P_{Ky3}|\gamma|) \tag{5.2}$$

In equation 5.2, F_z is the normal load acting on the tire, F_{z_0} a reference normal load and γ the camber angle; the other parameters P_{Ky1}, P_{Ky2} and P_{Ky3} are experimentally identified. $\lambda_{F_{z_0}}$, λ_{Ky} are scaling factors. Values used in the vehicle model are listed in Table 5.2.

Table 5.2: Coefficients used in MF-tire model

Mf-tire coefficients	Values
P_{Ky1} (parameter of MF-tire)	12.96 1/rad
P_{Ky2} (parameter of MF-tire)	1.712 1/rad
P_{Ky3} (parameter of MF-tire)	0.1217 1/rad
$\lambda_{F_{z_0}}$ (scaling factor of MF-tire)	1
λ_{K_y} (scaling factor of MF-tire)	1
F_{z_0} (reference normal load)	4120 N

The static loads on the front and rear axle for the vehicle used in this thesis are close to 6000 N and 6900 N, respectively; the weight distribution is thus 46-54. A longitudinal acceleration of 3 m/s^2 can produce a longitudinal load transfer of 550 N from front to rear axle. This means that a moderate acceleration can change the normal load on tires by 8-9%. Using formulation 5.2, the understeer coefficient of the vehicle was computed considering the effect of longitudinal accelerations between -3 and 3 m/s2. Figure 5.1 reports the value of k_{us} for longitudinal load transfers ΔN_x between -550 and 550 N. As can be observed, when no load transfer is generated, the vehicle presents an understeer coefficient close to -0.002 rad, associated with a moderate oversteer response. It is noticeable how negative load transfers (corresponding to deceleration) significantly emphasize this behavior. On the other side, positive load transfers can even turn the vehicle into an understeering one. Globally, a longitudinal load transfer below 10% the static load can change k_{us} by $8.4e^{-3}$ rad/kN.

To get a better idea of the significance of the result, it is interesting to evaluate the effect of a common device used to alter the vehicle's response again based on normal load distribution. Lateral load transfer while cornering distributes over the front and rear axle according to the roll stiffness ratio η, usually tuned with anti-roll bars. Owing to a non-linear effect of normal load on tire cornering stiffness, a load transfer from inner to outer tire decreases the cornering stiffness of an axle. Proper settings of anti-roll bars thus modify the oversteer/understeer tendency of a vehicle. Figure 5.2 shows the effect of lateral load transfer

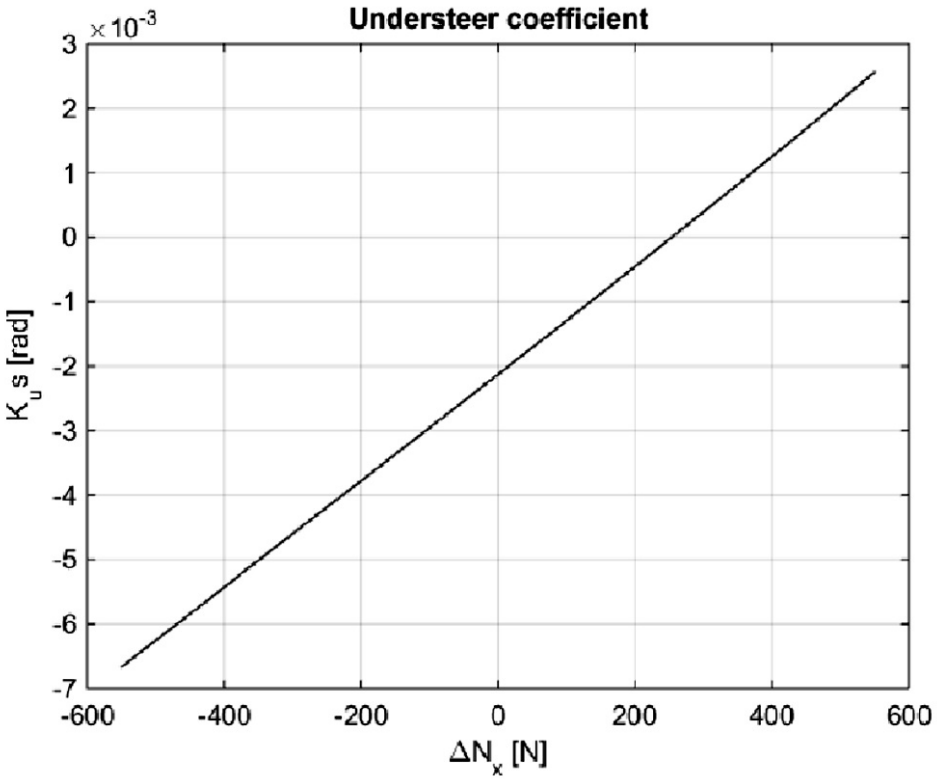

Figure 5.1: Understeer coefficient VS longitudinal load transfer

Δ_{N_y} on k_{us} for different values of η; maximum values for Δ_{N_y} are obtained with a lateral acceleration of 3 m/s^2 . When the load transfer is directed toward the rear axle, oversteer response is enhanced while the opposite effect can be obtained with values of η higher than 0.5. It is noteworthy that, for load transfers close to 15% the static normal load, the effect on k_{us} is at most $1.7e^{-3}$ rad/kN. Longitudinal load transfer is thus a powerful mean for changing vehicle's response due to direct increase/decrease of total normal load on an axle. Lateral load transfer relies instead on a non-linear effect of load transfer between the wheels of the same axle, thus resulting in a more limited effect.

Considering the effectiveness of longitudinal load transfer in affecting vehicle's behavior, this research explores the idea of controlling it by active suspensions. A vehicle with active suspensions is generally equipped with four actuators at the four corners, allowing the control of the relative motion between car-body and unsuspended masses. Actuators can only generate a system of internal forces; therefore, the only way to influence normal load distribution through active suspensions is to control the accelerations of the car-body. This control strategy

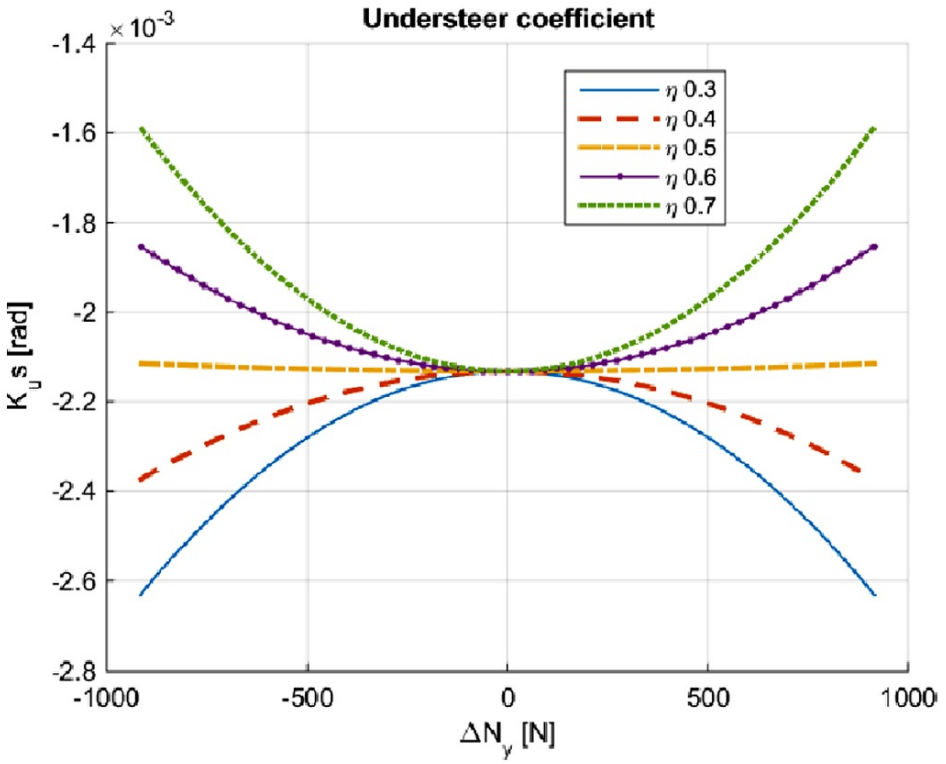

Figure 5.2: Understeer coefficient VS lateral load transfer for different roll stiffness ratios

can inevitably have an impact on riding comfort; however, considering that this system should activate only in an emergency condition to recover vehicle's stability and directionality, this can be regarded as a drawback of minor relevance. The following simple model shows how load transfer can be obtained by generating a suitable combination of heave and pitch acceleration.

Referring to Figure 4.7 in section 4.1.4, the total normal loads on front and rear axles can be determined as:

$$\begin{aligned} F_f &= F_{s_f} + \Delta_{N_{f_{ref}}} = \frac{m_s g l_r}{l} + \frac{m_s \ddot{z} l_r}{l} - \frac{m_s a_x h_{CoG}}{l} - \frac{I_{yy}\ddot{\theta}}{l} \\ F_r &= F_{s_r} + \Delta_{N_{r_{ref}}} = \frac{m_s g l_f}{l} + \frac{m_s \ddot{z} l_f}{l} + \frac{m_s a_x h_{CoG}}{l} + \frac{I_{yy}\ddot{\theta}}{l} \end{aligned} \tag{5.3}$$

In equation 5.3, F_{s_f} and F_{s_r} represent the static load acting on front and rear axle, respectively; $\Delta_{N_{f_{ref}}}$ and $\Delta_{N_{r_{ref}}}$ are instead the load transfers caused by longitudinal, vertical and pitch acceleration. Load transfers can be easily evidenced:

$$\begin{aligned}\Delta_{N_{f_{ref}}} &= \frac{m_s \ddot{z} l_r}{l} - \frac{m_s a_x h_{CoG}}{l} - \frac{I_{yy}\ddot{\theta}}{l} \\ \Delta_{N_{r_{ref}}} &= \frac{m_s \ddot{z} l_f}{l} + \frac{m_s a_x h_{CoG}}{l} + \frac{I_{yy}\ddot{\theta}}{l}\end{aligned} \tag{5.4}$$

Assuming that target values $\Delta_{N_{f_{ref}}}$ and $\Delta_{N_{r_{ref}}}$ are requested, the combination of vertical and pitch acceleration allowing to obtain them can be easily determined, solving equation 5.4 with respect to $\ddot{z}$ and $\ddot{\theta}$:

$$\begin{aligned}\ddot{z}_{ref} &= \frac{\Delta_{N_{f_{ref}}} + \Delta_{N_{r_{ref}}}}{m_s} \\ \ddot{\theta}_{ref} &= \frac{\Delta_{N_{r_{ref}}} l_r - \Delta_{N_{f_{ref}}} l_f - m_s a_x h_{CoG}}{I_{yy}}\end{aligned} \tag{5.5}$$

Under the hypothesis of a rigid body, equation 5.5 allows estimating the reference values for vertical and pitch accelerations of the chassis associated with desired values of normal loads at the contacts. It is interesting to point out that front and rear load transfers are independent variables, i.e., it is possible to control the load on front and rear axle separately. This is not allowed when the load transfer is produced by longitudinal acceleration alone.

It is clear that this control strategy can be applied only for a fraction of seconds due to the limits of the stroke of the actuators (related to the limits of relative motion between suspended and unsuspended masses). However, considering its potential effectiveness, it could result useful to maintain vehicle's stability during transient conditions. In the following, a scheme of control logic is proposed.

Proposed control logic

The general schematic of the control logic for actively control the longitudinal load transfer is shown in Figure 5.3; hereafter a description of each block is provided.

Reference setting: This block identifies the target heave and pitch accelerations ($\ddot{z}_{ref}$,$\ddot{\theta}_{ref}$) on the basis of vehicle's response. The input for this block is the difference between lateral acceleration a_y and the product, $v_x\dot{\psi}$.

For the sake of simplicity, in the following a_y and $\dot{\psi}$ are assumed positive in sign: this happens in a left-hand curve, according to the sign

convention adopted in the numerical model. The input of the control logic is in fact $|a_y| - v_x|\dot{\psi}|$ so that the turn direction is considered.

During steady-state cornering the difference $a_y - v_x\dot{\psi}$ is zero, while in transient its value may be positive or negative. Positive values indicate that the vehicle is generating lateral acceleration but the corresponding rotation along the vertical axis is too slow with respect to the regime value. In other words, yaw rate has to be increased, and this can be done by shifting the normal load from the rear to the front axle. If the term $a_y - v_x\dot{\psi}$ is negative, the vehicle is turning around a vertical axis too fast concerning the lateral acceleration; in this case yaw rate should be decreased by shifting the normal load from front to rear axle to stabilize the vehicle.

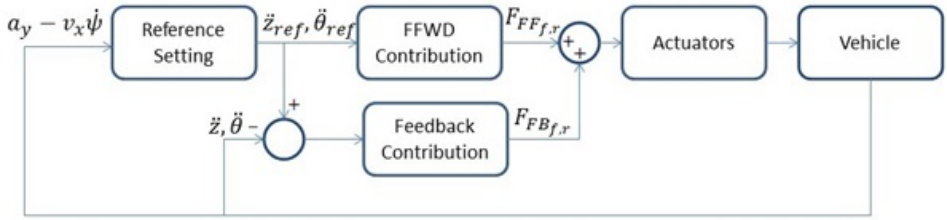

Figure 5.3: Schematic diagram of control logic

The normal load variations $\Delta_{N_{f_{ref}}}$ and $\Delta_{N_{r_{ref}}}$ are determined according to the graphs presented in Figure 5.4. Basically, variations of normal load are assumed to vary almost linearly with the term $a_y - v_x\dot{\psi}$. A dead zone is introduced to avoid control activation for small values of $a_y - v_x\dot{\psi}$. In addition, normal load variations on front and rear axle are saturated at 25% corresponding to static load. At this research stage, parameters of tables reported in Figure 5.4 were tuned empirically. Once normal load variations are identified, $\ddot{z}_{ref}$ and $\ddot{\theta}_{ref}$ are determined according to equation 5.5.

Feedforward contribution: This block provides forces of F_{FF_f} and F_{FF_r} by using $\ddot{z}_{ref}$ and $\ddot{\theta}_{ref}$. The following relations can be derived, under the hypothesis of rigid body [131]:

$$\begin{aligned} F_{FF_f} + F_{FF_r} &= m_s\ddot{z}_{ref} \\ -F_{FF_f}l_f + F_{FF_r}l_r &= I_{yy}\ddot{\theta}_{ref} \end{aligned} \tag{5.6}$$

Solving equations 5.6 leads to:

$$\begin{aligned} F_{FF_f} &= \frac{1}{l}(m_s\ddot{z}_{ref} - I_{yy}\ddot{\theta}_{ref}) \\ F_{FF_r} &= \frac{1}{l}(m_s\ddot{z}_{ref} + I_{yy}\ddot{\theta}_{ref}) \end{aligned} \tag{5.7}$$

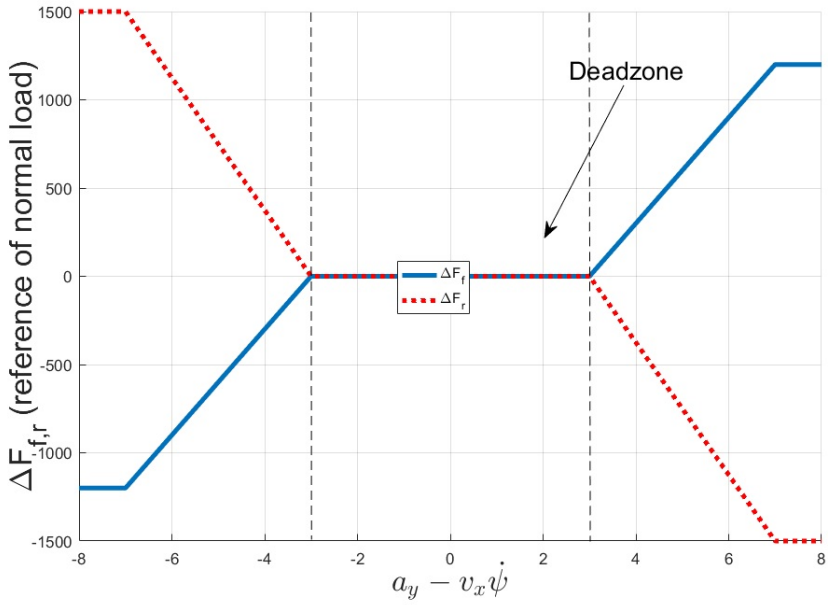

Figure 5.4: Reference of front and rear axles normal force according to lateral dynamics

Feedback contribution: The feedback block monitors the values of accelerations on the chassis and modifies output forces (F_{FB_f} and F_{FB_r}) based on the difference between reference and actual values. Corrective terms are determined according to equation 5.8

$$\begin{aligned} F_{FB_f} &= \frac{1}{l}(m_s(\ddot{z}_{ref} - \ddot{z}) - I_{yy}(\ddot{\theta}_{ref} - \ddot{\theta})) \\ F_{FB_r} &= \frac{1}{l}(m_s(\ddot{z}_{ref} - \ddot{z}) + I_{yy}(\ddot{\theta}_{ref} - \ddot{\theta})) \end{aligned} \tag{5.8}$$

5.2.3 Actuator model

Modeling of actuators is required to consider the delay introduced by their dynamics. No specific choice was made about the actuators technology: in the numerical model, they are considered as components in order to provide a force following a reference with a given bandwidth and limits on the maximum force and power absorption. The reference force is determined by the control logic passes through a second-order transfer function representing the dynamics of the actuators; a bandwidth of 20 Hz is assumed as shown in Figure 5.5. Force and power limits were set to 2 kN and 10 kW, respectively.

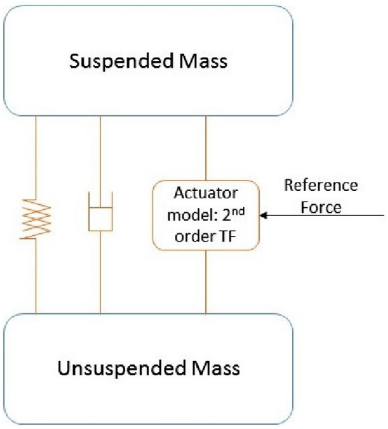

Figure 5.5: Scheme of a suspension

Maximum stroke of actuators plays a significant role in affecting the performance of the control: heave and pitch accelerations can be in fact applied only as long as relative motion between suspended and unsuspended masses is possible. So it is important to address that in setup and logic to avoid reaching the limits of suspension stroke and undesirable effects on vehicle ride height and comfort. At present research stage, no direct check on actuator position is introduced in the control logic. To prevent the actuator to reach its limits, actuators activate when $||a_y| - v_x|\dot{\psi}|| > 3$; as a consequence, forces are applied for brief moments to avoid reaching the stroke limitation. The position of actuators is controlled a posteriori to check its plausibility.

5.2.4 Numerical results

As seen from the description of the control logic, the stability of the vehicle is controlled by changing its oversteer/understeer response. Excess or lack of yaw rate is corrected through active suspensions which are employed to generate an appropriate longitudinal load transfer. The performance of the proposed control logic was tested numerically analyzing the dynamics of the vehicle model previously described when subjected to a series of open loop maneuvers. In particular, step steer and lane change were analyzed. Open loop maneuvers were intentionally used to put into evidence the vehicle's response, without any correction by a driver. Besides, selected maneuvers are quite typical in emergency situations like obstacle avoidance.
Figure 5.6 refers to a step steer maneuver performed at 100 km/h with a final steer angle of 90° (steer at wheels is up to 4°). The step steer is completed in 0.1 s and is performed on dry road (μ= 1).

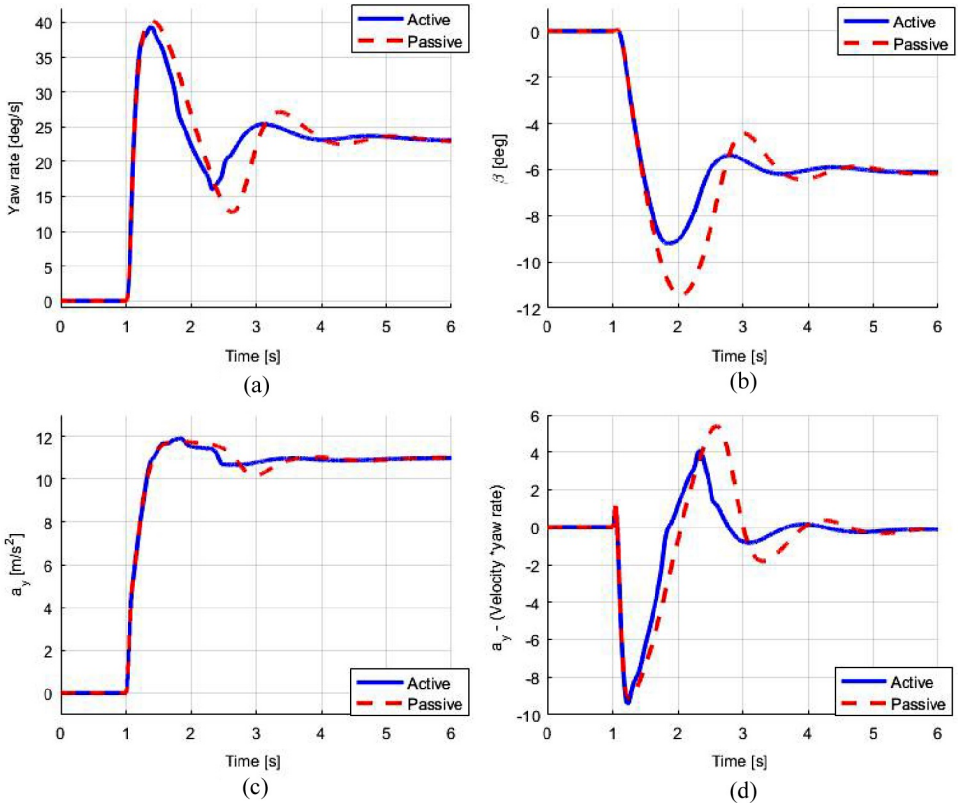

Figure 5.6: Simulation results relevant to step steer maneuver (90°) on a dry road

Figure 5.6(a) refers to the yaw rate signal and compares the passive vehicle (red dotted line) with the actively controlled one (blue line): the amplitude of the first peak at 1.3 s is similar for the two vehicles, while the following oscillations are clearly damped-out by the active control. The comparison between the signals of lateral acceleration (Figure 5.6(c)) shows that both vehicles reach the same regime condition but the controlled one displays lower overshoots. In other words, the control makes the vehicle more stable without decreasing its speed. The analysis of Figure 5.6(b) reveals that the control logic is able to reduce the peak of sideslip angle by 25% (from 12° to 9°). As last, Figure 5.6(d) shows the time history of $a_y - v_x\dot{\psi}$ for the two vehicles. Considering the red dotted line, it is possible to notice how the first phase of the maneuver (1.1–1.75 s) is characterized by an excess of yaw rate; in a second phase (2.3–2.5 s) yaw rate is instead too low compared to the level of lateral acceleration. The actively controlled vehicle displays a better behavior especially in the second part of the maneuver where the difference $a_y - v_x\dot{\psi}$ is closer to zero, indicating a condition

closer to steady state.

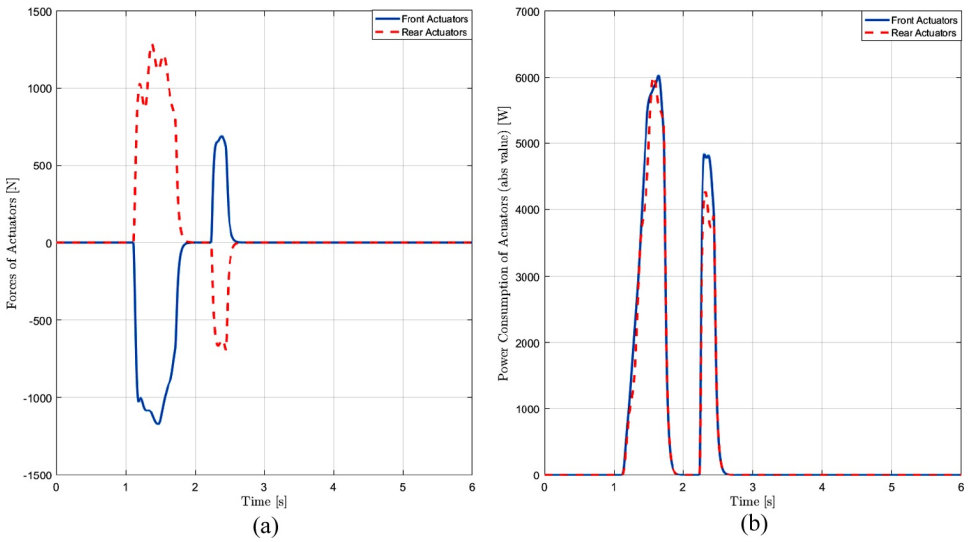

Figure 5.7: Actuator force and power corresponding to step steer maneuver

To have a better insight on control intervention, Figure 5.7 shows the time histories of forces developed by actuators and power consumption of actuators. As seen in Figure 5.7(a), the control activates in the first phase, when there is an excess of yaw rate. The controller's response increases the cornering stiffness of the rear axle while reducing the cornering stiffness of the front axle. Owing to the shortage of yaw rate in the second phase, the controller increases the normal force on the front axle and vice versa on the rear axle. The vehicle's response is moved towards a regime condition after controller actions. Figure 5.7(b) is relevant to the power consumption of each actuator in this maneuver.

Results shown in Figure 5.8, are referred to the same maneuver this time performed on a wet road ($\mu = 0.7$). Time histories on yaw rate and lateral accelerations (Figure 5.8(a) and (c)), show that the vehicle response becomes less stable with a slippery road; again the control is able to reduce overshoots, especially in yaw rate. Figure 5.8(b) is relevant to the sideslip angle of the vehicle and compares passive vehicle (red dotted line) with actively controlled one (blue line): the active one can effectively reduce the peak of sideslip angle by 15% (from 13° to 11°) in comparison with passive one. The first control intervention (1.1–1.75 s) is similar to what observed in Figure 8: as the vehicle develops an excess of yaw rate, the controller increases the cornering stiffness of rear axle while reducing the one on the front axle. The vehicle displays then an excess of lateral acceleration in the second

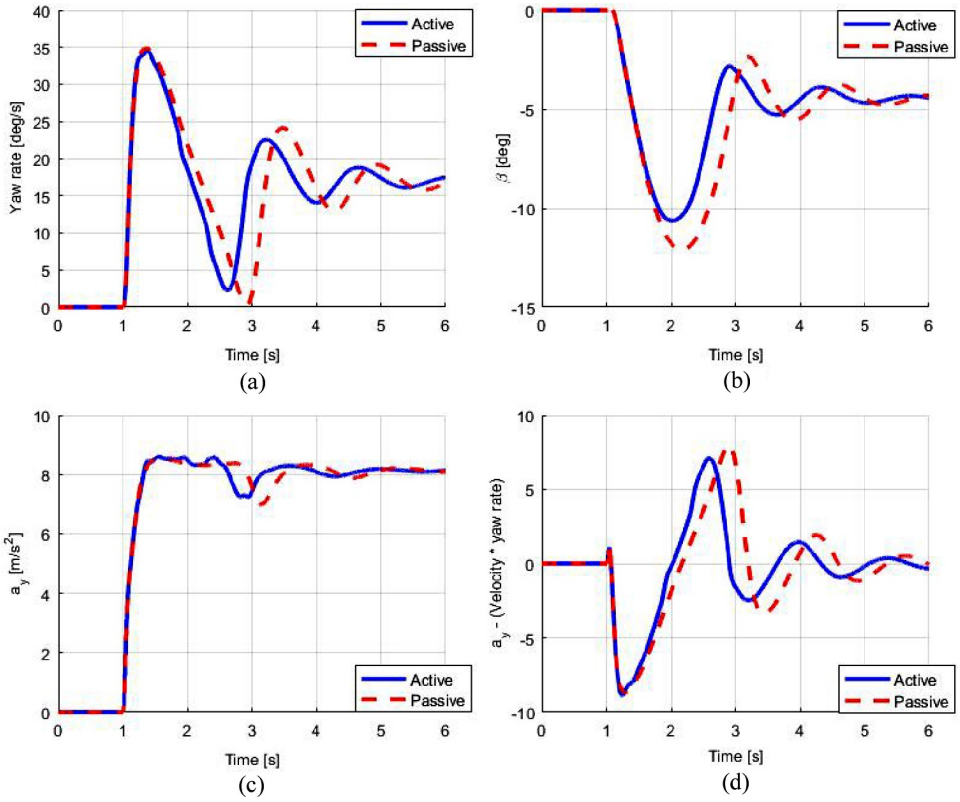

Figure 5.8: Simulation results relevant to step steer maneuver (90°) on a wet road

phase (2.3–2.7 s) and the controller activates to reduce the load on the rear axle and increase the load on the front one. This second phase lasts a little bit longer when the maneuver is performed on the wet road.

Lane change represents an emergency maneuver that a driver performs when trying to avoid an obstacle and recover the running direction. The open-loop test allows analyzing the response of the vehicle to the same driver's input when normal load control is active or not. Figure 5.9 refers to simulation results related to a lane change maneuver performed at 150 km/h with a final steer angle of 45° (corresponding to a tire rotation of about 2°). Figure 5.9(a) refers to the yaw rate: the first peak of the yaw rate is slightly smaller for the controlled vehicle; this small difference actually allows the vehicle to better follow the steering input. The actively controlled vehicle clearly anticipates the response of the passive one which takes too long to change the sign of yaw rate and recover the original running direction. As shown in Figure 5.9(c), the trajectories of the two vehicles are dramatically dif-

ferent: the actively controlled vehicle completes the lane change, while the passive one is less prompt and exits the maneuver with a totally wrong angle. This means that it would be much easier for a driver to complete this maneuver with the actively controlled vehicle.

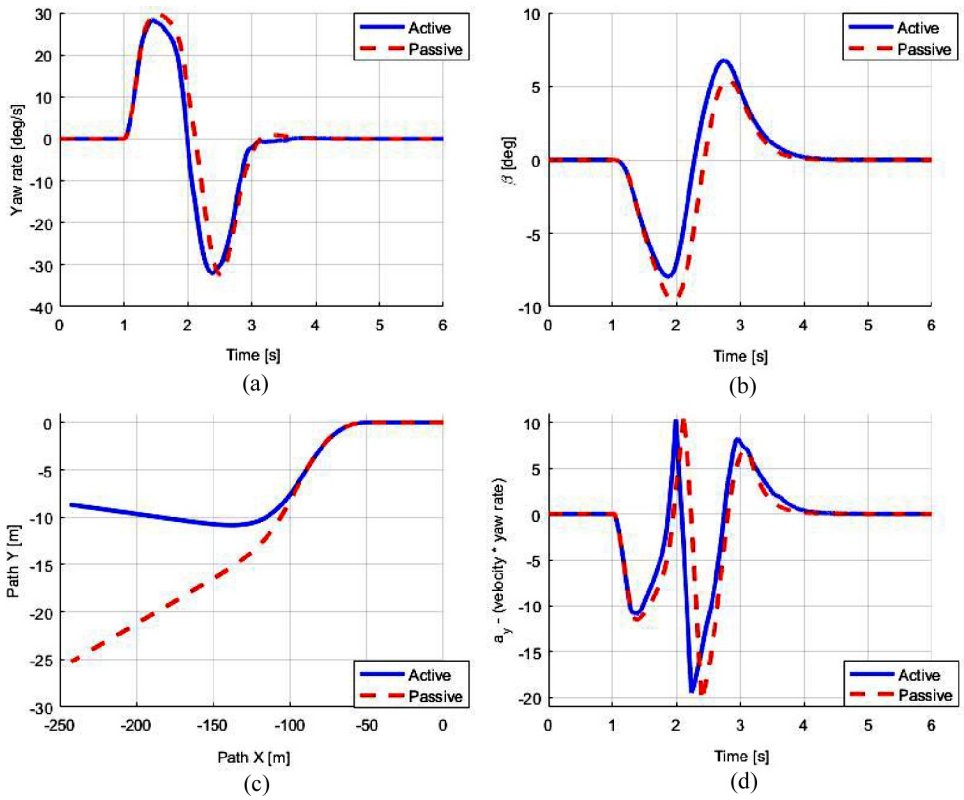

Figure 5.9: Simulation results relevant to lane change manoeuvre (45°) on a dry road

5.3 Active aerodynamics control

5.3.1 Introduction

This section investigates the effect of actively controlled spoilers on the normal load distribution on the front and rear axle in order to stabilize the vehicle under severe maneuvers. The control logic is tested using a non-linear numerical model of a vehicle equipped with two spoilers approximately located above front and rear axles. The spoilers are controlled independently to change the angle of attack of spoilers so that they can produce downforce or lift-force to alter the normal load distribution between front and rear axles. So the control logic is able to

change the vehicle's response regarding oversteer or understeer. Therefore, this section is dealt with altering normal load distribution by using front and rear spoilers to generate down and lift forces in a way that vehicle can overcome oversteer and understeer tendency in cornering maneuvers at high speeds. A precise model of the actuating system is included so that delays bandwidth and motor specifications of actuators are considered. Numerical simulations have been carried out considering step steer, lane change, fishhook and step steer maneuvers and comparing the response of passive and active vehicles. Robustness of the control to changing of friction coefficients was also verified numerically.

5.3.2 Control logic of active aerodynamics

As stated in the introduction, the aim of proposed active control in this thesis is to change the angle of attack of the front and rear spoilers so that the desired distribution of normal load is obtained. In particular, the control logic tries to regulate the normal load on front and rear axle to avoid excessive oversteer or understeer response, especially during transients. The controller consists of two layers, where the upper layer monitors the vehicle condition (understeering/oversteering), while the lower layer calculates the angle of spoiler and controls the actuators with respect to vehicle condition. As shown in Figure 5.10, the control process can be divided into three phases:

1. In the first one, a look-up table is used to determine the desired normal load distribution according to current vehicle dynamics;
2. In the second phase, look-up tables are utilized again to determine the angles of attack of front and rear spoilers so that that target normal loads can be obtained;
3. As for last an actuation system is used to effectively move the spoilers.

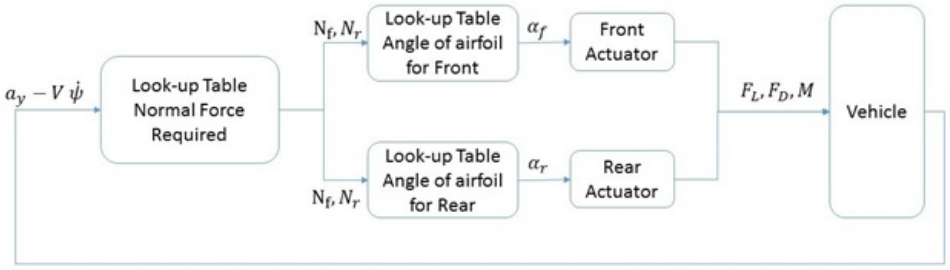

Figure 5.10: Schematic of the control strategy

5.3.3 Reference of normal loads for front and rear axles

Active aerodynamics offers the opportunity of increasing total normal load on the tires without increasing the vehicle's weight [15]. This clearly improves the road holding and the maximum lateral acceleration [164]. In parallel, active aerodynamics allows the continuous regulation of balance, i.e., normal load distribution between front and rear axle. This effect has an obvious impact on understeer/oversteer behavior since increasing the normal load on one axle has a direct influence over its cornering stiffness. The simple 2D model of Figure 5.11 shows how forces and moments produced by the spoilers allow controlling the distribution of normal loads between front and rear axle [32].
where
F_{D_i}=drag force of front and rear spoiler
F_{L_i}=lift/down force of front and rear spoiler
M_i=torque of front and rear spoiler
h_f=height of front spoiler (0.6 m)
h_r=height of rear spoiler (0.8 m)
d=longitudinal distance of front spoiler to CoG (1.86 m)
e=longitudinal distance of front spoiler to CoG (1.65 m)

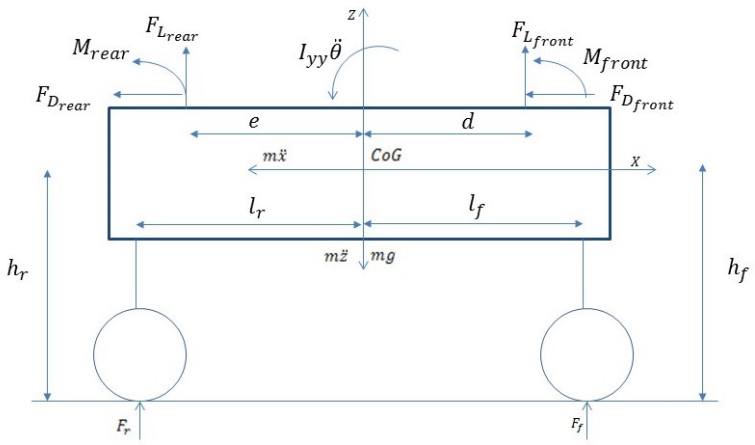

Figure 5.11: 2D schematic of the vehicle model

Considering the schematic of Figure 5.11 and using equation 5.3, normal force of front and rear axle can be obtained as follows:

$$\begin{aligned} N_f &= -\frac{F_{D_f} + F_{D_r} + M_f + M_r + F_{L_f}(l_f - d) + F_{L_r}(l_r + e)}{l} \\ N_r &= -\frac{F_{D_f} + F_{D_r} + M_f + M_r - F_{L_f}(l_f - d) - F_{L_r}(l_r + e)}{l} \end{aligned} \tag{5.9}$$

Controlling the angle of attack of the front and rear spoilers changes the values of front and rear aerodynamic forces and moments in order to control normal load distribution. Since aerodynamic forces can change the total value of vertical force on axles, normal loads on the front and rear axle can be controlled independently. The first step of control logic consists in determining the desired values of load transfers. A simple approach is used which is explained in the previous section, based on the index I_{lat}:

$$I_{lat} = a_y - v_x\dot{\psi} \tag{5.10}$$

The goal of proposed control logic is to keep I_{lat}, as low as possible in order to have a predictable behavior of the vehicle. In addition, this control implicitly supports the driver's command: when the driver set a steering angle while traveling at a speed v_x, the control logic helps the vehicle to reach a steady state condition and compensate excessive or insufficient yaw rate. Based on the index of I_{lat}, the control logic tries to alter the front-rear normal load distribution according to the relations reported in Figure 5.12 which was tuned with a series of numerical simulations to understand required forces by the vehicle in different speeds in order to stabilize the vehicle. The numbers of simulation have been done to develop the table according to required forces with respect to I_{lat} to stabilize the vehicle.

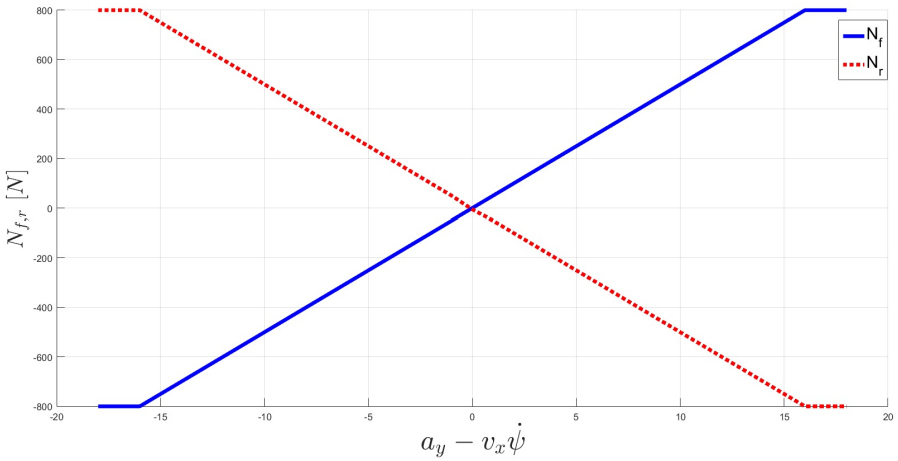

Figure 5.12: load transfer as function of I_{lat}, for front and rear axles

5.3.4 Reference of angle of attack for front and rear spoilers

Once the reference load transfers are determined, the angles of attack of the front and rear spoilers have to be set, so that combination of

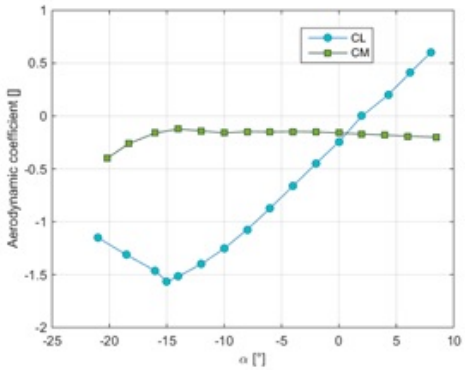

Figure 5.13: Lift-force and moment coefficient of spoiler

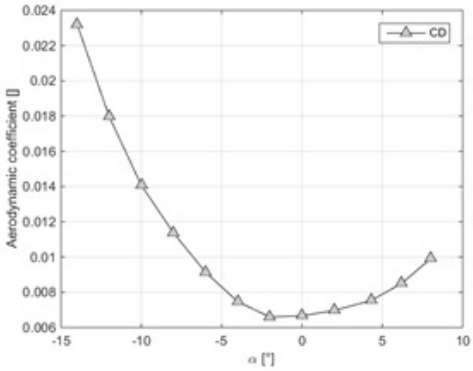

Figure 5.14: Drag coefficient of spoiler

drag force, lift force and aerodynamic moment allows obtaining the desired load transfer. A convenient way for describing the aerodynamic characteristics of a spoiler is to plot the values of the coefficients against the angle of attack, which is the angle between the plane of the wing and the direction of (relative) wind. For this work the aerofoil reported in [1] was considered. The aerodynamic coefficients of the aerofoil used for numerical simulations are reported in Figures 5.13 and 5.14 where they are plotted as the function of the angle of attack.

A cambered profile is chosen so that a downforce is developed when the angle of attack is zero. Main dimensions of front and rear spoilers applied on the car are reported in Table 5.3.

Table 5.3: Main dimensions of adopted spoilers

spoiler dimension	value
Cord length	0.2 m
Cord width	1.3 m
Cord area	0.26 m^2

The identification of the angles of attack required to obtain the desired normal loads is performed through look-up tables defined according the process described in the following. A number of numerical simulations was carried out considering the vehicle running on straight track at 100, 150, 200 and 250 km/h. For each speed, different com-

binations of the angle of attack of front and rear spoilers (respectively α_f and α_r) were considered: in particular, each angle of attack was changed in the range 8° to -15° with a resolution of 1°. The relations N_f (α_f, α_r, v_x) and N_r (α_f, α_r, v_x) were thus identified: Figures reports these functions for a speed of 150 km/h.

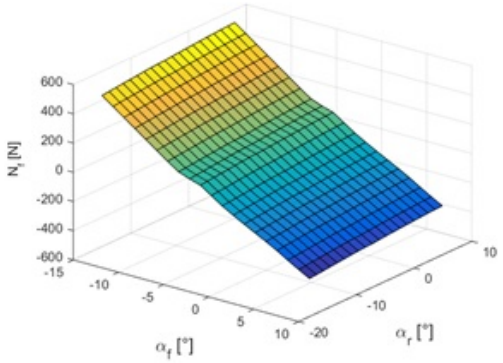

Figure 5.15: Aerodynamic loads on front as function of the angles of attack at 150 km/h

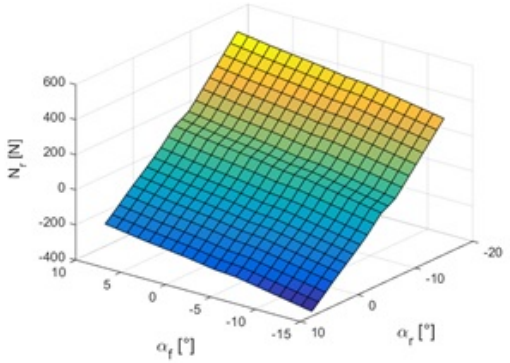

Figure 5.16: Aerodynamic loads on rear as function of the angles of attack at 150 km/h

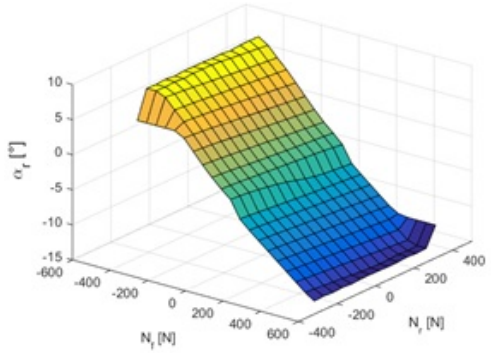

Figure 5.17: Angle of attack for front spoiler required to obtained a desired load transfer on rear axle (V=150 km/h)

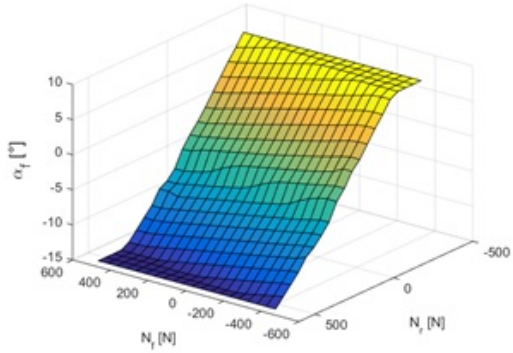

Figure 5.18: Angle of attack for rear spoiler required to obtained a desired load transfer on rear axle (V=150 km/h)

It is possible to determine the relations N_f (α_f, α_r, v_x) and N_r (α_f, α_r, v_x) by using the same simulations data in order to identify the angles of attacks required to generate desired load transfers (Figures 5.17 and 5.18). A look-up table approach is used to determine the values of angles of attack for given speed and the combination of front and

rear load transfers. In this approach, aerodynamic forces and moments are computed according to a quasi-static theory neglecting the effect of car-body motion on the angle of attack. Also, the response of the rear spoiler is assumed not influenced by the wake of the front one.

5.3.5 Spoilers actuation

The active aerodynamic system consists of two separate actuators, which rotate the spoilers and adjust the desired angle of attack. The controllers of these actuators are the lower layer of the controller system. The actuator of the system is an electric linear actuator which is controlled by using a PID controller. Parameters of the motor are derived from a commercial electric motor to ensure to have a bandwidth of 5 Hz when a vehicle travels at 200 km/h. This bandwidth is adequate for controlling vehicle handling. All parameters, bandwidth, and delay are considered in developing the actuator. Specifications of the actuator are reported in Table 5.4.

Table 5.4: Specifications of actuator

Actuator specification	value
maximum current	100 A
maximum torque	5 Nm
maximum angular velocity	100 rad/s
electrical resistance	0.0046 Ω
electrical inductance	0.00001 H
moment of inertia	$8.9621 \times 10^{(-7)}\ kgm^2$
transmission ratio	0.15
transmission efficiency	0.9

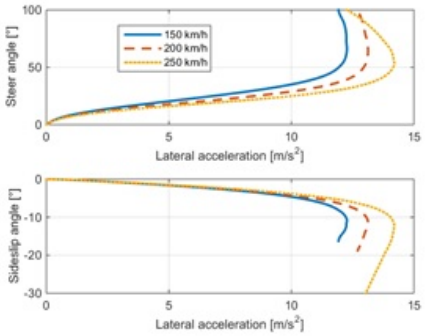

Figure 5.19: Simulation results of step steer maneuver for various velocities on dry road - passive vehicle

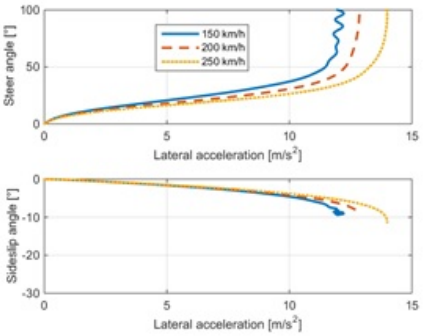

Figure 5.20: Simulation results of step steer maneuver for various velocities on dry road - actively controlled vehicle

5.3.6 Numerical analysis

In this section, the performance of the active aerodynamic system is evaluated by using the results of computer simulations. In particular, the analysis is carried out considering a series of open loop maneuvers; in this way, the response of the vehicle itself (i.e., without driver's intervention) can be assessed. First results presented are related to slow ramp steer up to 100° (steer at wheels is up to 4.5°) maneuvers to analyze the steady state response of the vehicle. In particular, the vehicle is running on dry asphalt at 150, 200 and 250 km/h while the steering wheel reaches 100° in almost 5 s.
Figure 5.19 depicts the response of the passive vehicle in terms of steer angle VS lateral acceleration and sideslip angle VS lateral acceleration. It is interesting to point out that how an increasing speed allows reaching higher lateral accelerations due to characteristics of the controller; i.e., the spoilers develop downforce also when the angle of attack is zero. The understeer gradient in the linear zone decreases with increasing speed. However, when considering the lateral acceleration developed as the function of steer angle, its value decreases after reaching the maximum. This is particularly evident at 250 km/h. In addition, the absolute value of sideslip angle of the vehicle significantly increases for lateral accelerations higher than 12 m/s2.

The controlled vehicle responds to the same input as shown in Figure 5.20. Increasing speed always leads to higher lateral accelerations around the same values obtained with the passive vehicle. For 200 km/h and 250 km/h, there is a monotonic relation between lateral acceleration and steering angle; this is partially true also for the test

at 150 km/h where, due to the lower value of downforce, the control struggles to achieve the same result. The proposed control logic thus makes the vehicle more predictable and easier to control. The same indication can be drawn looking at the sideslip angle diagram: even when the acceleration is close to 14 m/s2, the sideslip angle is slightly above 11°. It is noteworthy to highlight that the control logic is trying to decrease I_{lat} which can lead to improving the vehicle's response also in quasi steady-state conditions.

The second simulation run is for the fishhook maneuver on a dry surface road to evaluate the performance of yaw stability of control logic. Figure 5.21 shows the comparison plots of the passive and active vehicle. They show that the vehicle - with the controller ON and OFF – had the same steering input (fishhook of magnitude 90 degrees) and constant speed (200 km/h). This particular steering input was chosen because the actual vehicle was found to spin out for this steering input during tests. In other words, this was a limit maneuver for the vehicle and the effect of controller intervention is clearly seen in the lateral acceleration and yaw rate response plots. The test vehicle with controller 'OFF' is seen to spin out in this maneuver. For the maneuver of the fishhook, it is observed that the peak value of sideslip angle for the control logic is significantly reduced by 95% (-180°to -9°) compared to that for passive one, as shown in Figure 5.21(b). Moreover, the peak value of the yaw rate which is shown in Figure 5.21(a) significantly decrease. Figures 5.21(d) and (e) show the time history of normal forces of the front and rear axle when the controller turns ON and OFF. Figure 5.21(c) represents the lateral acceleration behavior of the vehicle. As seen in the Figure 5.21(c), passive and active vehicle have completely different behavior because the passive one is out of control. Figure 5.21(f) shows the time history of the angle of attack for front and rear spoilers which dotted lines demonstrate the reference angle of airfoils, and solid lines represent the actual angle of attack of airfoils.

Figure 5.22 refers to a lane change maneuver performed at 200 km/h with a final steer angle of 45°(steer at wheels is 2°) on the dry road. The Figure 5.22(a) refers to the yaw rate of the vehicle and compares passive vehicle (red dotted line) with actively controlled one (blue line): the active control allows reducing the overshoots reducing the time required to reach the regime condition. The analysis of Figure 5.22(b) reveals that how the control allows reducing the peak of sideslip angle by 96% (from -180°to -6°), thus indicating a significant improvement in vehicle's stability. The Figure 5.22(c) shows the time history of a_y-$v_x\dot{\psi}$ for the two vehicles. Considering the red dotted line, it is possible to notice that how the first phase of the maneuver (1-1.9 s) is characterized

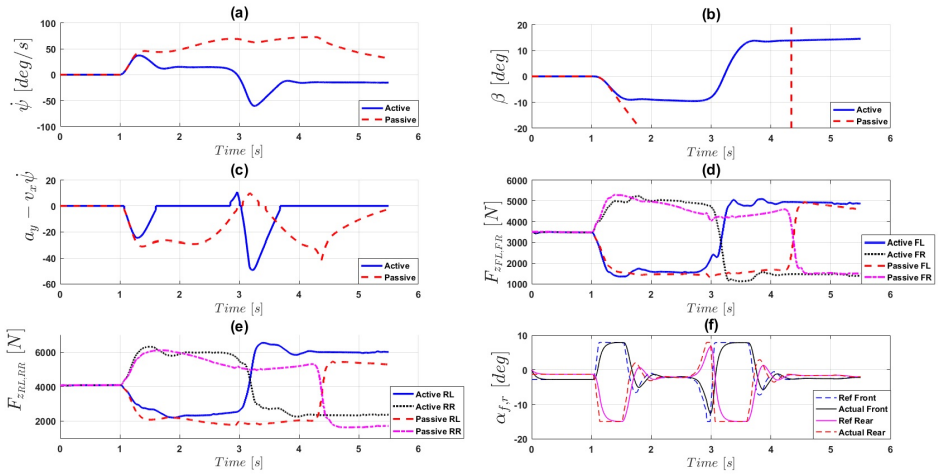

Figure 5.21: Simulation results relevant to fishhook manoeuver (90°) on dry asphalt

by an excess of yaw rate; in a second phase (1.9-2.2s), the yaw rate is too low compared to the level of lateral acceleration. The control intervention allows increasing of yaw rate unbalance in the leading to a better response also in the second phase. The controller is needed to stabilize the vehicle when the driver has to make a lane change maneuver. The controller is utilized to control the load transfer of the vehicle while lane changing. One of the most advantages of this control logic is to increase the maneuverability of the vehicle. As seen in the Figure 5.22(d), the control logic can remarkably influence tracking of the desired trajectory in severe condition in fast transient by changing longitudinal load transfer, but the passive one fails to track the desired trajectory.

The third simulation run is for the lane change maneuver on a wet surface road. The wet road is one of the toughest conditions which vehicles are facing with. The friction coefficient of road decreases suddenly under this condition. This can lead to deteriorating the dynamic capability of the vehicle. This simulation illustrates the capability of active aerodynamics system to compensate the reduction of the friction coefficient. Results of the third simulation are shown in Figure 5.23. The Figure 5.23(b) is relevant to the sideslip angle of the vehicle and compares passive vehicle (red dotted line) with actively controlled one (blue line): the active one can effectively reduce the peak value of sideslip angle by 96% (from -180° to -7°) in comparison with passive one. As seen in Figure 5.23(c), one can understand the behavior of vehicle by analyzing a_y-v_x $\dot{\psi}$. In the first phase of maneuver (1-1.6 s)

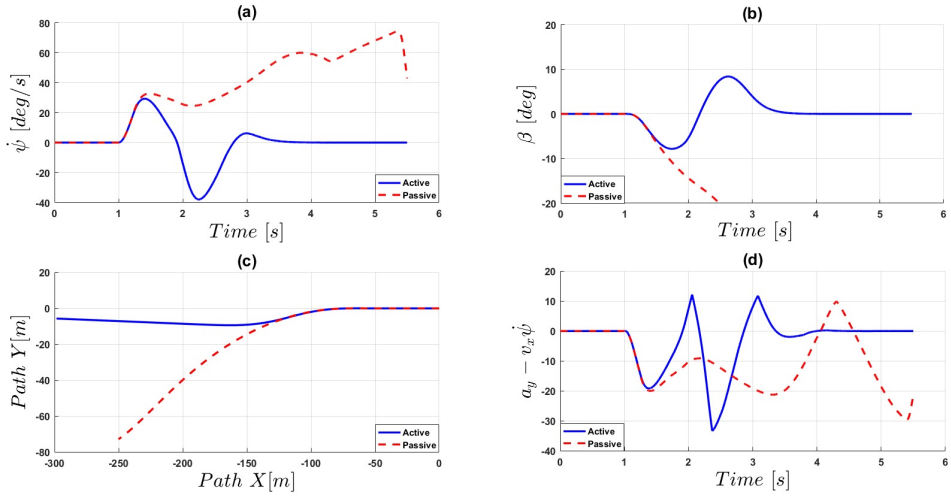

Figure 5.22: Simulation results relevant to lane change manoeuver (45°) on dry asphalt

the vehicle starts to oversteer then the controller action is to increase cornering stiffness of rear axle by increasing normal force for reducing yaw rate where the angle of front spoiler is positive (lift force), and angle of the rear spoiler is negative (downforce). In the second phase of maneuver (2-2.2 s) the vehicle undergoes understeer regime and controller increase the normal load on the front axle to raise yaw rate of the vehicle. In the third phase of maneuver (2.2-2.8 s) the vehicle starts to oversteer then the controller takes action to raise cornering stiffness of rear axle by amplifying normal force for decreasing yaw rate. The vehicle moves to the understeering regime in the fourth phase (2.8-3.9 s) then the controller activates to reduce the load on the rear axle and increase the load on front one. Due to the shortage of yaw rate in the fourth phase, the controller increases the normal force on the front axle and vice versa on the rear axle. The vehicle's response is moved towards a regime condition after controller actions. The angles of wings for front and rear are completely against each other due to aim of longitudinal load transfer ash shown in Figure 5.23(f).

The last simulation which is reported in Table 5.5 is related to step steer maneuver performed at various speeds with a final steer angle of 30°. The step steer is completed in 0.1 s and is performed on the dry road (μ= 1). Table 5.5 compares the overshoot of vehicle sideslip angle and the overshoot of yaw rate in the controlled and uncontrolled cases. When the controller is active, the vehicle significantly reduces the overshoot of sideslip angle and yaw rate compared with the un-

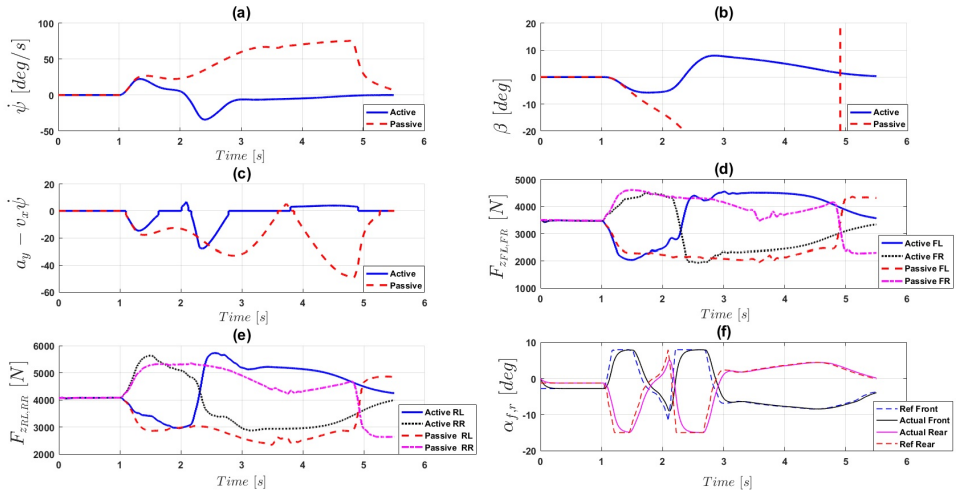

Figure 5.23: Simulation results relevant to lane change manoeuver (45°) on wet asphalt

controlled vehicle where the passive vehicle is not able to perform the maneuver at high speeds due to the instability. However, the overshoot of sideslip angle of the active vehicle in the maneuver with 150 km/h is slightly more than the maneuver with 200 km/h due to lack of sufficient speed to generate down/lift forces in order to decrease sideslip angle and stabilize the vehicle.

Table 5.5: Simulation results of step steer maneuver with final steer of 30° at various velocities

Velocity	150 km/h		200 km/h		250 km/h	
	β[°]	$\dot{\psi}$[deg/s]	β[°]	$\dot{\psi}$[deg/s]	β[°]	$\dot{\psi}$[deg/s]
Passive	9.05	21.2	—	—	—	—
AAC	5.1	18.02	5.05	19.35	5.2	20.27

5.4 Active rear steering(ARS)

5.4.1 Introduction

The design of active steering subsystem controller will be carried out in this section. The literature review in Chapter 2 shows that variety of control algorithms have been applied to different active steering systems to improve steering response of the vehicle. So for investigation of the benefits of the active steering system, ARS will be developed and examined in this section. The control target of steerability can be converted into a reference behavior where the ideal behavior of the vehicle in response to driver steer inputs represents. Therefore, the responsibility of the active subsystem controller is minimizing the deviation between reference response and actual vehicle response. Consequently, in this thesis, ARS controller is designed to track control strategy.

5.4.2 Vehicle model for ARS

As discussed in Chapter 2, the vehicle handling characteristics can be modified by actively steering the rear axle in the opposite or same direction of the front one. Figure 5.24 illustrates the same-direction case for the ARS bicycle model with the rear wheel steer angle δ_r included. By modifying the expression of the rear lateral tire force in the bicycle model which influences rear tire sideslip angle α_r, the equation of motion of ARS bicycle model can be obtained. For obtaining the equation of motion of ARS model, first we need to obtain the rear tire slip angle α_r. In a similar way to the front tire sideslip angle α_f, the rear tire slip angle α_r can be derived as follows:

$$\alpha_r = \delta_r - \frac{v_y - l_r\dot{\psi}}{v_x} \tag{5.11}$$

Thus the following equations of motion of the 4WS bicycle model can be derived:

By applying Newton's second law, the vehicle dynamic equations can be derived under consideration of lateral and yaw motions which is in the following:

$$mV(\dot{\beta} + \dot{\psi}) = F_f cos\delta_f + F_r cos\delta_r \tag{5.12}$$

Yaw motion, or moments about the vertical z-axis through the CoG:

$$I_{zz}\ddot{\psi} = F_f cos\delta_f l_f + F_r cos\delta_r l_r \tag{5.13}$$

Hence, the vehicle motion equations are expressed by

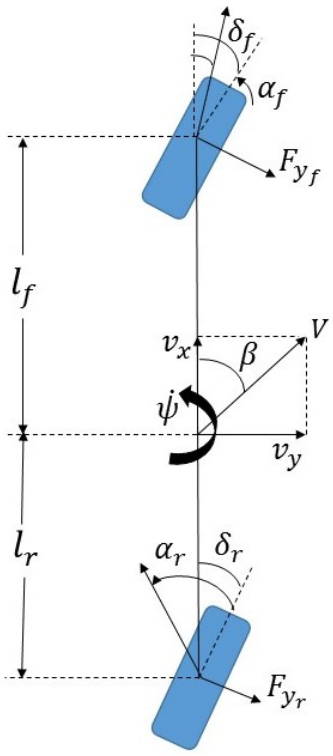

Figure 5.24: Bicycle model for ARS vehicles with kinematic quantities and forces

$$\begin{aligned} mV(\dot{\beta}+\dot{\psi}) &= \{-(C_{\alpha_f}+C_{\alpha_r})\beta - \frac{-(l_f C_{\alpha_f} - l_r C_{\alpha_r})}{V}\dot{\psi} \\ &\quad + C_{\alpha_f}\delta_f + C_{\alpha_r}\delta_r\} \\ I_{zz}\dot{\psi} &= \{-(l_f C_{\alpha_f} + l_r C_{\alpha_r})\beta - \frac{-(l_f^2 C_{\alpha_f} - l_r^2 C_{\alpha_r})}{V}\dot{\psi} \\ &\quad + l_f C_{\alpha_f}\delta_f - l_r C_{\alpha_r}\delta_r\} \end{aligned} \tag{5.14}$$

By defining the state vector x=$[\beta\ \dot{\psi}\ ]^T$, input vector u=$[\delta_f\ \delta_r\ ]^T$ and output vector y=$[\beta\ \dot{\psi}\ ]^T$, the vehicle model can be expressed in the state-space form as follows:

$$\begin{aligned} \dot{x} &= Ax + B\delta_{f,r} \\ y &= Cx \end{aligned} \tag{5.15}$$

where

$$
\begin{aligned}
A &= \begin{bmatrix} \dfrac{-(C_{\alpha_f}+C_{\alpha_r})}{mV} & \dfrac{C_{\alpha_r}l_r - C_{\alpha_f}l_f}{mV^2} - 1 \\ \dfrac{(C_{\alpha_r}l_r - C_{\alpha_f}l_f)}{I_{zz}} & \dfrac{-(C_{\alpha_f}l_f^2 + C_{\alpha_r}l_r^2)}{I_{zz}V} \end{bmatrix} \\
B &= \begin{bmatrix} \dfrac{C_{\alpha_f}}{mV} & \dfrac{C_{\alpha_r}}{mV} \\ \dfrac{C_{\alpha_f}l_f}{I_{zz}} & -\dfrac{C_{\alpha_r}l_r}{I_{zz}} \end{bmatrix} \\
C &= \begin{bmatrix} 1 & 0 \\ 0 & 1 \end{bmatrix}
\end{aligned}
\tag{5.16}
$$

where the reference of sideslip angle to zero and yaw rate reference is set to:

$$
\dot{\psi}_{ref} = \frac{v_x}{l(1 + \dfrac{k_{us}}{l}v_x^2)}\delta_f \tag{5.17}
$$

5.4.3 Linear Quadratic Regulator Control

In this section, the design of an optimal control system by is explained by a state space formulation. The desired characteristic of the planet behavior is utilized into a mathematical expression for achieving the purpose. By selecting a performance index or cost function, the system can be optimized. Minimizing cost function or performance index makes the system to give the desired response. Therefore, an optimal control system can be achieved by minimizing a performance index. By assuming that u(t) is a control input The cost function J is in the following:

$$
J = \frac{1}{2}\int_0^{\inf}(x^T Q x + u^T R u)dt \tag{5.18}
$$

where

Q=a positive semi-definite
R=a positive definite

By solving Algebraic Riccati Equation for minimizing the cost function, Q and R matrices can be derived. The parameters Q and R can be utilized in the role of design parameters in order to penalize the state variables and the control signals. The larger these values are, the more you penalize these signals. Generally, it is called expensive control strategy by choosing a large value for R for stabilizing the system with less energy. However, a cheap control strategy is the strategy when R is set to a small value which means that the purpose of a designer is not to penalize the control signal. Likewise, Setting a large value for Q implies that the stabilization of the system can be done with the minimum possible changes in the state by the controller and choosing a small value for Q represents less concern about the changes in the states. Therefore, there is a trade-off between selecting the values for Q and R. This approach is based on finding the positive definite solution of Algebraic Riccati Equation [131], given below:

$$A^T K + KA + Q - KBR^{-1}B^T K = 0 \tag{5.19}$$

and the control input to the system is:

$$u = -R^{-1}BK(t)x \tag{5.20}$$

5.4.4 Actuator model

The corrective steering command from the controller is constrained by the bandwidth of the steering actuator, which is approximated by a second-order system function H_a [129]:

$$H_a = \frac{\omega_n^2}{s^2 + 2\zeta\omega_n s + \omega_n^2} \tag{5.21}$$

where ω_n is the natural frequency and ζ is the damping ratio of the steering actuator. It was suggested that an actuator bandwidth of about 15 Hz is required to obtain acceptable performance for a vehicle, while the damping ratio is assumed as 0.7 [143]. The relation between natural frequency and bandwidth is as follows:

$$\omega_{BW} = \omega_n(\sqrt{(1 - 2\zeta^2) + \sqrt{\zeta^4 - 4\zeta^2 + 2}}) \tag{5.22}$$

5.4.5 Numerical results

In order to evaluate the stand-alone ARS controller designed above, tests of the controller will be performed on various conditions and maneuvers.

Steady-state cornering

The simulation results of steady-state cornering or ramp steering at 150 km/h while the steering wheel reaches 150° in 4 seconds under two different road surface conditions are shown in Figure 5.25. Here the steering angle is plotted as a function of lateral acceleration for both passive and controlled vehicles. Under both road surface conditions, the passive vehicle is seen to reach the handling limit at low levels of steering angle and becomes out of control.

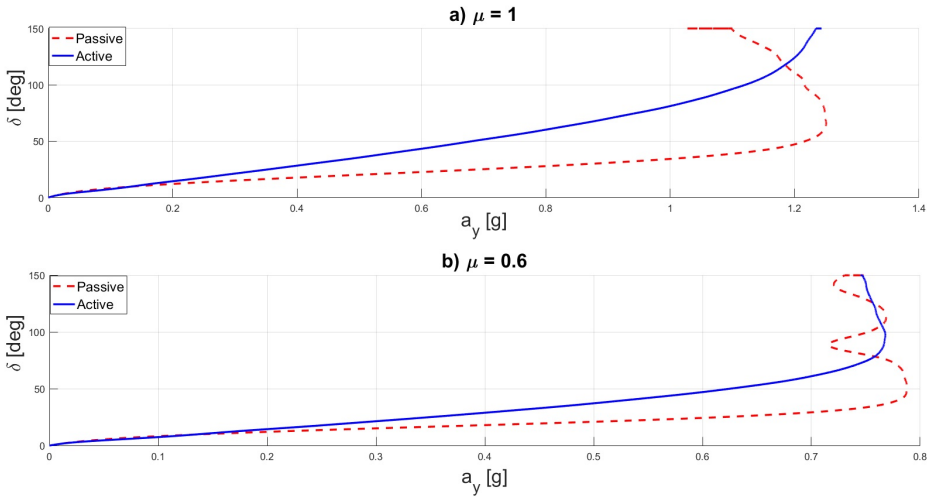

Figure 5.25: simulation results of ramp steer maneuver for two different road surface conditions; $\mu = 1$ (a), $\mu = 0.6$ (b)

As seen in Figure 5.25, the vehicle with ARS system is to be linear to much higher levels of lateral acceleration up to the handling limit. Therefore, in the wider range of handling situations, the vehicle with ARS behaves in a more predictable manner compared with passive vehicle. These kinds of behaviors are indeed expected due to the exploiting of the linear reference model which is utilized for ARS controller and most of the time behaves linearly to steering inputs of the driver. The results illustrate that the active steering extends the linear handling region of the vehicle and prevents from entering into the non-linear region. Thus, from the driver's point of view, the vehi-

cle becomes more controllable. Moreover, This specific maneuver also depicts that ARS is robust to the variations of road surface friction.

Step steer

The simulation results related to step steer maneuver are shown in Figure 5.26. The passive and the controlled vehicle are seen to show a big difference in this maneuver. Compared to the passive vehicle, one can, however, observe that the controlled vehicle has better tracking behavior and is able to track the reference of yaw rate while the passive one is completely lost the reference as demonstrated in Figure 5.26(a). Figure 5.26(b) depicts the sideslip angle of vehicle where the vehicle with ARS can significantly reduce it compared with passive one. As seen in Figure 5.26(c), the active vehicle is able to reach the regime condition while the passive one is not. Figure 5.26(d) shows the reference and actual signals of actuator for rear steering.

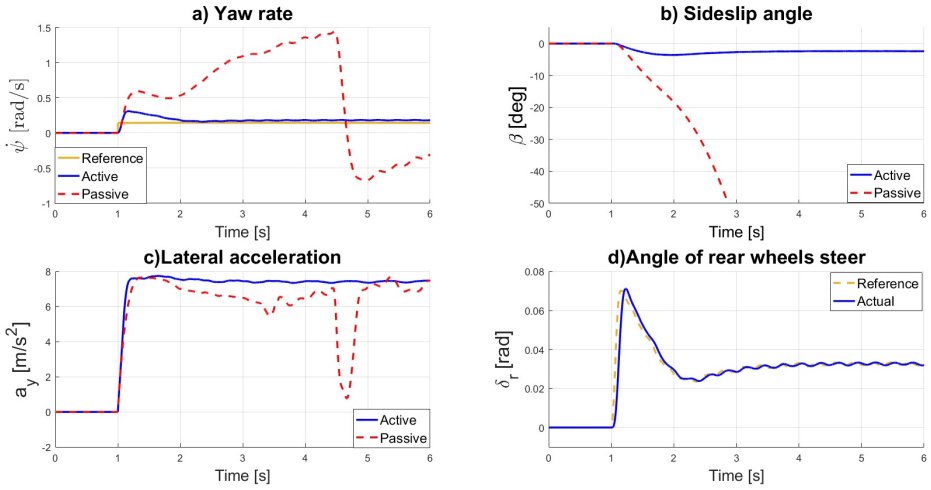

Figure 5.26: Simulation results of constant speed step steer (90°) at 150km/h

Single lane change

The simulation results are shown in Figure 5.27. In Figure 5.27(a), the vehicle with the ARS controller is seen to track the reference yaw rate properly while the passive one is out of the trajectory at the first moment of steering. As seen in Figure 5.27(b), the active vehicle reduces sideslip angle of the vehicle by 99% with respect to passive one (180°). Also ARS reduces the peak of lateral acceleration and is able to reach

steady state condition in 3s as shown in Figure 5.27(c). The reference and actual signals of actuator of rear steering is demonstrated in Figure 5.27(d).

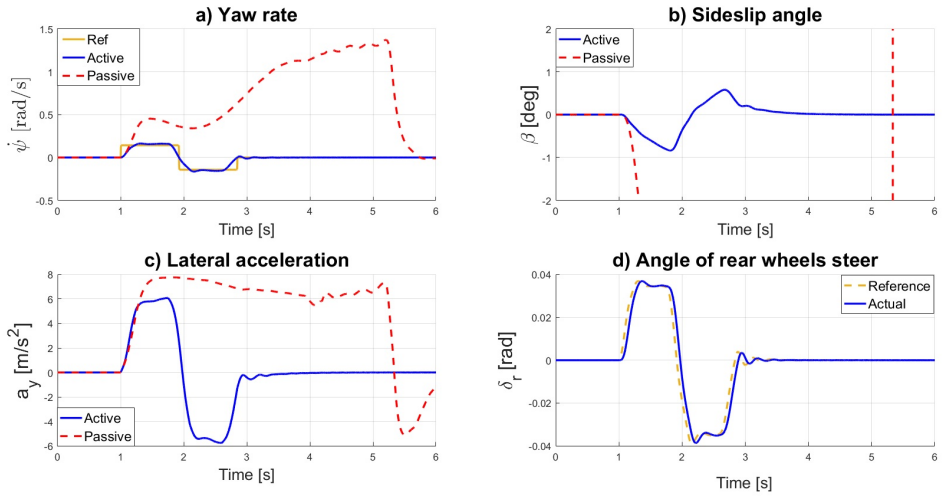

Figure 5.27: Simulation results of single lane change input with amplitude of 45° at 150km/h

5.5 Hydraulically interconnected suspension (HIS)

5.5.1 Introduction

The working principle of HIS is shown in Figure 5.28. The HIS is composed of double acting hydraulic cylinders, variable orifice valves, accumulators, pipeline and pressure sensors. And there are four hydraulic circuits in a HIS system as seen in Figure 5.28.

The performance of the HIS depends on piston volume, system mean pressure, fluid and material properties, valve and cylinder characteristics, accumulator performance, and other system parameters. The characteristics as mentioned earlier determine anti-roll capacity. The nonlinear characteristics of the components and the compressibility of the oil and are considered according to the software of LMS Lmagine Lab AMESim as shown in Figure 5.29. The model includes accumulators, valves, hoses, hydro-pneumatic pistons, fittings, and other components that are commonly used in hydraulic systems. Further details will be provided on how some of the major components are included in the AMESim model of Figure 5.29.

Some of the components used in the system are described in the following:

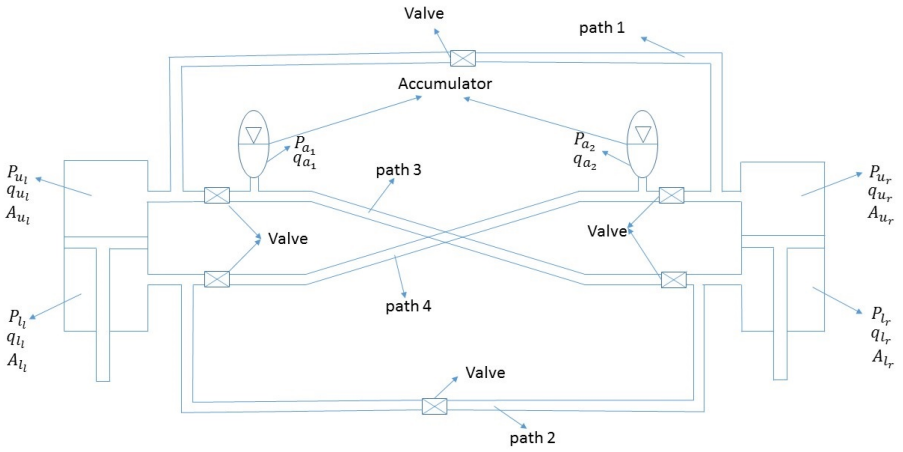

Figure 5.28: Schematic diagram for hydraulic circuit of half-car HIS system

Accumulator

The accumulator is a nitrogen-filled diaphragm-type hydraulic accumulator. The accumulator consists of two chambers separated by an elastomeric diaphragm. One chamber is filled with pre-charged gas and the other with fluid (commonly a Newtonian fluid such as oil). When the fluid pressure in the hydraulic circuit becomes higher than the pre-charged pressure, fluid enters the accumulator chamber and compresses the gas. A drop in fluid pressure in the circuit pushes the stored fluid back into the system.

Valve

The hydraulic suspension system includes a series of variable orifice valves that throttle the fluid as it passes through them, hence generating a damping force. In this analysis, the valve is modeled as a variable orifice. When the pressure difference is higher than a preload (or threshold pressure), the orifice opens according to the pressure difference across it to allow fluid passage. The orifice diameter and preload pressure are critical to the relationship between the damping force and velocity across the damper (i.e., damping curve), as has been detailed

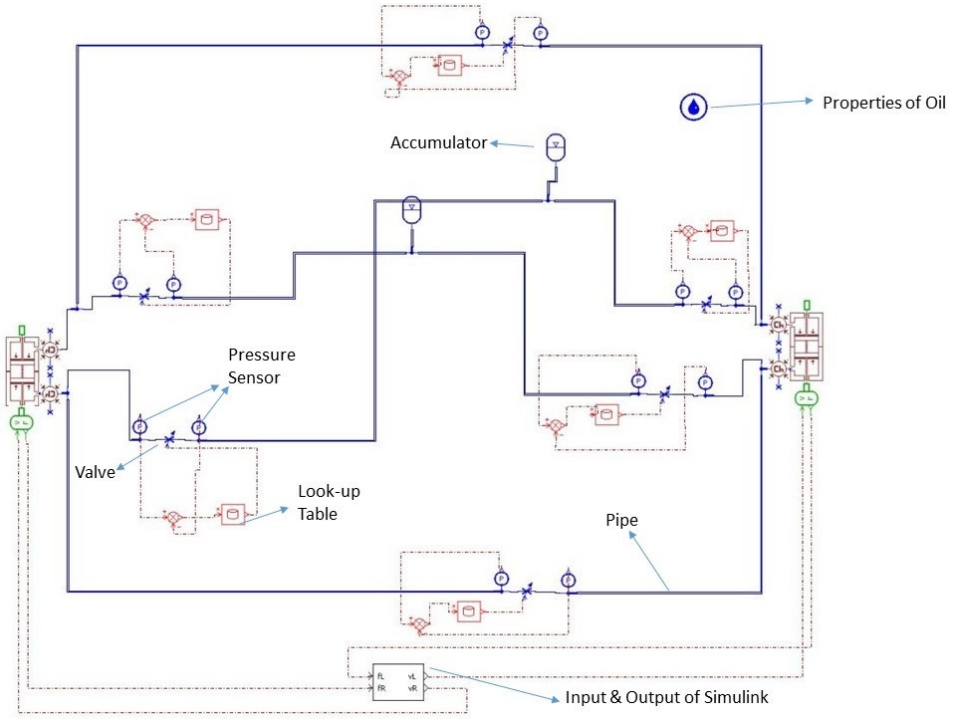

Figure 5.29: Scheme of HIS in AMESim software

in many past studies.

5.5.2 HIS Operating System

Out-of-phase and In-phase are the two main modes of operation for HIS system.

Out-of-phase (roll mode)

In the out-of-phase mode, the two pistons move in opposite directions (paths 3 and 4). When the vehicle turns left, the body will lean rightwards due to the centrifugal force, causing the left piston goes up, and the right piston goes down, fluid flows out of the left top chamber into the right-bottom chamber. The only place for the displaced fluid is in the accumulator in path three as shown in Figure 5.28. Pressure then rises in this line and falls in another line due to the simultaneous fluid flow out of the accumulator in path four as shown in Figure 5.28. Meanwhile, the accumulators in the circuit absorb the extra oil because of the volume difference between the two chambers above and below the piston, due to the damper rod volume. The accumulators also serve to stabilize the hydraulic pressure in the circuit. A force induced by the

pressure difference tends to resist the change, thus including additional resistance to body roll, much the same as an anti-roll bar.

In-phase mode

Parallel circuits (paths 1 and two as demonstrated in Figure 5.28) are corresponding to the in-phase mode. When the vehicle passes steady state condition, it starts tilting due to the torque that remained from transient regime so, in order to avoid tilting of the vehicle, parallel lines of HIS activate to balance between right and left sides of the vehicle.

5.5.3 Mathematical Model of Half Car

The heave and roll motions of half car model are given as follows,

$$\begin{aligned} m_s\ddot{z}_s = \{&-k_{s_{fl}}(z_s - \frac{\phi_{t_f}}{2} - z_{u_{fl}}) - c_{s_{fl}}(\dot{z}_s - \frac{\dot{\phi}_{t_f}}{2} - \dot{z}_{u_{fl}}) \\ &- k_{s_{fr}}(z_s + \frac{\phi_{t_f}}{2} + z_{u_{fr}}) - c_{s_{fr}}(\dot{z}_s + \frac{\dot{\phi}_{t_f}}{2} - \dot{z}_{u_{fr}}) \\ &+ F_{HIS_{fl}} + F_{HIS_{fr}}\} \end{aligned} \tag{5.23}$$

$$\begin{aligned} I_{xx}\ddot{\phi} = \{&\frac{k_{s_{fl}}(z_s - \frac{\phi_{t_f}}{2} - z_{u_{fl}})t_f}{2} + \frac{c_{s_{fl}}(\dot{z}_s - \frac{\dot{\phi}_{t_f}}{2} - \dot{z}_{u_{fl}})t_f}{2} \\ &\frac{-k_{s_{fr}}(z_s + \frac{\phi_{t_f}}{2} + z_{u_{fr}})t_f}{2} - \frac{c_{s_{fr}}(\dot{z}_s + \frac{\dot{\phi}_{t_f}}{2} - \dot{z}_{u_{fr}})t_f}{2} \\ &+ m_s a_y h_{CoG} - \frac{F_{HIS_{fl}}t_f}{2} + \frac{F_{HIS_{fr}}t_f}{2}\} \end{aligned} \tag{5.24}$$

$$\begin{aligned} m_s\ddot{z}_{u_{fl}} = \{&k_{s_{fl}}(z_s - \frac{\phi_{t_f}}{2} - z_{u_{fl}}) - c_{s_{fl}}(\dot{z}_s - \frac{\dot{\phi}_{t_f}}{2} - \dot{z}_{u_{fl}}) \\ &- k_{t_{fl}}(z_{u_{fl}} - z_{g_{fl}}) - F_{HIS_{fl}}\} \end{aligned} \tag{5.25}$$

$$\begin{aligned} m_s\ddot{z}_{u_{fr}} = \{&k_{s_{fr}}(z_s - \frac{\phi_{t_f}}{2} - z_{u_{fr}}) - c_{s_{fl}}(\dot{z}_s - \frac{\dot{\phi}_{t_f}}{2} - \dot{z}_{u_{fr}}) \\ &- k_{t_{fr}}(z_{u_{fr}} - z_{g_{fr}}) - F_{HIS_{fr}}\} \end{aligned} \tag{5.26}$$

5.5.4 The Mathematical nonlinear model of HIS

The left and right side of the HIS structure is analyzed. The oil inside the cylinder chambers is considered compressible. The output force of HIS can be written as:

$$\begin{aligned} F_l &= P_{l_l} A_{l_l} - P_{u_l} A_{u_l} \\ F_r &= P_{l_r} A_{l_r} - P_{u_r} A_{u_r} \end{aligned} \tag{5.27}$$

The flow equation is:

$$\begin{aligned} \Delta P_l = P_{l_l} - P_{u_l} &= \frac{1}{2} \frac{Q_l}{C_d A_l}^2 sign(z_l) \\ \Delta P_r = P_{l_r} - P_{u_r} &= \frac{1}{2} \frac{Q_r}{C_d A_r}^2 sign(z_r) \end{aligned} \tag{5.28}$$

Relation between relative velocity of piston to the cylinder and flow of damping hole is in the following:

$$\begin{aligned} Q_l &= A_{l_l} z_l \\ Q_r &= A_{l_r} z_r \\ P_{v_l} &= P_{u_l} - C_d Q_l \\ P_{v_r} &= P_{u_r} - C_d Q_r \end{aligned} \tag{5.29}$$

The pressure and volume of accumulator- P_{a_i} and V_{a_i} (i =1, 2), respectively-are related to the pre-charge values, P_p and V_p, as follows:

$$P_p V_p^2 = P_{p_1} {V_{p_1}}^{\gamma} = P_{p_2} {V_{p_2}}^{\gamma} = constant \tag{5.30}$$

The volume of accumulator can be written as:

$$\begin{aligned} V_{a_l} &= V_0 + A_{l_l}(z_l + \frac{t_f \phi}{2}) - A_{u_l}(z_l - \frac{t_f \phi}{2}) \\ V_{a_r} &= V_0 + A_{l_r}(z_r - \frac{t_f \phi}{2}) - A_{u_r}(z_r + \frac{t_f \phi}{2}) \end{aligned} \tag{5.31}$$

The properties of HIS systems are listed in Table 5.6.

5.5.5 Numerical Results

Open-loop maneuver is conducted to investigate the performance of HIS.

Table 5.6: Properties of the hydraulic interconnected suspension system

HIS properties	Values
density of oil (ρ)	$870 kgm^{-3}$
viscosity of oil (μ_{vis})	0.0051 Nsm^{-2}
bulk modulus of oil (β_{oil})	1400 Mpa
pipeline diameter (d_p)	0.0162 m
accumulator volume (V_a)	0.00032 m^3
pre-charge Pressure of Accumulator P_a	1 Mpa
piston area (A_{i_j})	0.025 m^2

Ramp steer

Ramp steer maneuver is simulated on a dry asphalt in various speeds. Particularly, the velocities of the vehicle are 80, 100 and 120 km/h where the steering angle reaches 100° in 4 s. Figure 5.30(a) and Figure 5.30(b) depicts the response of the passive and active vehicle in terms of steer angle VS roll angle and sideslip angle VS roll angle, respectively. It is observed that there is an improvement regarding roll angle by comparing active and passive figures. In the figure of $\delta - \phi$, reducing in roll angle can be notified by exploiting HIS. Moreover, it is interesting to emphasis that HIS is also beneficial for yaw control by decreasing the slightly sideslip angle of the vehicle while it is not significant improvement regarding a_y.

Step steer

After analyzing the performance of HIS in steady-state conditions, step steer maneuver is chosen in order to evaluate the performance of HIS in the transient condition. The step steer is completed in 0.1 s and is performed on a dry road (μ= 1) at the velocity of 100 km/h. Figure 5.31 depicts roll angle, roll velocity and roll acceleration, respectively. By looking at Figure 5.31, one can understand the effects of HIS in reducing the roll motion, avoiding oscillations and stabilizing the vehicle much faster than the passive one.

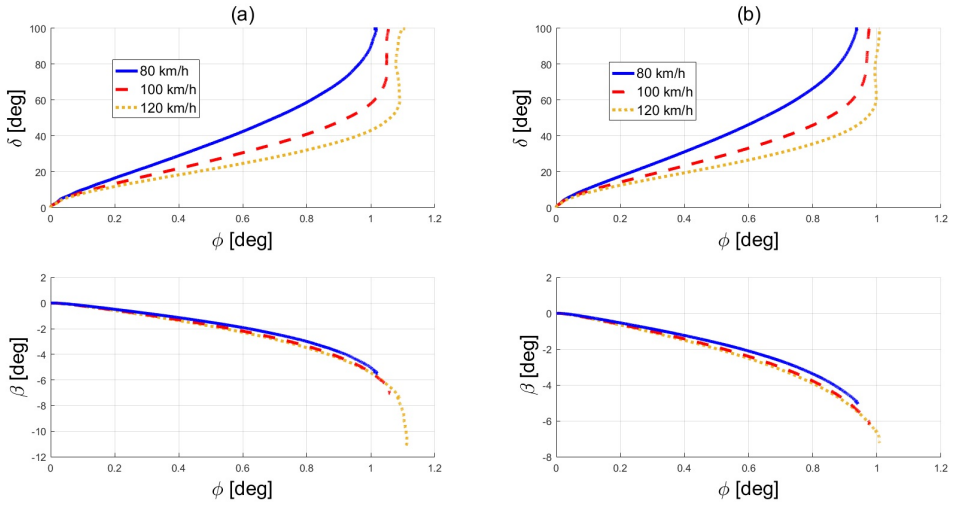

Figure 5.30: Simulation results of ramp steer maneuver for various velocities on dry road; passive vehicle (a), vehicle with Hydraulically Interconnected Suspension (b)

5.6 Active Anti-Roll Bar (AARB)

This section will focus on understanding the vehicle dynamic behavior under the influence of active anti-roll bar mechanism. In order to simulate the vehicle behavior, a linear four degrees half car model is developed as well as active anti-roll bar model. The objective of this section is to show the capability of active anti-roll bar to enhance the behavior of vehicle dynamics under several roll induced maneuvers.

5.6.1 Introduction

As some of the requirements for achieving good handling characteristics are contradictory to those required for a ride, a compromise must be made to achieve a reasonable ride-handling balance. This trade-off is engineered mostly by varying body stiffness, suspension tuning, and anti-roll bars. While body stiffness is a passive component, extensive research has been done on active suspension, and the technology is successfully implemented in most premium cars today. However, the amount of research on development in active ARB has been relatively lacking. Earliest active ARB systems were hydraulic, and until recently, they have been the predominant choice for electromechanical systems.

Active ARB systems provide the ability to vary the effective stiffness of the chassis and thus, reducing the amount of trade-off required in balancing ride and handling characteristics. Supported by suitable

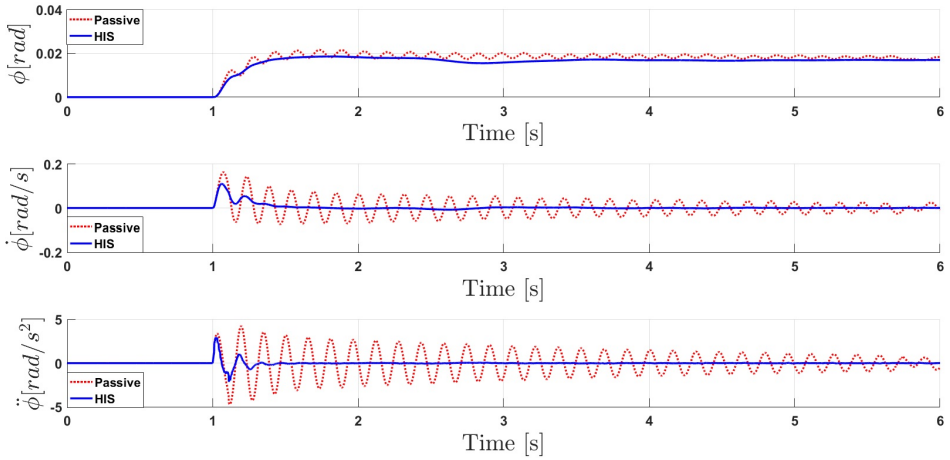

Figure 5.31: Simulation results of step steer maneuver with final amplitude of 90° at 100 km/h

actuator control for ARB, the chassis can be made stiffer to provide better agility during cornering or made softer in rough road conditions to improve ride comfort characteristics.

The second target of the AARB system is to reduce the body sideslip angle and body yaw rate oscillations during dynamic maneuvers, like a double lane change. This target can be obtained through a dynamic variation of the roll stiffness distribution between the two axles of the car.

5.6.2 Control theory

This section explains the theory behind a controller implemented for active anti-roll bar. The LQG control method as described in section 5.4.3 in chapter 5 is used to control the active anti-roll bar. The state variables are defined as
x=$[\beta\ \dot{\psi}\ \phi\ \dot{\phi}\ ]^T$
Two AARB are used for front and rear axle in order to reduce roll angle and minimize vehicle sideslip angle. An LQR controller is applied to minimize the roll angle ϕ and roll rate $\dot{\phi}$, i.e., the set-point is set to zero. Also, another aim of AARB is to track the reference of yaw rate and minimize sideslip angle of the vehicle. The strategy for minimizing sideslip angle ($\beta_{ref} = 0$) and tracking the reference of yaw rate (equation 5.17) is to apply inverse torque for front and rear axle, which is, in this case, the characteristic of the vehicle is going to be understeer tendency.

The input to the system is steering angle, δ_f while the outputs of

the system are sideslip angle,β, yaw rate, $\dot{\psi}$, roll rate, $\dot{\phi}$, and roll angle ϕ. The transfer function equations for single track model with roll dynamics system is written as follows:

$$\begin{aligned} I_{zz}\ddot{\psi} - I_{xz}\ddot{\phi} &= l_f(C_{\alpha_f}(\beta + \frac{l_f\dot{\psi}}{v_x} - \delta_f)) - l_r(C_{\alpha_r}(\beta - \frac{l_r\dot{\psi}}{v_x})) \\ mv_x(\dot{\beta} + \dot{\psi}) - m_s h_r\ddot{\phi} &= C_{\alpha_f}(\beta + \frac{l_f\dot{\psi}}{v_x} - \delta_f) + C_{\alpha_r}(\beta - \frac{l_r\dot{\psi}}{v_x}) \\ I_{xx}\ddot{\phi} - I_{xz}\ddot{\psi} &= (m_s g h_r - k_\phi)\phi - c_\phi\dot{\phi} + m_s h_R(v_x(\dot{\beta} + \dot{\psi}) - h_R\ddot{\phi}) \end{aligned} \tag{5.32}$$

Therefore the state equation matrix can be written as:

$$\dot{x} = Ax + Bu \tag{5.33}$$

where

$$E_1 = \begin{bmatrix} mv_x & 0 & 0 & -m_s h_r \\ 0 & I_{zz} & 0 & -I_{xz} \\ 0 & 0 & 1 & 0 \\ -m_s h_r v_x & -I_{xz} & 0 & I_{xx} + m_s h_r^2 \end{bmatrix}$$

$$E_2 = \begin{bmatrix} -C_{\alpha_f} - C_{\alpha_r} & -mv_x - \dfrac{C_{\alpha_f} l_f + C_{\alpha_r} l_r}{v_x} & 0 & 0 \\ -C_{\alpha_f} l_f + C_{\alpha_r} l_r & \dfrac{-C_{\alpha_f} l_f^2 - C_{\alpha_r} l_r^2}{v_x} & 0 & 0 \\ 0 & 0 & 0 & 1 \\ 0 & m_s h_r v_x & m_s g h_r - k_\phi & c_\phi \end{bmatrix}$$

$$E_3 = \begin{bmatrix} 0 & 0 & 0 & 0 \\ 0 & 0 & 0 & 0 \\ 0 & 0 & 0 & 0 \\ \frac{t_f}{2} & -\frac{t_f}{2} & \frac{t_r}{2} & -\frac{t_r}{2} \end{bmatrix}$$

(5.34)

where
A=E_2/E_1
B=E_3/E_1
u=$[F_{ARB_{fl}}\ F_{ARB_{fr}}\ F_{ARB_{rl}}\ F_{ARB_{rr}}]^T$=the control force vector
k_ϕ=stiffness of anti-roll bar (232320 N/m)
c_ϕ=damping coefficient of anti-roll bar (5000 Ns/m)
h_R=height of roll center
I_{xz}=moment of inertia about x-z axis (30.065 kgm^2)

5.6.3 Numerical results

This section describes the evaluation of active anti-roll bar in various maneuvers.

Ramp steer

Ramp steer maneuver is selected to evaluate on a dry road condition (μ=1) where the steering angle reaches to 100° in 4 s at 150 km/h. As by looking to Figure 5.32(a), an active vehicle is able to reduce the overshoot of yaw rate and also vehicle can easily reach steady state condition. Figure 5.32(b) shows the reduction of vehicle sideslip angle (β) from -7° to -5° which means 28% reduction in vehicle sideslip angle. Figure 5.32(c) illustrates the time history of $a_y - v_x\dot{\psi}$ and active vehicle avoids vehicle from understeer and oversteer conditions. The time history of normal forces of each wheel is presented in Figures 5.32(d) and (e). The effect of active anti-roll bar in reducing of roll angle can be proved by looking at Figure 5.32(f).

Double lane change

Figure 5.33 shows double lane change maneuver where the magnitude of the steering angle is 45° on a dry road condition at 120 km/h. Figure 5.33(a) compares the yaw rate ($\dot{\psi}$) of passive and active vehicles and by looking at the Figure 5.33(a) the active vehicle influences tracking of desired trajectory. The vehicle sideslip (β) is remarkably reduced in the active vehicle compared with passive one as shown in Figure Figure 5.33(b). Figure 5.33(c) demonstrates the time history of $a_y - v_x\dot{\psi}$ which means that passive vehicle is losing its stability at the beginning of the cornering while active anti-roll bar significantly stabilizes the vehicle. Figures 5.33(d) and (e) illustrates the time history of normal forces of each wheel. The roll angle of the vehicle can be slightingly reduced by

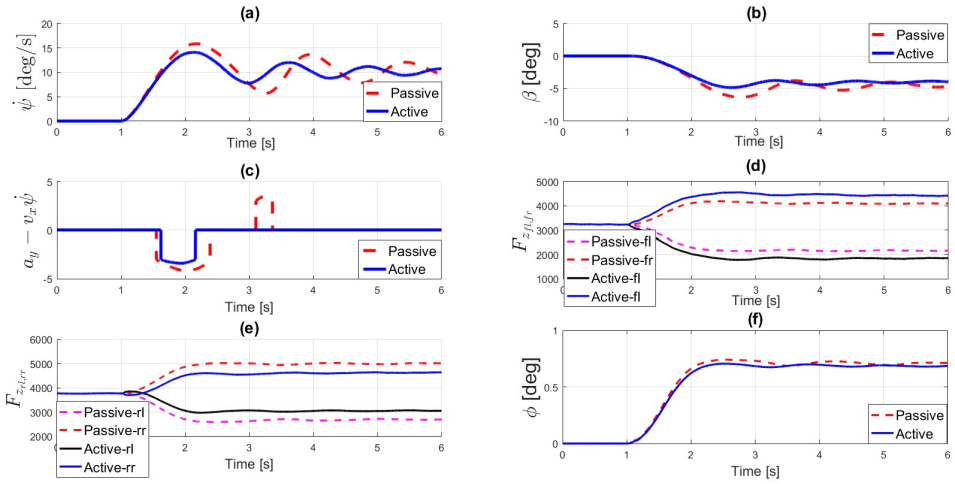

Figure 5.32: Simulation results of ramp steer input with final amplitude of 100° at 150km/h

active vehicle. Moreover, an AARB eliminates the oscillation of roll angle compared with passive vehicle.

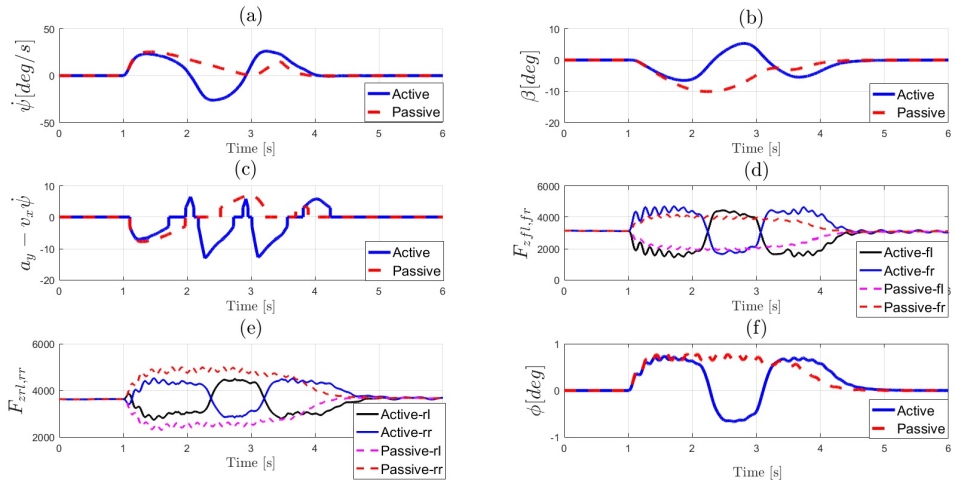

Figure 5.33: Simulation results of double lane change input with final amplitude of 45° at 120km/h

5.7 Electronic stability control (ESC)

5.7.1 Introduction

Electronic Stability Control (ESC) systems are designed to correct for understeer and oversteer conditions. ESC uses input from various sensors along with an advanced control strategy to sense the incidents of steering instability. It selectively brakes the rear or front tires at an individual corner to generate a correcting yaw moment that can counteract the oversteer/understeer dynamics.

5.7.2 Control strategy

According to the current state of technology, direct measurements of the yaw rate, lateral acceleration, velocity and the steering angle are quite feasible. This approach is based on the detection of understeering and oversteering conditions before the limit conditions are reached. The controller model described here is developed using Simulink, with simulations carried out in MATLAB. The vehicle model is based on VI-CarRealTime commercial software that intended to emulate actual vehicle dynamics. The difference between lateral acceleration and multiplication of velocity and yaw rate is employed as the control variable for yaw stability ($I_{lat} = a_y - v_x\dot{\psi}$). If the index ($I_{lat}$) has a positive value, then the vehicle is said to be understeering. If the index is negative, the vehicle is said to be oversteering. Depending on the sign of the index and the direction of a turn, control system selectively brakes individual wheels to generate a corrective yaw moment which maintains vehicle stability. A simple ABS functionality has been incorporated in the ESC system. The longitudinal slip ratio for all four tires is obtained from VI-CarRealTime. Two thresholds are set for longitudinal slip (0.01 and 0.02). If any of these ratios exceed the thresholds, then the brake pressure calculated by the ESC system is reduced to prevent wheel lock-up. The desired value for yaw rate is the same as the used in the previous section (Equation 5.17).

The look-up table is designated to determine the magnitude of brake pressure based on the magnitude of differences between $\dot{\psi}_{ref}$ and $\dot{\psi}$ as depicted in Figure 5.34. The look-up table uses the nearly linear relationship between residual of yaw rate and brake pressure and brake pressure. The slope of this linear relationship determines the rate of increase in brake pressure for a given yaw rate residual magnitude. The look-up table in the ABS module gives the factor by which brake pressure is reduced when slip ratios exceed the threshold. Changing this table would modify reduction in brake pressures.

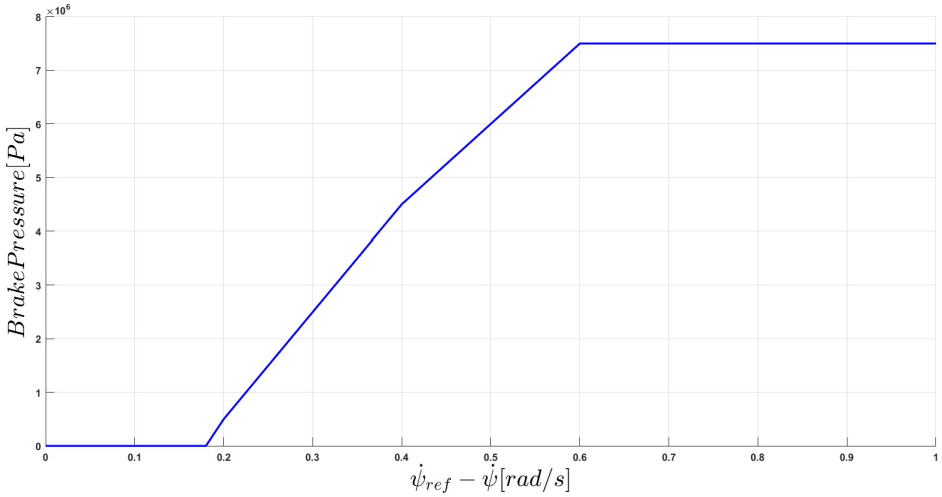

Figure 5.34: Lookup able of brake pressure

5.7.3 Numerical results

The performance of the ESC is evaluated by using the results of computer simulations.

Ramp steer

The analysis is related to slow ramp steer (up to 100°) maneuver on the dry road surface ($\mu = 1$) to analyze the steady state response of the vehicle. In particular, the vehicle is running on a dry road at 100, 120 and 150 km/h while the steering wheel reaches 100° in 4 s. Figure 5.35(a) depicts the response of the passive vehicle in terms of steer angle VS lateral acceleration and sideslip angle VS lateral acceleration. The understeer gradient in the linear zone decreases with increasing speed. However, when considering the lateral acceleration developed as the function of steer angle, its value decreases after reaching the maximum. In addition, the absolute value of sideslip angle of the vehicle significantly increases for lateral accelerations higher than 12 m/s2. The controlled vehicle responds to the same input as shown in Figure 5.35(b). Increasing speed always leads to higher lateral accelerations around the corresponding values obtained with the passive vehicle. For 100 km/h, 120 km/h and 150 km/h, there is a monotonic relation between lateral acceleration and steering angle. The proposed control logic thus makes the vehicle more predictable and easier to control. The same indication can be drawn looking at the sideslip angle diagram: even when the acceleration is close to 12 m/s^2, the sideslip angle

is slightly above 14°. It is noteworthy that the control, trying to zero $a_y - v_x\dot{\psi}$, can improve the vehicle's response also in quasi steady-state conditions.

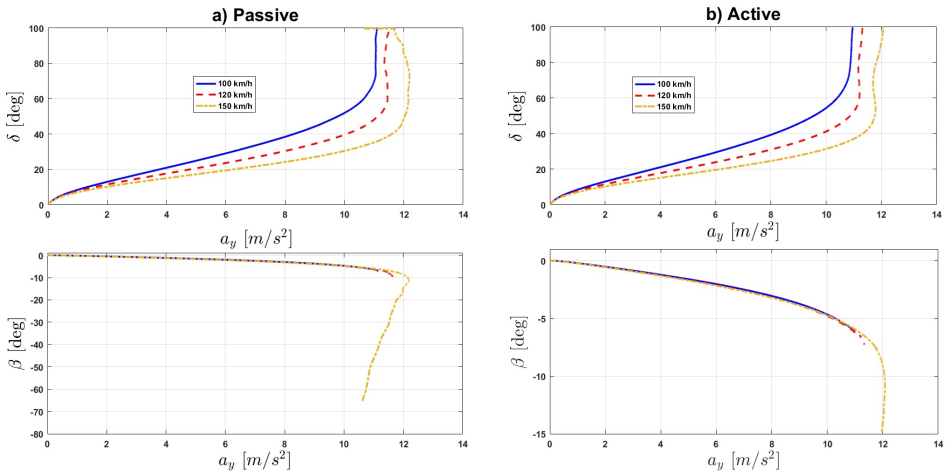

Figure 5.35: Simulation results of ramp steer maneuver for various velocities on dry road; passive vehicle (a), actively controlled vehicle (b)

Step steer

Figure 5.36 is related to step steer maneuver which is performed in 0.1 s on dry road condition (μ=1) at 100 km/h. Figure 5.36(a) compares the yaw rate of the vehicle when the controller ON and OFF. It can be seen that yaw rate is significantly reduced the overshoot of it when ESC is ON mode. It in noteworthy to point out that ESC allows reducing the time required to reach the regime condition. Moreover, ESC is able to decrease the sideslip angle of the vehicle in order to stabilize the vehicle as shown in Figure 5.36(b).

5.8 Torque vectoring

5.8.1 Introduction

Torque vectoring can be used as a stability control system by the distribution of drive torque through the wheels for generating a corrective yaw moment about the z-axis of the vehicle. Torque vectoring can generate the corrective yaw moment by distributing torque asymptotically to left/right wheels of an axle or front/rear axles. The logic of torque vectoring system is in the following [86]:

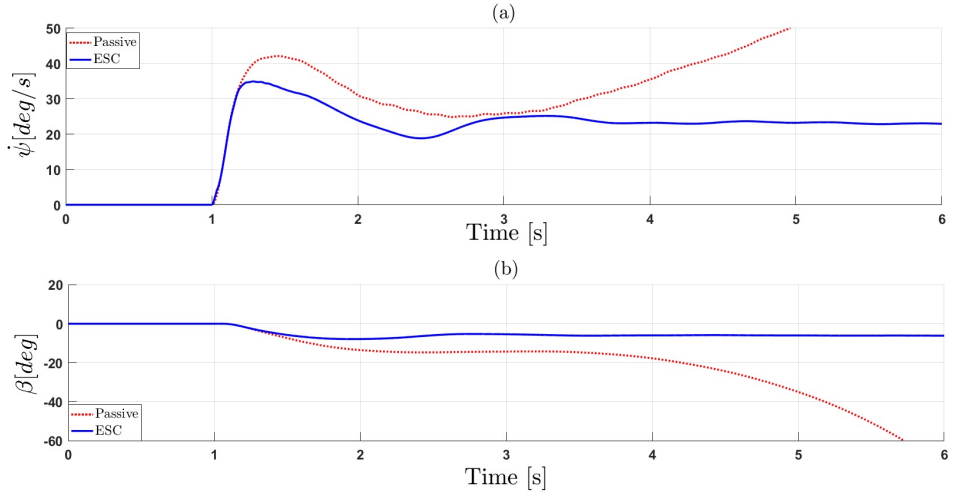

Figure 5.36: Simulation results relevant to step steer maneuver (90°) on dry asphalt

1. When the vehicle is in oversteer condition, more torque is transferred to the front-inside wheel because the adhesion potential has been reached at the rear axle in order to generate the corrective yaw moment.
2. When the vehicle is in understeer condition, more torque is transferred to the rear-outside wheel because the adhesion potential has been exceeded on the front axle in order to generate the corrective yaw moment.

The torque vectoring system can also affect the driving dynamics by altering the front-to-rear torque distribution. This is an advantage for controlling the interconnection between the longitudinal and lateral tire forces where altering one force automatically affects the other. This strategy can change the lateral force potential at the front/rear axles in order to enhance the ability of the drive to steer the vehicle. Also, it reduces the potential of lateral force at front/rear axles by increasing the longitudinal traction force. The detailed description of strategy with respect to understeer/oversteer conditions is in the following [86]:
1. In an understeer condition, by transmission of more engine torque to the rear axle, the vehicle can be controlled.
2. In an oversteer condition, by transmission of more engine torque to the front axle, the vehicle can be controlled.

Despite the similarity between torque vectoring system and electronic stability control (ESC) system, torque vectoring is more effective particularly at high speeds and during emergency maneuver near the

handling limits of the vehicle [204]. In other words, TV is focused on performance, for instance, it can keep or even increase vehicle speed during the intervention and TV does not aim to reduce wheel's speed so that it would be easier for the driver to control it. The advantage of torque vectoring is keeping constant the total driving force of the vehicle. However, ESC is hindering total driving force by the effect of braking and reduction of drive torque which leads to raises the insufficiency of the vehicle by removing the power that has already generated. Also, from driver's point of view, it is disruptive because of the unexpected speed reduction. In addition, torque vectoring allows to increase driving safety, to enhance driving performance in a wide range of operation even in normal driving conditions, while ESC or active braking is valid only in a limited operation time to ensure the safety of the vehicle. However, it is noteworthy to point out that torque vectoring is an effective system only when a driving torque exists which means that torque vectoring cannot intervene in the case that the driver releases the throttle or brakes the vehicle. In such cases, an ESC system must intervene in order to maintain the stability of the vehicle. In addition, understeer characteristic through torque vectoring can be illustrated in Figure 5.37. As seen in the figure, torque vectoring system can intervene in three regions based on the dynamic behavior of the vehicle and the control logic.

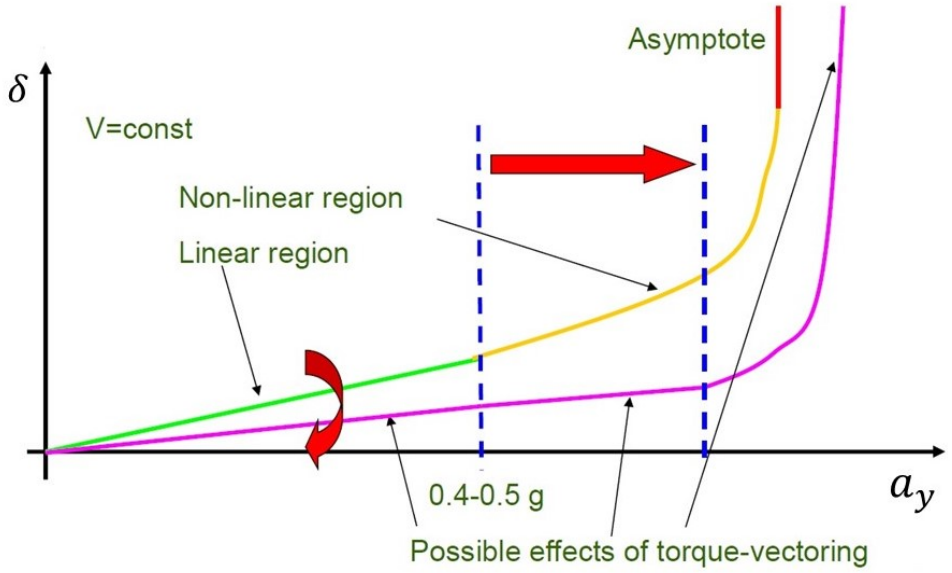

Figure 5.37: Understeer characteristic through torque vectoring control

5.8.2 Torque vectoring control

The aim of the torque vectoring system in this thesis is to distribute the corrective yaw moment from the controller to the individual wheels for stabilizing the vehicle driving dynamics. Assuming that M_z is the total required corrective yaw moment, the tire forces on each axle must be adapted so that each axle produces a portion of the total corrective yaw moment:

$$M_z = M_{z_f} + M_{z_r} = \varepsilon_f M_z + \varepsilon_r M_z \tag{5.35}$$

where
$M_{z_{f,r}}$ = the portions of the required corrective yaw moment at the front and rear axles
$\varepsilon_{f,r}$ = the percentages of the total required corrective yaw moment Mz that must be generated at the front and rear axles
In addition, the correlation between ε_f and ε_r describes the front-to-rear torque vectoring distribution where $\varepsilon_f + \varepsilon_r = 100\%$.

The generated yaw moment on each axle can be written as follows:

$$M_{z_f} = F_{x_{fl}} \frac{t_f}{2} + F_{x_{fr}} \frac{t_f}{2} \tag{5.36}$$

Since the magnitudes of $F_{x_{fl}}$ and $F_{x_{fr}}$ are the same, the corrective yaw moment for front axle can be derived:

$$M_{z_f} = F_{x_f} t_f \Rightarrow F_{x_f} = \frac{M_{z_f}}{t_f} \tag{5.37}$$

$$M_{z_r} = F_{x_{rl}} \frac{t_r}{2} + F_{x_{rr}} \frac{t_r}{2} \tag{5.38}$$

Since the magnitudes of $F_{x_{rl}}$ and $F_{x_{rr}}$ are the same, the corrective yaw moment for rear axle can be derived:

$$M_{z_r} = F_{x_r} t_r \Rightarrow F_{x_r} = \frac{M_{z_r}}{t_r} \tag{5.39}$$

LQR control

The vehicle dynamics controller is designed as a Linear Quadratic Regulator (LQR) as described in detail in section 5.4.3 . Controlled state variables are the vehicle sideslip angle (β) and yaw rate ($\dot{\psi}$). The controller is based on a bicycle vehicle model where equations of motion are in the following:

$$\begin{bmatrix} \dot{\beta} \\ \ddot{\psi} \end{bmatrix} \begin{bmatrix} \frac{-(C_{\alpha_f}+C_{\alpha_r})}{mv_x} & \frac{C_{\alpha_r}l_r - C_{\alpha_f}l_f}{mv_x} - v_x \\ \frac{(C_{\alpha_r}l_r - C_{\alpha_f}l_f)}{I_{zz}v_x} & \frac{-(C_{\alpha_f}l_f^2 + C_{\alpha_r}l_r^2)}{I_{zz}v_x} \end{bmatrix} \begin{bmatrix} \beta \\ \dot{\psi} \end{bmatrix} + \begin{bmatrix} \frac{C_{\alpha_f}}{m} \\ \frac{C_{\alpha_f}l_f}{I_{zz}} \end{bmatrix} \delta + \begin{bmatrix} 0 & 0 \\ \frac{t_f}{I_{zz}} & \frac{t_r}{I_{zz}} \end{bmatrix} \begin{bmatrix} F_{x_f} \\ F_{x_r} \end{bmatrix} \tag{5.40}$$

by considering single track vehicle model, references for vehicle sideslip angle (β) and yaw rate ($\dot{\psi}$) can be written as follows[21, 197, 103]:

$$\dot{\psi}_{ref} = \begin{cases} \dfrac{v_x}{l(1+\frac{k_{us}}{l}v_x^2)}\delta_f, & |\dot{\psi}| < \frac{a_y}{v_x} \\ \frac{\mu g}{v_x}, & |\dot{\psi}| \geq \frac{a_y}{v_x} \end{cases} \tag{5.41}$$

$$\beta_{ref} = (\frac{l_r}{v_x} - \frac{l_f m v_x}{l C_r})\dot{\psi}_{ref} \tag{5.42}$$

5.8.3 Numerical results

Performances of the implemented torque vectoring control system are assessed through simulations where it will be accomplished with the previously described 14 DOF vehicle model. Open loop maneuvers will be carried out on different adhesion surfaces.

Ramp steer

The simulation results of steady-state cornering (ramp steer) with the magnitude of 100° under two different road surface conditions at various velocities are shown in Figures 5.38 and 5.39. Here the steering angle δ and vehicle sideslip angle β are plotted as a function of lateral acceleration for both passive and controlled vehicles. Under dry road surface condition, by increasing velocity, the passive vehicle started to lose its stability especially at 175 km/h and 200 km/h. The sideslip angle of the passive vehicle significantly increased by increasing the velocity of the vehicle. However, torque vectoring control remarkably influenced vehicle dynamics behavior in a positive way. The sideslip angle of the

vehicle was significantly reduced which this enables a driver to complete cornering maneuvers. Under rainy or wet road surface condition, by looking at figure of vehicle sideslip angle and lateral acceleration, the uncontrolled vehicle was not able to complete the maneuvers due to the severity of maneuver because the interaction between tire and road is insufficient to generate necessary forces to stabilize the vehicle, while the active vehicle can finish the maneuver by generating enough traction force to overcome the improper situation. Under both road surface conditions, the passive vehicle was seen to be out of control at low levels of lateral acceleration and become gradually unstable when the vehicle approached the handling limit. However, the vehicle with torque vectoring controller was seen to be linear to much higher levels of lateral acceleration until the handling limit and therefore behaved in a more predictable manner over an even wider range of handling conditions than the passive vehicle under both road surface conditions. This is indeed expected due to the utilization of the linear reference model which is selected for the torque vectoring control system and always responds linearly to driver inputs.

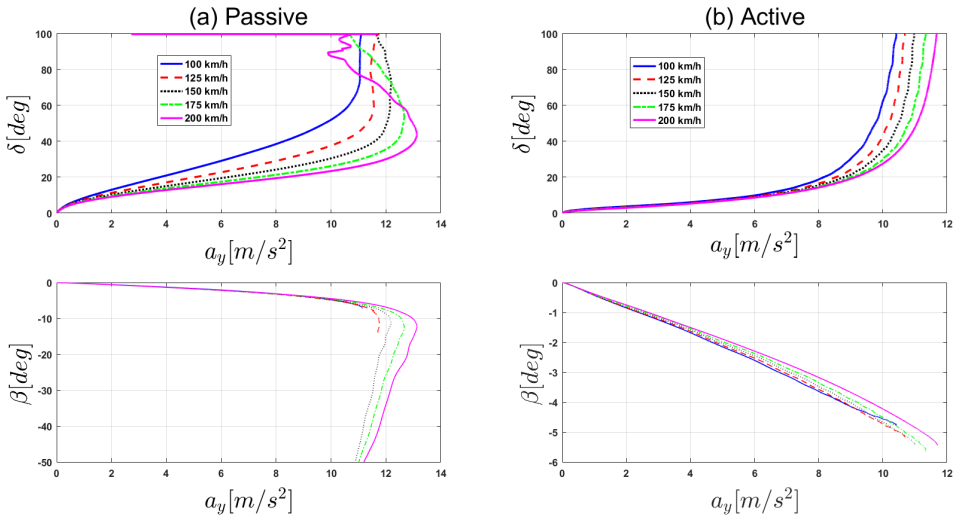

Figure 5.38: Simulation results of ramp steer maneuver for various velocities on dry road ($\mu = 1$); passive vehicle (a), actively controlled vehicle (b)

These results depict that the torque vectoring control system extends the linear handling region of the vehicle and prevents entering into the nonlinearity. Therefore, from the driver's perspective, the vehicle becomes more controllable. In addition, this specific maneuver also demonstrates good robustness of torque vectoring controller with

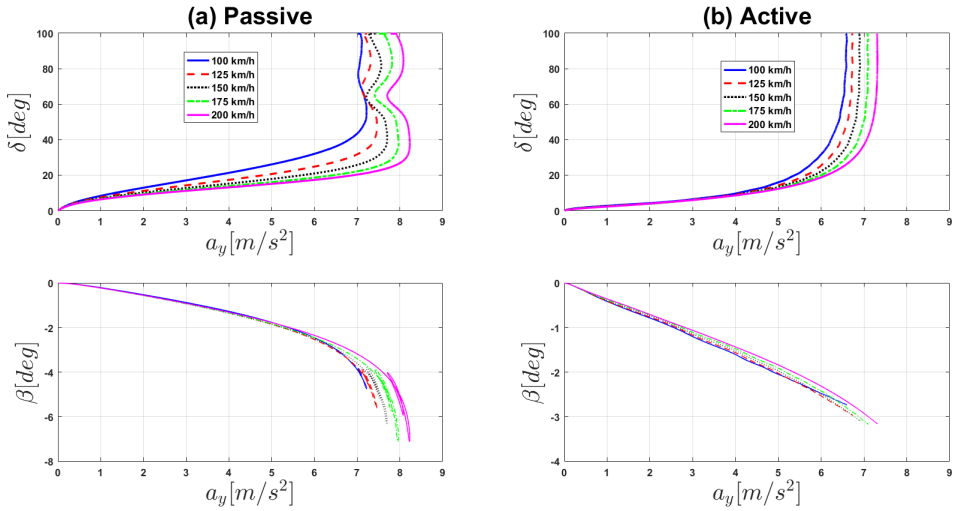

Figure 5.39: Simulation results of ramp steer maneuver for various velocities on wet road ($\mu = 0.6$); passive vehicle (a), actively controlled vehicle (b)

respect to vehicle speed and road surface friction variations.

Double lane change

In another test, double lane change maneuver with the magnitude of 45° on the dry road surface was tested to evaluate the performance of torque vectoring control system and the results of TV ware compared with passive vehicle. As seen in Figure 5.40(a) and Figure 5.40(b), A 33% and 50% reduction in the overshoot of yaw rate and vehicle sideslip angle is observed for the active vehicle, respectively. Moreover, the active vehicle is able to track the reference of yaw rate in order to perform the maneuver. Figure 5.40(c) shows a number of forces which are performed by torque vectoring control system on front wheels based on yaw rate and vehicle sideslip angle. Time history of $a_y - v_x\dot{\psi}$ is illustrated in Figure 5.40(d) which demonstrates that controller starts to operate when the amount of $a_y - v_x\dot{\psi}$ is abruptly increasing.

5.9 Summary

The dynamic stability subsystem controllers have been designed in this chapter. Each subsystem has been examined for illustrating the relative merits. A brief summary of each subsystem is described in the following:

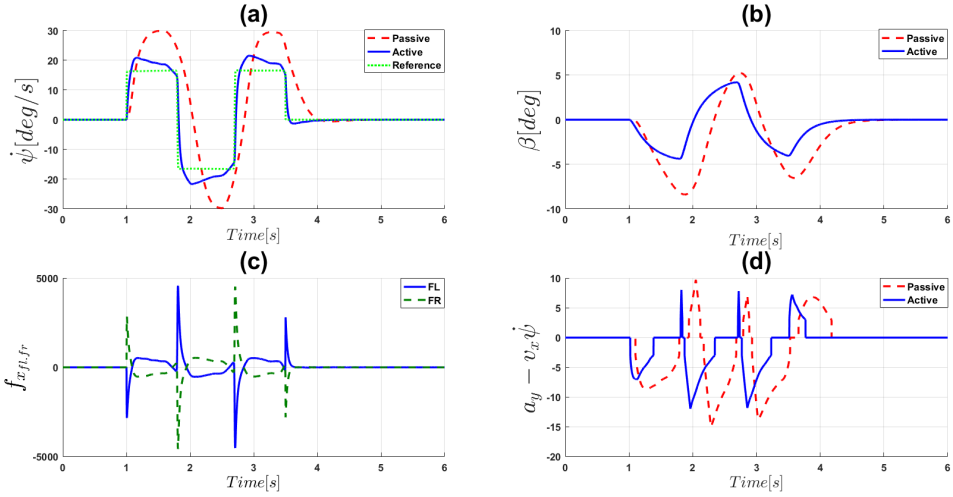

Figure 5.40: Simulation results of double lane change maneuver at 125 km/h on dry road

Active suspension

The first section presented the analysis of a lateral-stability control based on active suspensions. In particular, the proposed control logic exploits the actuators of active suspensions to generate a system of inertia forces on the car-body able to alter the normal load distribution on the axles. The control aims to change normal load distribution between front and rear axle to influence the understeer/oversteer response of a vehicle. A high-level control logic was designed to determine the variation of normal load on front and rear axle required to stabilize the vehicle. The normal load control was then implemented considering a feedforward contribution based on a simple linear 2D model of the vehicle and a feedback contribution based on the acceleration measured on board. Bandwidth and delays of suspension actuators were taken into account. Open loop maneuvers (step steer and lance change) were performed to analyze the response of the vehicle in critical conditions. Numerical results showed the effectiveness of the control in improving vehicle stability and also its robustness towards changing in friction coefficient. Results related to this controller are encouraging and show the potential of longitudinal load transfer in controlling the vehicle. In particular, such a control is able to improve stability without affecting promptness. Power requirements represent probably the main drawback of this approach: up to 10 kW (per actuator) were needed for using this control logic.

Active aerodynamics control

The implementation of an active aerodynamic system for sports car has been studied. The proposed system controls the angle of attack of the front and rear spoilers to get the desired distribution of normal loads on the front and rear axles. A high-level control logic was designed to determine the variation of normal load on front and rear axle required to stabilize the vehicle. This aim of the logic is zeroing the difference between lateral acceleration and the product between vehicle's speed and yaw rate. This control presents the advantage of being based on quantities commonly measured or estimated on board and allows the vehicle to react in a very predictable way to keep an almost direct relationship between lateral acceleration and yaw rate. The normal load control was then implemented by changing the angle of attack of the front and rear spoilers according to look-up tables. Bandwidth and delays and motor specifications of actuators were taken into account. Several open loop maneuvers (slow ramp steer, lance change, fishhook and step steer) were performed to analyze the response of the vehicle in critical conditions, comparing the stability of the passive and active vehicle by yaw rate, lateral acceleration, and sideslip angle. Numerical results showed the effectiveness of the control in improving vehicle's stability and also its robustness towards changing in friction coefficient.

Active four wheel steering

In this section, active four-wheel steering system was introduced to improve vehicle maneuverability at low speeds, enhance stability at high speeds, and improve vehicle transient response to steering input. The first aim can be achieved by the reduction of the radius of turn via steering the rear wheels in an opposite direction with the front ones at low speeds. For achieving the second goal which is increasing stability at high speeds, the rear wheels must steer in the same direction of front ones to generate lateral force in rear wheels for matching it with lateral force of front wheels. The control logic was designed using an LQR controller based on a simplified bicycle handling model. Numerical results illustrated the effectiveness of active four-wheel steering for enhancing the stability and maneuverability of the vehicle. Also, by simulation results, it was proved that it was robust to variations of road friction coefficient.

Hydraulically interconnected suspension

The second section discussed analyzed the principle of hydraulically interconnected suspension in order to enhance the comfort, smoothness, and safety of the vehicle. A new and improved hydraulically interconnected suspension was proposed; thereby a new solution appears by adding parallel paths to the system to eliminate torque, which remained from transient phase, in steady state phase. The parameters of the new structure were set to establish the mathematical model of it. In order to analyze new structure HIS, hydraulically interconnected suspension was tested by utilizing AMEsim software and MATLAB SIMULINK by considering all details of HIS properties. Results demonstrated that hydraulically interconnected suspension is able to significantly reduce roll motion in cornering maneuvers. Moreover, it positively affected yaw motion by reducing roll motion.

Active anti-roll bar

The aim of analyzing active anti-roll bar is to improve vehicle's performance in terms of handling, ride comfort and safety by developing a control algorithm. In this thesis, a strategy developed was exploiting two active anti-roll bar at the front and rear axles in order to control the normal forces of four wheels. By generating two torques at the front and rear axles in an opposite direction, vehicle's performance can be improved. According to the simulation results, the proposed system has a capability of achieving better performance regarding reducing roll motion and enhancing stability and safety.

Electronic stability control

This section explained the construction and working of the ESC model. This is a simplified model which utilized differential braking to control vehicle response. The control variables utilized are lateral acceleration, yaw rate and longitudinal velocity for the stabilization of yaw motion. The implemented control system utilized the differential of reference and measured yaw rate to generate brake by look-up table on the specific wheel based on oversteering, understeering and direction of a turn. The performance of this simplified model will be evaluated through simulation runs and comparison with a passive vehicle. Results demonstrated that this approach gave satisfactory performance.

Torque vectoring system

In this section, torque vectoring controller was developed based on an LQR controller. Torque vectoring system aims to distribute the calculated corrective yaw moment to the individual wheel to maximizes use of all tires for the enhancement of vehicle handling. Several maneuvers were carried out in simulation to demonstrate the performance and effectiveness of the torque vectoring system.

Chapter 6

Design of Integrated Vehicle Active Control Systems

6.1 Introduction

By analyzing each active subsystem, one can understand that each active subsystem has its functional limitations and its effective range of vehicle handling. For covering the entire range of handling, it is needed to integrate several subsystems. Working several active subsystems in a combined mode does not mean to have better performance compared with each subsystem because of undesired interactions between different subsystems. Consequently, it is needed to develop integrated vehicle dynamics control for obtaining an improved vehicle handling performance. In this chapter, an integrated vehicle dynamics control system will be developed by utilizing the centralized approach described in Chapter 2 for exploiting cooperative interaction and preventing interferences between different active subsystems.

6.1.1 Design objectives

Interferences among several stand-alone controllers can lead to handling limit because of conflicts in control targets. Therefore, to prevent undesirable interactions among several stand-alone controllers and to decrease performance trade-offs in the handling of the vehicle, two methods are suggested to coordinate the control actions of the subsystems. The proposed integrated vehicle dynamics control system will be designed for obtaining the following targets:

- For maintaining the vehicle stability close to and at the limit of handling

- For enhancement of the performance of the vehicle on cornering maneuvers
- For improvement and enhancing the performance and safety of the vehicle at high speeds
- For enhancing the steerability of the vehicle
- For reducing trade-off between road holding and comfort of passengers

By considering the Table 2.1, control targets, feasibility of each subsystem for integration and power consumption of these subsystems, the following subsystems are selected for integration:
1. Active rear steering (ARS) to control lateral force of tires
2. Torque vectoring (TV) to control longitudinal force of tires
3. Active aerodynamics control (AAC) to control normal force of tires
4. Hydraulic interconnected suspension (HIS) to decrease trade-off between road holding and passengers comfort and prevent roll motion in cornering maneuvers

Table 6.1: Brief description of active chassis control systems

	ARS	TV	HIS	AARB	AAC	ESC	ASS
Comfort			F_z	F_z			F_z
Safety	F_y	F_x		F_z	F_z	F_x	F_z
Performance	F_y	F_x		F_z	F_z		F_z

The integrated vehicle control system is designed, implemented and tested in MATLAB Simulink. Initially, three chassis controls are integrated by optimal control (LQR) described in section 5.4.3, then the performance of the integrated control is evaluated for different maneuvers and is compared with passive vehicle and stand-alone controllers in order to verify the influence of the integrated vehicle control system on vehicle performance. Secondly, three chassis controls are integrated by utilizing the fuzzy logic system. This integration system is also verified by comparison with the passive vehicle and standalone controllers under various maneuvers. Next, Two methodologies are compared to each other and discuss pros and cons of each integration system. Finally, the integration of four chassis controls is implemented by using

the fuzzy logic system. Note that, even though the Hydraulic Interconnected Suspension (HIS) is implemented, the behavior of HIS is not integrated.

6.2 Combined Control

Before the final integration is developed, combined control of the three and four standalone chassis control systems designed in Chapter 5 will be evaluated. In the combined control structure, the subsystem controllers operate in parallel. In other words, the standalone chassis control systems are usually active based on the reference tracking. The characteristics of the combined control system are in the following:

- No communication between the controllers
- Each controller has its own reference model

The analysis and evaluation of the combined control will be done in the next section for comparing with the integrated control scheme in order to assess the performance of the integrated vehicle dynamics system. This comparison assists to make a better analyzing and understanding of the advantages and disadvantages of the proposed integrated control scheme.

6.3 Integration of ARS, TV and HIS

Therefore, to prevent undesirable interaction between the active rear steering and torque vectoring subsystems and decrease performance trade-offs in vehicle handling, two integration schemes are introduced to coordinate the control action of the two subsystems. Initially, the system is designed with two methods (LQR and fuzzy logic), then it is implemented in MATLAB SIMULINK where all the adjusting and setting is carried out. All the information required by the controllers is assumed to be obtained via VI-CarRealTime commercial software.

6.3.1 LQR method

Linear quadratic regulator (LQR) described in section 5.4.3 is used to integrate two standalone controllers ARS and TV. The state variables of LQR are vehicle sideslip angle, and yaw rate and outputs of it are rear wheel steering and yaw moment. Bicycle model which is described in section 4.1.4 is used to define the lateral vehicle dynamics. The vehicle model can be written in the state-space form as follows:

$$A = \begin{bmatrix} \dfrac{-(C_{\alpha_f} + C_{\alpha_r})}{mV} & -1 + \dfrac{C_{\alpha_r} l_r - C_{\alpha_f} l_f}{mV^2} \\ \dfrac{(C_{\alpha_r} l_r - C_{\alpha_f} l_f)}{I_{zz}} & \dfrac{-(C_{\alpha_f} l_f^2 + C_{\alpha_r} l_r^2)}{I_{zz} V} \end{bmatrix}$$
$$B = \begin{bmatrix} \dfrac{C_{\alpha_r}}{mV} & 0 \\ \dfrac{-C_{\alpha_r} l_r}{I_{zz}} & -\dfrac{1}{I_{zz}} \end{bmatrix} \tag{6.1}$$

where control output is u=[δ_r M_z]. M_z is the amount of a required yaw moment in order to stabilize the vehicle which is applied by TV by modifying the distribution of driving torque to the wheels and δ_r is the required angle for rear wheels which is calculated by the controller in order to apply by ARS.

Numerical results

Three different maneuvers were carried out to analyze and investigate the effect of integrated vehicle dynamics system. All these maneuvers are commonly utilized in vehicle tests and can emulate vehicle's performance in extreme cases. Moreover, these maneuvers are selected to analyze the vehicle behavior in steady-state and transient conditions.

Ramp steer

These maneuvers were carried out for constant speed profile values of 100 km/h, 125 km/h, 150 km/h, 175 km/h and 200 km/h. A slowly increasing steering angle up to 150° with a rate of angle increase of 37.5° per second was utilized. Simulation results are illustrated in Figures 6.1. The figure depicts the response of the vehicle in terms of steer angle vs. lateral acceleration, and the slope of the curve represents the understeer gradient. A positive slope displays understeer, zero slope represents neutral steer, and a negative slope indicates oversteer. Some vehicles will remain understeer over the entire operating range. Other vehicles can be understeer at the low levels of lateral acceleration and alter to oversteer condition at the high levels of lateral acceleration and illustrate limit oversteer [137]. By looking at the figures, one can understand that increasing speed allows reaching higher levels of lateral acceleration. In passive and HIS vehicle, by considering the lateral

acceleration developed as a function of steer angle, its value decreases after reaching the maximum. This is particularly evident at 150 km/h, 175 km/h and 200 km/h. For ARS vehicle, there is a linear relationship between the steering angle and lateral acceleration, but by increasing velocity especially at 175km/h and 200 km/h, the vehicle is going to lose stability. For TV vehicle, it can be said that vehicle has a good performance and good stability at different levels of lateral acceleration and various speeds. On the other hand, the performance of integrated vehicle dynamics system (LQR) has a superior capability in controlling vehicle compared with other standalone controllers and passive vehicle, and it does not allow the vehicle to reach handling limit. This is because of utilizing bicycle vehicle model (linear) to design the integrated system; therefore the behavior of the vehicle is linear most of the time even at high levels of lateral acceleration.

In addition, Tables 6.2 and 6.3 which are related to ramp steer maneuver compare the understeer coefficient at two different levels of lateral acceleration to understand the dynamic behavior of the vehicle in terms of understeer coefficient. By looking at the Table 6.2, it can be observed that the performance of Passive and HIS vehicles are almost the same and ARS vehicle has a higher understeer coefficient due to the characteristic of active steering which provides more understeer tendency to the vehicle. When it comes to comparing the TV vehicle and the LQR integrated vehicle, the understeer coefficients of the TV at 100 km/h, 125 km/h, and 150 km/h are superior to LQR, but at high speeds, the performance of integrated vehicle dynamics system (LQR) is better.

Table 6.2: Comparison of understeer coefficient k_{us} where $a_y/g = 0.4$ in ramp steer maneuver with final steer amplitude of 150° at various velocities

0.4 g	100 km/h	125 km/h	150 km/h	175 km/h	200 km/h
Passive	0.0061	0.0058	0.0054	0.0051	0.0047
HIS	0.0061	0.0058	0.0054	0.0050	0.0047
ARS	0.0522	0.0415	0.0349	0.0299	0.0263
TV	-0.0153	-0.0081	-0.0044	-0.0022	-0.0008
LQR	-0.0172	-0.0091	-0.0045	-0.0016	0.0004

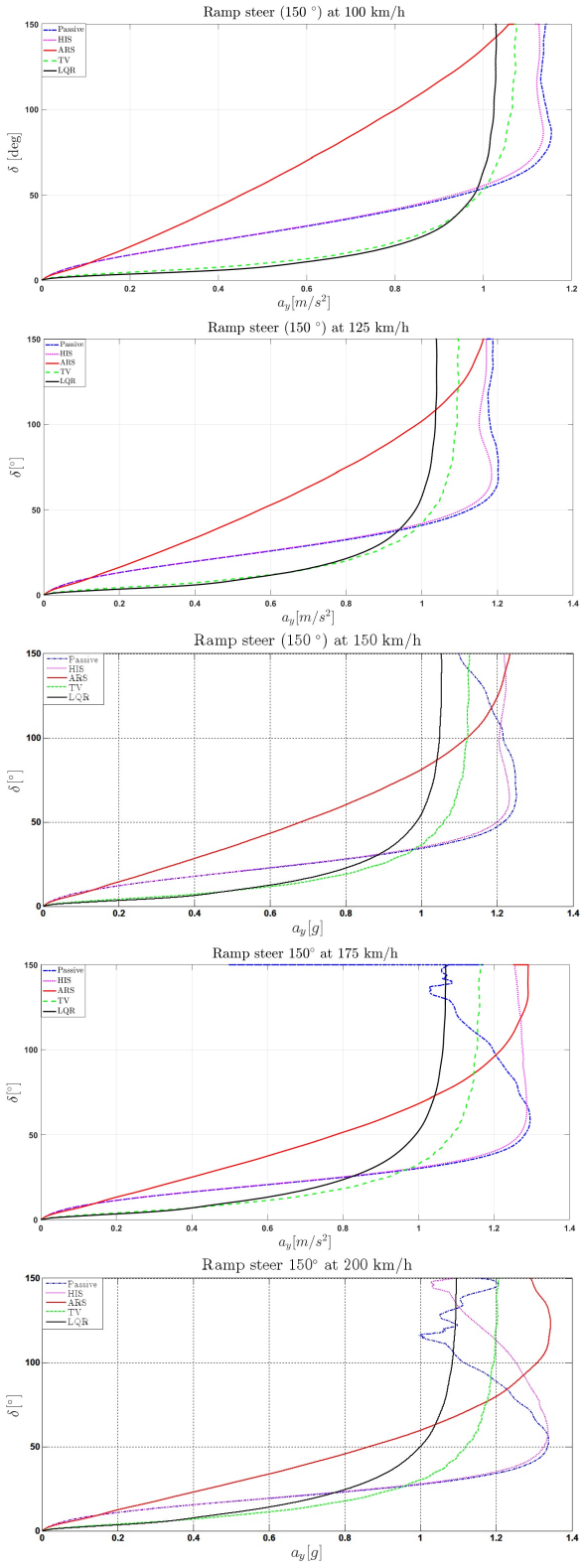

Figure 6.1: Simulation results of ramp steer input with final amplitude of 150° at various velocities

Table 6.3 compares the understeer coefficient of active chassis controllers at the lateral acceleration of 0.7 g. As mentioned before, ARS has a higher understeer coefficient due to the nature of the controller. When the vehicle is traveling at 100 km/h, the performance of TV is better compared with LQR, but at the speeds of 125 km/h and 150 km/h the performance of LQR is improved, however by increasing the speed (175 km/h and 200 km/h) TV has a superior performance.

Table 6.3: Comparison of understeer gradient k_{us} where $a_y/g = 0.7$ of ramp steer maneuver with final steer amplitude of 150° at various velocities

0.7 g	100 km/h	125 km/h	150 km/h	175 km/h	200 km/h
Passive	0.0055	0.0049	0.0045	0.0042	0.0039
HIS	0.0059	0.0050	0.0047	0.0043	0.0040
ARS	0.0540	0.0427	0.0353	0.0301	0.0266
TV	-0.0087	-0.0026	0.0059	0.0023	0.0032
LQR	-0.0108	-0.0024	0.0025	0.0055	0.0075

6.3.2 Fuzzy logic method

This control strategy needs to regulate the active regions of the two standalone chassis control system regarding the vehicle states in order to prevent control objective conflicts. Therefore, this control strategy requires some states of the vehicle to determine the activation process for the controllers. The range of the operating system is from the low levels of lateral acceleration (normal driving) to the high level of it or handling limit.

The working principle of the control strategy will be described as follows:

The coordinator function weights the input from dynamic yaw control depending on several states, including steering angle, yaw rate, longitudinal velocity and vehicle sideslip angle. This coordinator is divided into two parts. The first one consists of a fuzzy system responsible for generating the weighting parameter (W_1) for Active Rear Steering (ARS). The other part is the same methodology which is responsible for generating weighting parameter (W_2) for torque vectoring

system (TV). This fuzzy system represents functions W_1=f(δ, $\dot{\psi}$, v_x, β) and W_2=f(δ, $\dot{\psi}$, v_x, β).

The identification of W_1 and W_2 required to obtain the desired behavior is performed through look-up tables defined according to the process described in the following. Some numerical simulations were carried out considering the vehicle running under various step steer maneuvers (δ=30°,60° and 90°) at 100 and 150 km/h. For each steering angle and speed, different combinations of W_1 and W_2 were considered: in particular each weight was changed in the range 0 to 1 with a resolution of 0.25.

The fitness function adopted is the sum of some partial cost functions. The integrated vehicle control system has to able to optimize yaw rate in order to have the desired response. The following equation is the fitness function adopted in this learning process, where L_i is the weighting constant for each partial cost function.

$$f(\delta, \dot{\psi}, v_x, \beta) = L_1 \frac{\beta_{reg}}{\beta_{reg_{target}}} + L_2 \frac{\dot{\psi}_{os}}{\dot{\psi}_{os_{target}}} + L_3 \frac{\beta_{os}}{\beta_{os_{target}}} + L_4 \frac{\dot{\psi}_{target}}{\dot{\psi}_{reg}} \tag{6.2}$$

where
β_{reg} = The value of vehicle sideslip angle in regime condition
$\beta_{reg_{target}}$ = The target value of vehicle sideslip angle in regime condition
$\dot{\psi}_{os}$ = The overshoot of yaw rate
$\dot{\psi}_{os_{target}}$ = The target value for overshoot of yaw rate
β_{os} = The overshoot of vehicle sideslip angle
$\beta_{os_{target}}$ = The target value for overshoot of vehicle sideslip angle
$\dot{\psi}_{target}$ = The target value for yaw rate
$\dot{\psi}_{reg}$ = The value of yaw rate in regime condition
L_i (i=1,2,3,4) = weighting constants

The weighting constants used in this fitness function were based on an initial set of simulations and relative importance of each partial cost function and chosen to give reasonable and representative vehicle behavior. In this thesis, two sets of L_i was chosen:

- The first one is based on normal or safe driving. This means that our priority for choosing to weight constant is to give more weights on safety cost functions.
  L_1=0.1
  L_2=0.1
  L_3=0.1

L_4=0.7

- The second one is based on sport driving. This means that our priority for choosing to weight constant is to give more weights on performance cost functions.
  L_1=0.33
  L_2=0.33
  L_3=0.33
  L_4=0

As the fuzzy coordinator has four inputs and two outputs, the inputs were grouped two by two as W(δ, v_x) and W(β, $\dot{\psi}$) and their relationships are shown in Figures 6.2, 6.3, 6.4, 6.5, 6.6, 6.7, 6.8 and 6.9 After selection of W with respect to inputs, the outputs of each table, which is related to a standalone controller, sum up and divide by two for providing a weight for each controller. Note that the values of tables are different for each mode (normal or sport) of driving.

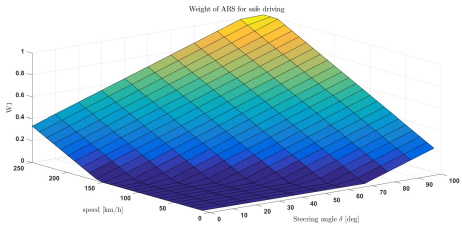

Figure 6.2: Coordinator of W_1 for safe driving based on δ and v_x

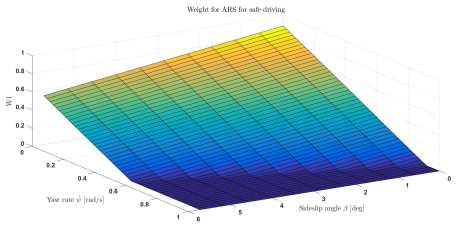

Figure 6.3: Coordinator of W_1 for safe driving based on β and $\dot{\psi}$

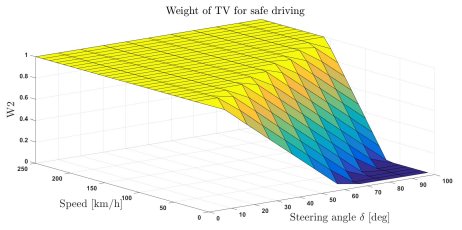

Figure 6.4: Coordinator of W_2 for safe driving based on δ and v_x

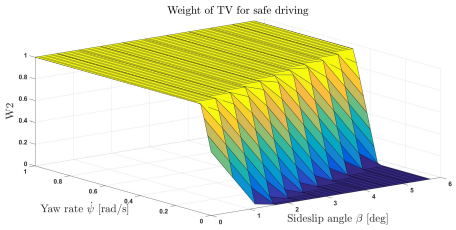

Figure 6.5: Coordinator of W_2 for safe driving based on β and $\dot{\psi}$

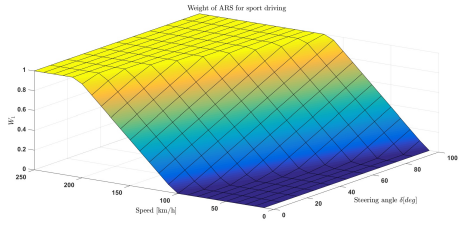

Figure 6.6: Coordinator of W_1 for sport driving based on δ and v_x

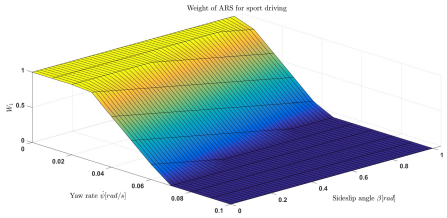

Figure 6.7: Coordinator of W_1 for sport driving based on β and $\dot{\psi}$

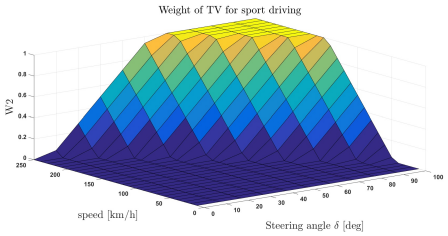

Figure 6.8: Coordinator of W_2 for sport driving based on δ and v_x

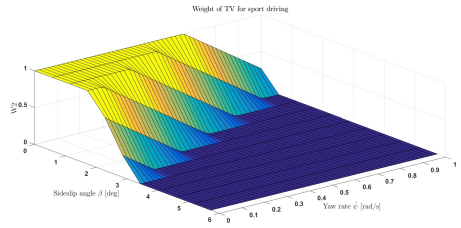

Figure 6.9: Coordinator of W_2 for sport driving based on β and $\dot{\psi}$

Numerical results

Ramp steer

These maneuvers are carried out for constant speed profile values of 100 km/h, 125 km/h, 150 km/h, 175 km/h and 200 km/h. A slowly increasing steering angle up to 150° with a rate of angle increase of 37.5° per second was utilized. Simulation results are illustrated in Figures 6.10. The figure depicts the response of the vehicle in terms of steer angle vs. lateral acceleration, and the slope of the curve represents the understeer gradient. By increasing the speed of the vehicle in the maneuver, the vehicle can reach the higher level of acceleration as seen in the Figure 6.10. As discussed the behavior of the standalone chassis control system in this maneuver in the previous section, the dynamic behavior the integrated vehicle dynamics control (fuzzy logic) will be discussed. The performances of the Fuzzy-safe and Fuzzy sport have completely different due to the priority of each integrated vehicle dynamics system. In other words, the priority of Fuzzy-safe is to stabilize the vehicle and to avoid the vehicle from hazardous situations while the priority of fuzzy-sport is to let the vehicle to approach to the handling limit such that the driver enjoys driving. Then the control system intervenes to prevent the vehicle from losing stability.

Moreover, Tables 6.4 and 6.5 which are related to ramp steer maneu-

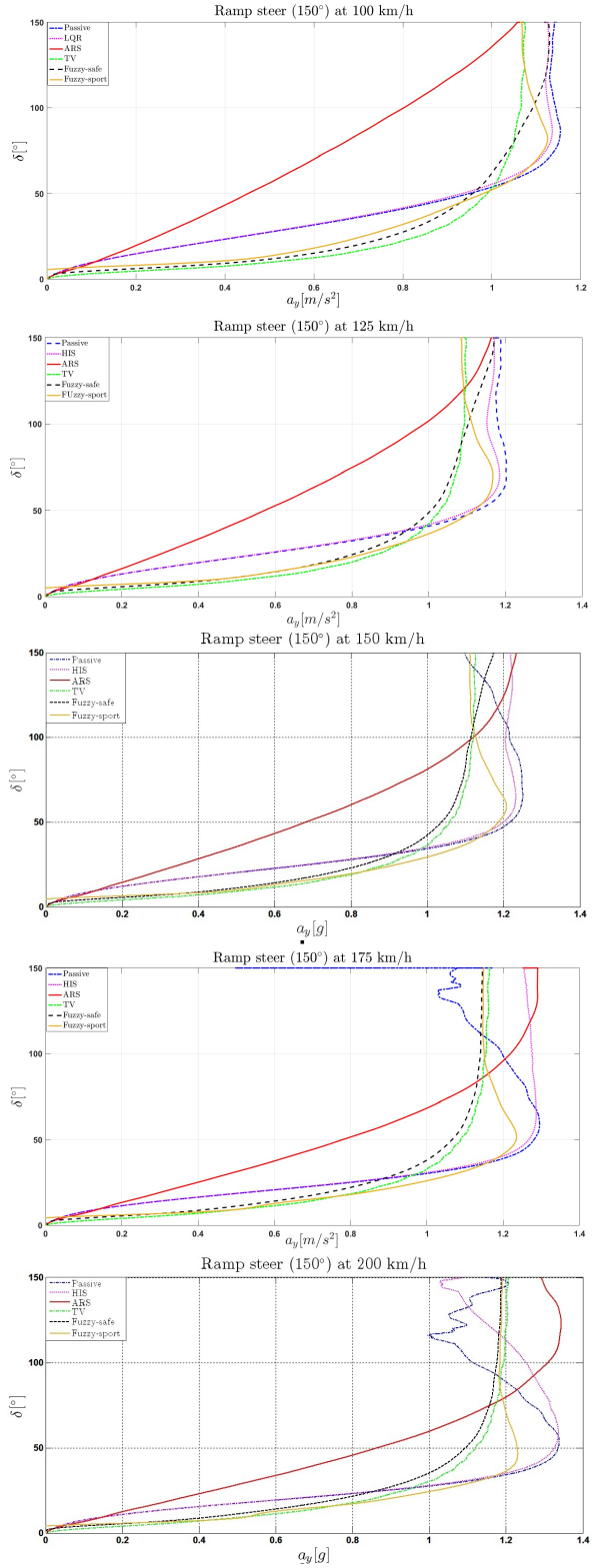

Figure 6.10: Simulation results of ramp steer input with final amplitude of 150° at various velocities

ver compare the understeer gradient at two different levels of lateral acceleration to understand the dynamic behavior of the vehicle regarding understeer gradient. Table 6.4 shows the understeer coefficient when the lateral acceleration of the vehicle is 0.4 g. Again, ARS vehicle has a higher understeer coefficient at various velocities due to the characteristic of active steering. By comparing the understeer coefficient of TV, Fuzzy-safe, and Fuzzy-sport, the performance of Fuzzy-sport is better at low speeds, but by increasing the speed, the performance of the Fuzzy-safe is improved in terms of understeer coefficient.

Table 6.4: Comparison of understeer coefficient k_{us} where $a_y/g = 0.4$ of ramp steer maneuver with final steer amplitude of 150° at various velocities

0.4 g	100 km/h	125 km/h	150 km/h	175 km/h	200 km/h
Passive	0.0061	0.0058	0.0054	0.0051	0.0047
HIS	0.0061	0.0058	0.0054	0.0050	0.0047
ARS	0.0522	0.0415	0.0349	0.0299	0.0263
TV	-0.0153	-0.0081	-0.0044	-0.0022	-0.00085
Fuzzy-safe	-0.0133	-0.0064	-0.0026	-0.00042	-0.00096
Fuzzy-sport	-0.0112	-0.0065	-0.0039	-0.0030	-0.0012

The Table 6.5 reports the understeer coefficient at the high level of lateral acceleration (0.7g). By looking at the table, one can understand that by increasing the speed, the understeer coefficient is changing from negative value to positive value in TV, Fuzzy-safe, and Fuzzy-sport. This means that the behavior of the vehicle is going to understeer condition when the vehicle is traveling at high speeds. Fuzzy-sport has a better performance till 150 km/h compared with Fuzzy-safe and TV, but beyond that velocity, the performance of TV is better.

6.3.3 Comparison of two methods

This section compares between the two integrated schemes. In order to compare, various maneuvers were carried out to understand the vehicle's behavior under different levels of acceleration.

Table 6.5: Comparison of understeer coefficient k_{us} where $a_y/g = 0.7$ of ramp steer maneuver with final steer amplitude of 150° at various velocities

0.7 g	100 km/h	125 km/h	150 km/h	175 km/h	200 km/h
Passive	0.0055	0.0049	0.0045	0.0042	0.0039
HIS	0.0059	0.0050	0.0047	0.0043	0.0040
ARS	0.0540	0.0427	0.0353	0.0301	0.0266
TV	-0.0087	-0.0026	0.00059	0.0023	0.0032
Fuzzy-safe	-0.0046	0.00029	0.0032	0.0048	0.0063
Fuzzy-sport	-0.0009	-0.00029	0.0010	0.0020	0.0027

Ramp steer

Results presented in Figure 6.11 are related to ramp steer up to 150° maneuvers to analyze the steady state response of the vehicle. In particular, the vehicle is running on dry asphalt at 100 km/h, 125 km/h, 150 km/h, 175 km/h and 200 km/h while the steering wheel reaches 150° in almost 4 s with a rate of 37.5 °/s. Figure 6.11 depicts the response of the different types of vehicles regarding steer angle vs. lateral acceleration.

The performance of LQR is almost the same at various speeds, and the LQR method provides the lowest lateral acceleration even at high speeds. The combined controller can achieve good performance with the higher level of lateral acceleration compared to LQR. When it comes to Fuzzy-safe, it is interesting to point out that the controller allows to reach the higher level of the lateral accelerations by increasing the speed of the vehicle due to characteristics of the controller and the performance of the controller is good especially at high speeds. The dynamic behavior of Fuzzy-sport is different, and it reaches to the higher level of lateral acceleration at the low level of steering angle, and by increasing the steering angle, the controller reduces the lateral acceleration due to the possibility of losing stability.

Table 6.6 compares the understeer coefficient of the vehicle at 0.4 g. Fuzzy-sport is acting better at 100 km/h and 125 km/h, and by increasing the velocity of the vehicle at 150 km/h and 175 km/h, Fuzzy-

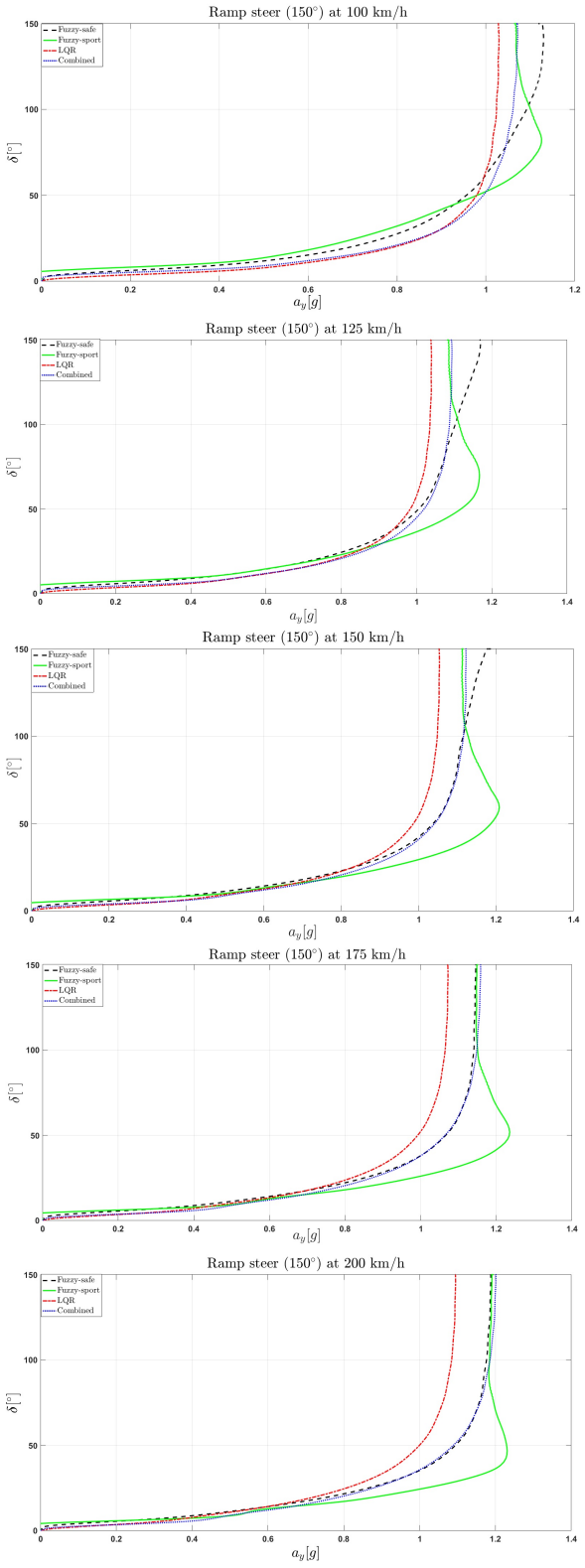

Figure 6.11: Simulation results of ramp steer input with final amplitude of 150° at various velocities

safe has a better performance compared with others. At 200 km/h, the Combined controller has a lowest $k_u s$ among the other controllers.

Table 6.6: Comparison of understeer gradient k_{us} where $a_y/g = 0.4$ of ramp steer maneuver with final steer amplitude of 150° at various velocities

0.4 g	100 km/h	125 km/h	150 km/h	175 km/h	200 km/h
Combined	-0.0162	-0.0088	-0.0047	-0.0024	-0.0008
LQR	-0.0172	-0.0091	-0.0045	-0.0016	0.00048
Fuzzy-safe	-0.0133	-0.0064	-0.0026	-0.00042	-0.00096
Fuzzy-sport	-0.0112	-0.0065	-0.0039	-0.0030	-0.0012

The understeer coefficients of various integrated methods at 0.7g in ramp steer maneuver at different velocities are reported in the Table 6.7. As it can be seen in the Table 6.7, understeer coefficients are changing from negative to positive which means that the behavior of the controller is changing from oversteer to understeer tendency by increasing the speed of the vehicle. The best performance among the controllers is the Fuzzy-sport due to minimum value compared with other controllers at different velocities.

Table 6.7: Comparison of understeer gradient k_{us} where $a_y/g = 0.7$ of ramp steer maneuver with final steer amplitude of 150° at various velocities

0.7 g	100 km/h	125 km/h	150 km/h	175 km/h	200 km/h
Combined	-0.01	-0.0024	0.0016	0.0039	0.0053
LQR	-0.0108	-0.0024	0.0025	0.0055	0.0075
Fuzzy-safe	-0.0046	0.00029	0.0032	0.0048	0.0063
Fuzzy-sport	-0.0009	-0.00029	0.0010	0.0020	0.0027

Table 6.8 shows the overshoots of yaw rate and sideslip angle for step steer maneuver at 75 km/h with final steer of 45° in 0.1 seconds in two modes which the first mode is with the constant speed named "Power

ON" and the second mode is when the driver releases the throttle named "Power OFF". By looking at the Table 6.8, the minimum overshoot of the yaw rate and sideslip angle of the vehicle in the mode of Power ON and Power OFF belongs to Fuzzy-sport scheme. The performances of Fuzzy-safe and Combined are also acceptable, while LQR is not able to stabilize the vehicle in the Power OFF mode and the vehicle is going to lose controllability. The results demonstrate that the effective region of LQR scheme in low speeds is not satisfactory.

Table 6.8: Simulation results of step steer maneuver with final steer of 45° at 75 km/h in two modes: a) Power ON = constant speed b) Power OFF = releasing throttle

Mode	**Power ON**		**Power OFF**	
	$\boldsymbol{\beta_{os}}$ [°]	$\boldsymbol{\dot{\psi}_{os}}$ [deg/s]	$\boldsymbol{\beta_{os}}$ [°]	$\boldsymbol{\dot{\psi}_{os}}$ [deg/s]
LQR	7.6478	28.6285	22.5582	75.5256
rule-based-safe	3.3984	23.9084	3.8720	28.8543
rule-based-sport	2.6606	23.2947	2.5746	23.3807

Simulation results of step steer maneuver at 100 km/h with final steer 45° in 0.1 seconds in Power ON and Power OFF modes for different control schemes is reported in Table 6.9. The best performance belongs to Fuzzy-safe in two modes. It is interesting to point out that the overshoot of yaw rate of Fuzzy-sport is lower than the Fuzzy-safe scheme while the overshoot of the vehicle sideslip angle of Fuzzy-safe is less than Fuzzy-sport. Also, the performance of LQR scheme is acceptable in both modes of maneuver.

6.4 Integration of ARS, TV, AAC and HIS

This section dedicates to the integration of four subsystems. The method is the same as in the previous section 6.3.2. This strategy needs to determine an active region of three standalone active chassis control systems to prevent conflicts between the controllers' objectives and to avoid over-correction behavior. As mentioned before, even though the HIS is implemented, but the behavior of HIS is not integrated. A quantitative measure of this logic is based on the steering angle, velocity,

Table 6.9: Simulation results of step steer maneuver with final steer of 45° at 100 km/h in two modes: a) Power ON = constant speed b) Power OFF = releasing throttle

Mode	**Power ON**		**Power OFF**	
	β_{os} [°]	$\dot{\psi}_{os}$ [deg/s]	β_{os} [°]	$\dot{\psi}_{os}$ [deg/s]
Combined	4.6123	22.5459	5.1837	30.0196
LQR	6.8855	21.4029	9.2861	36.1774
Fuzzy-safe	4.4624	22.4370	5.0888	28.1758
Fuzzy-sport	4.7053	23.2669	7.1662	27.5479

Table 6.10: Simulation results of step steer maneuver with final steer of 45° at 125 km/h in two modes: a) Power ON = constant speed b) Power OFF = releasing throttle

Mode	**Power ON**		**Power OFF**	
	β_{os} [°]	$\dot{\psi}_{os}$ [deg/s]	β_{os} [°]	$\dot{\psi}_{os}$ [deg/s]
Combined	4.7588	19.5773	5.5767	24.6966
LQR	5.8725	17.0964	8.4272	25.9852
Fuzzy-safe	5.0177	20.9125	6.1063	24.6127
Fuzzy-sport	6.3925	22.7296	178.2711	86.0781

yaw rate and vehicle sideslip angle. It is assumed that the road surface coefficient and the vehicle sideslip angle are measured or estimated by VI-Grade commercial software. The AAC logic utilizes $a_y - v_x\dot{\psi}$ as the measure of operating point; however, TV and ARS uses $\dot{\psi}_{ref} - \dot{\psi}$ and $\beta_{ref} - \beta$ as the measure of operating point when the system working in a standalone mode. Therefore, it can be a conflict between the object of AAC, TV, and ARS. To overcome this, it needs to design and develop a logic that can prevent the objective conflict. So that the logic of the AAC should be changed to eliminate the probable conflict between AAC and other controllers. The new logic of AAC is according to the wights which are based on the steering angle, velocity, sideslip angle, and yaw rate. The developed integrated control system has four inputs and four outputs. The steering angle, velocity, vehicle sideslip angle, and yaw rate are fed back to the integrated control system as inputs and used to determine the weight of the controllers. The Fuzzy based integrated controller activates the ARS, TV, and AAC according to the states of the vehicle. For instance, the integrated scheme provides more weight to the AAC when the vehicle is traveling at high speed or increasing speed. In the following the detailed description of the controller strategy will be explained:

The coordinator function weights the input from dynamic yaw control depending on several states, including steering angle, yaw rate, velocity and vehicle sideslip angle. This coordinator is divided into four parts. The first one includes a fuzzy system responsible for generating the weighting parameter (W_1) for the front spoiler of AAC which adjusts the angle of attack and the second (W_2) alters the angles of the rear spoiler. The third part is the same methodology which is responsible for generating weighting parameter (W_3) for Active Rear Steering (ARS). The fourth part is related to Torque Vectoring System (TV). This fuzzy system represents functions W_1=f(δ, $\dot{\psi}$, v_x, β), W_2=f(δ, $\dot{\psi}$, v_x, β), W_3=f(δ, $\dot{\psi}$, v_x, β) and W_4=f(δ, $\dot{\psi}$, v_x, β).

The identification of W_1, W_2, W_3 and W_4 required to obtain the desired behavior is performed through look-up tables defined according to the process described in the following. Some numerical simulations were carried out considering the vehicle running under various step steer maneuvers (δ=30°, 60° and 90°) at 150, 200 and 250 km/h. For each steering angle and speed, different combinations of W_1, W_2, W_3 and W_4 were considered: in particular, each weight was changed in the range 0 to 1 with a resolution of 0.5. The fitness function adopted is the sum of a number of a partial cost function which is described in the previous section as an equation 6.2. In this control strategy, constants L_i (i=1, 2, 3 and 4) are demonstrated as follows:

L_1=0.33
L_2=0.33
L_3=0.33
L_4=0

As the fuzzy coordinator has four inputs and three outputs, the inputs were grouped two by two as W(δ, v_x) and W(β, $\dot{\psi}$) and their relationships for the front and rear spoilers are shown in Figures 6.12, 6.13, 6.14 and 6.15. After selection of W with respect to inputs, the outputs of each look-up table, which is related to a standalone controller, sum up and divide by two in order to weight the controller.

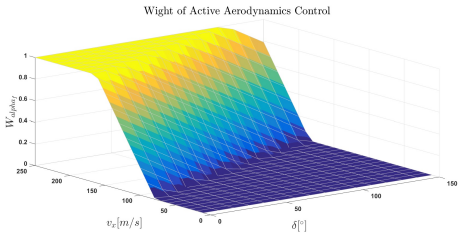

Figure 6.12: Coordinator of W_1 based on δ and v_x

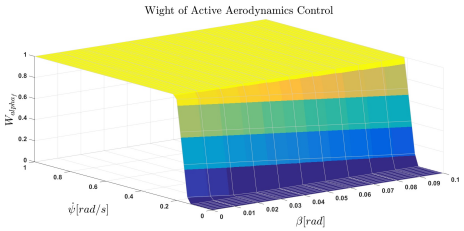

Figure 6.13: Coordinator of W_1 based on β and $\dot{\psi}$

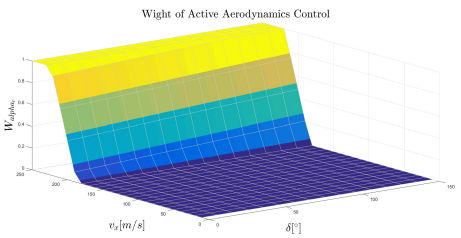

Figure 6.14: Coordinator of W_2 based on δ and v_x

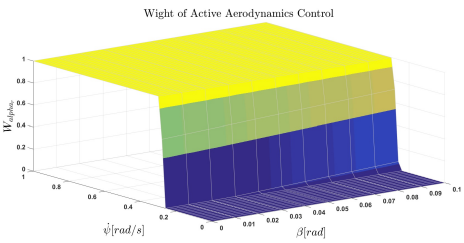

Figure 6.15: Coordinator of W_2 based on β and $\dot{\psi}$

6.4.1 Numerical Results

To assess the stability, performance and comfort of the vehicle under different situations and different range of vehicle handling, various maneuvers are set to understand the performance of the integrated scheme. First, the proposed integrated control scheme will be evaluated in steady-state maneuver (ramp steer). Then, it will be assessed in transient maneuver (step steer).

Figure 6.16 depicts the ramp steer maneuver at different velocities for three types of vehicle: passive, combined and fuzzy. The vehicle is

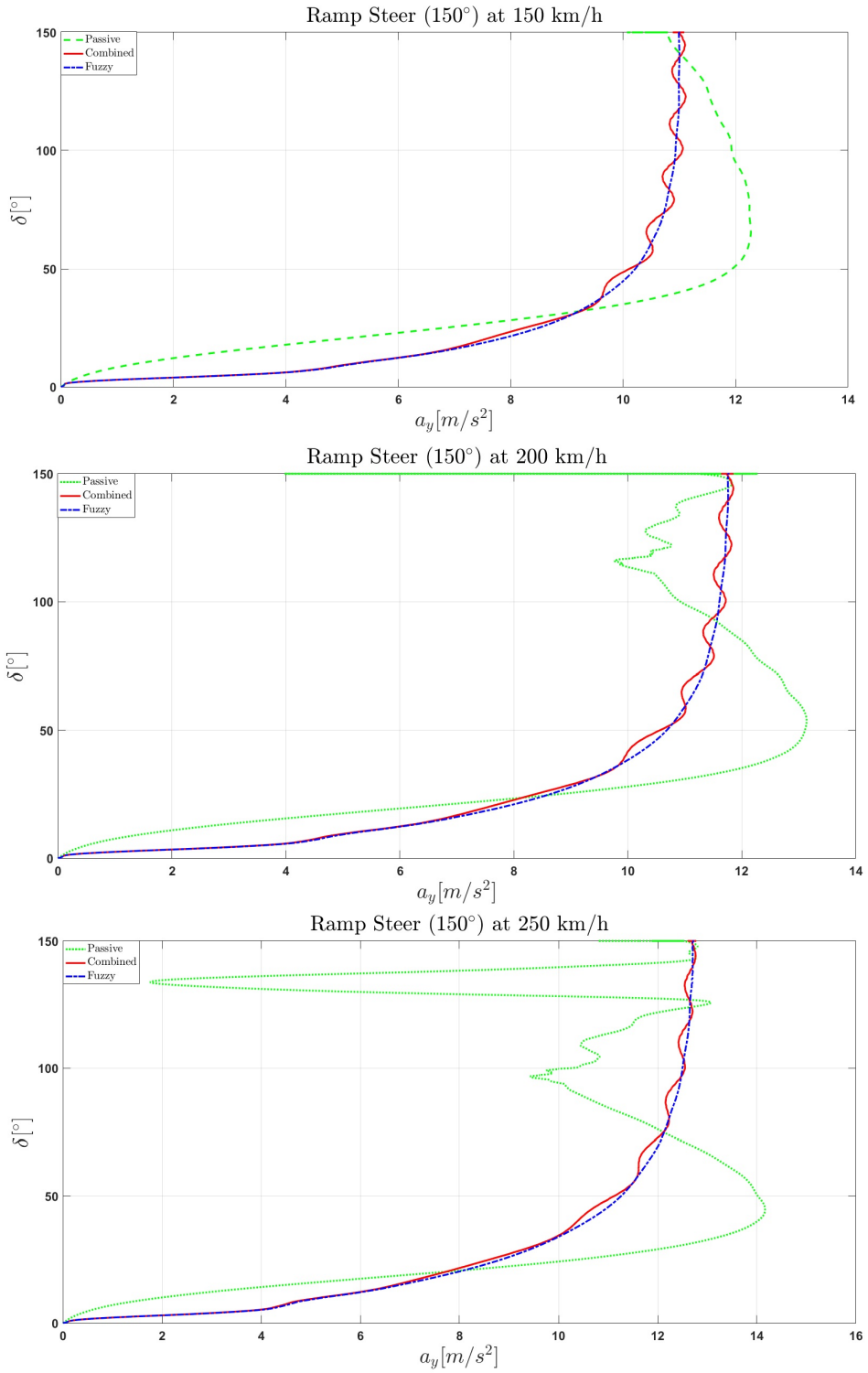

Figure 6.16: Simulation results of ramp steer input with final amplitude of 150° at various velocities

running on dry asphalt at 150 km/h, 200 km/h, and 250 km/h while the steering wheel reaches 150° in almost 4 s with a rate of 37.5 °/s. The passive vehicle has a high level of lateral acceleration at different velocities compared to Combined and Fuzzy vehicles, and it loses its stability in all the maneuvers. The Combined vehicle has some instability from 150 km/h up to 250 km/h. This occurs due to the objective conflicts between the subsystems. Therefore, the combined vehicle is not able to be effective by the superpositioning of the subsystems. When it comes to fuzzy approach, one can understand that the coordinator can effectively manage the subsystems to prevent the objective conflicts and increase the potential of each subsystem.

Table 6.11 illustrates the understeer coefficient of ramp steer maneuver at various velocities where the lateral acceleration is 0.4g. The passive vehicle is in understeer condition due to the positive value at different speeds. When it comes to comparing Fuzzy and Combined, it can be recognized that the Fuzzy has a better performance due to the lower value compared to Combined control regarding understeer coefficient.

Table 6.11: Comparison of understeer coefficient k_{us} where $a_y/g = 0.4$ of ramp steer maneuver with final steer amplitude of 150° at various velocities

0.4 g	150 km/h	200 km/h	250 km/h
Passive	0.0054	0.0047	0.0041
Combined	-0.0046	-0.0007	0.00079
Fuzzy	-0.0047	-0.0008	-0.00068

Table 6.12 refers to the understeer coefficient in ramp steer maneuver at different velocities where the lateral acceleration is 0.7g. The passive vehicle has a different response at various velocity, which is an understeer at 150 km/h and it changes to an oversteer situation at 200 km/h then it alters to an understeer condition at 250 km/h. By comparing the Combined control and Fuzzy scheme, the performance of Fuzzy has a better performance in terms of understeer coefficient at all velocities because of lower value.

Figure 6.17 refers to a step steer maneuver performed at 250 km/h with a final steer angle of 45° (steer at wheels is up to 2°). The step steer is completed in 0.1 s and is performed on a dry road (μ= 1) in Power ON mode which means that the velocity is constant during the

Table 6.12: Comparison of understeer coefficient k_{us} where $a_y/g = 0.7$ of ramp steer maneuver with final steer amplitude of 150° at various velocities

0.7 g	150 km/h	200 km/h	250 km/h
Passive	0.0045	-0.0334	0.0035
Combined	0.0021	0.0059	0.0071
Fuzzy	0.0017	0.0054	0.0066

maneuver. Figure 6.17(a) compare the vehicle yaw rate of the combined control and fuzzy scheme, and the performance of both control scheme is almost the same. Figure 6.17(b) represents the roll angle of the vehicle, and the performance of the fuzzy is better in terms of the comfort of the vehicle, and it can successfully eliminate the oscillation in roll motion. When it comes to the lateral acceleration of the vehicle which is demonstrated in Figure 6.17(c), and there is some instability in combined control due to the oscillation. However, the fuzzy scheme can significantly remove the oscillation. Figure 6.17(d) depicts the spoilers' the angle of attack in combined control and fuzzy scheme, and it can be seen that the working principle of the AAC in two different control scheme is entirely different. So that, by changing the logic of the AAC, the latter can efficiently affect the performance of the vehicle.

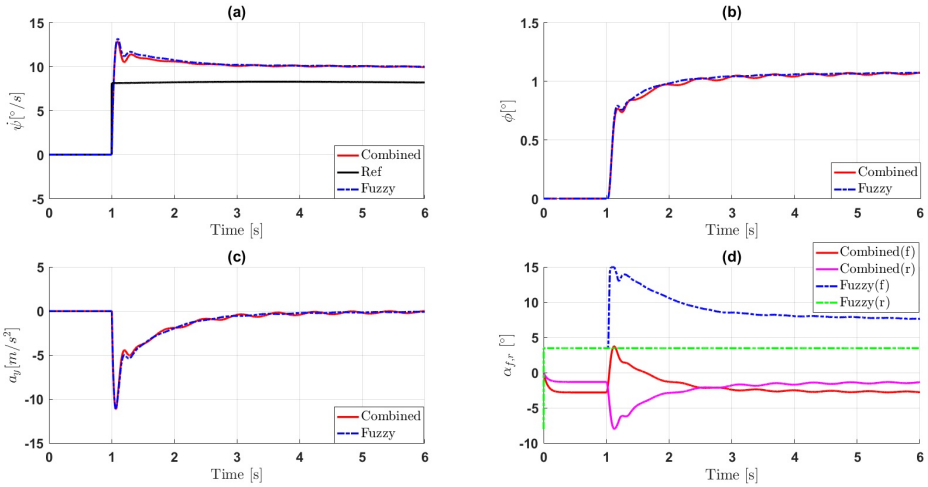

Figure 6.17: Simulation results of step steer input with final amplitude of 45° at 250km/h in Power ON mode

Simulation results for the step steer input at 250 km/h with a final steer angle of 45° are plotted in Figure 6.18 in Power OFF mode which means the driver release the throttle during the maneuver. The yaw rate of the vehicle illustrated in Figure 6.18(a) is almost the same in both control schemes. As seen in the Figure 6.18(b), there is an oscillation in the roll angle of the vehicle which causes discomfort to the passengers, while fuzzy scheme can remarkably eliminate the oscillation. By comparing two controllers in terms of lateral acceleration which is shown in Figure 6.18(c), the combined control has again instability which leads to decreasing the safety and performance of the vehicle whereas the fuzzy scheme has a superior performance regarding lateral acceleration. The angle of attack of spoilers is depicted in Figure 6.18(d), and it can be seen that the AAC of the fuzzy utilize the spoilers to generate downforce especially the front spoiler, while the AAC of the combined control employed spoilers to create lift force.

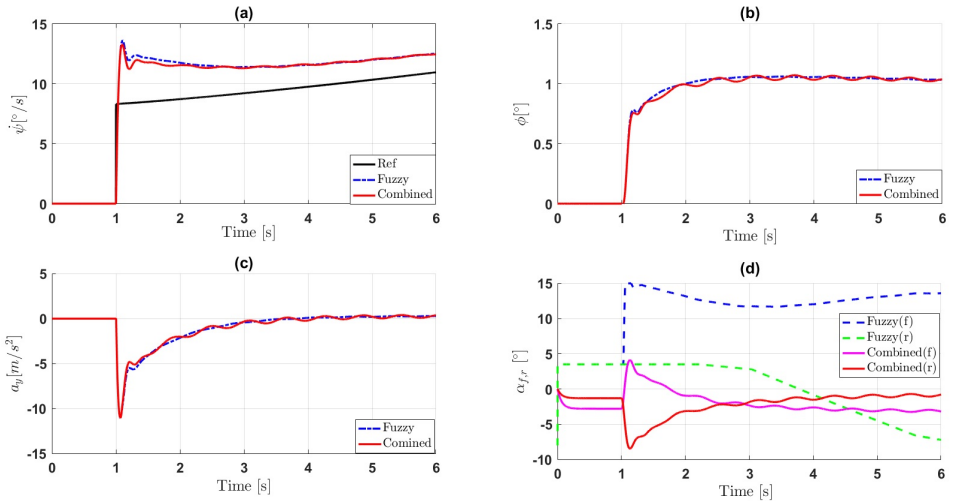

Figure 6.18: Simulation results of step steer input with final amplitude of 45° at 250km/h in Power OFF mode

The mentioned above simulation is done on a wet road ($\mu = 0.5$) to assess the performance of the proposed integrated scheme on a different road surface as shown in Figure 6.19. In terms of yaw rate, the performance of both fuzzy and combined control is almost the same which is illustrated in Figure 6.19(a). But when it comes to roll angle and lateral acceleration as depicted in Figures 6.19(b) and 6.19(c), respectively, there is some instability in the performance of the combined control. However, the Fuzzy scheme has a better performance with respect to the roll angle and lateral acceleration. The spoilers' the angle of attack for both the combined and fuzzy system are demonstrated in

Figure 6.19(d).

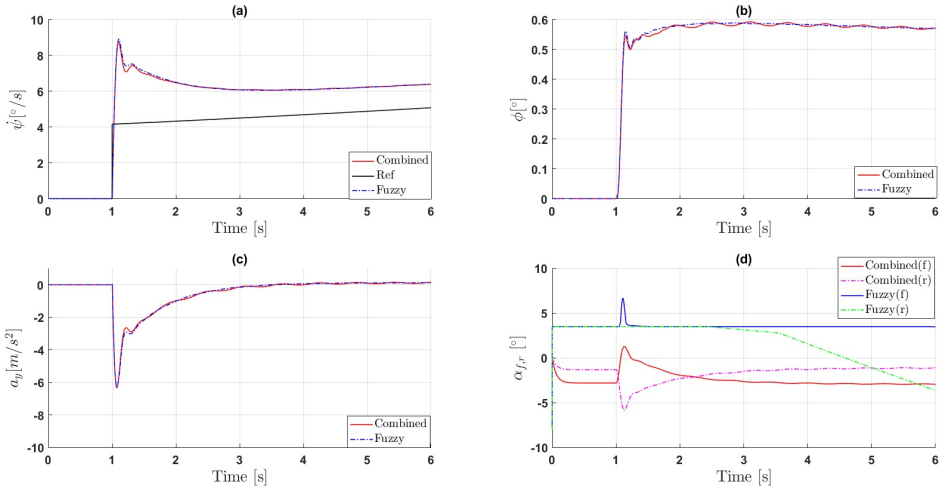

Figure 6.19: Simulation results of step steer input with final amplitude of 45° at 250km/h in Power OFF mode on a wet road

In a nutshell, the fuzzy scheme performs better than the combined control in terms of roll angle and lateral acceleration by reducing the oscillation which causes discomfort and instability. However, the yaw rate of the vehicle is the same in two controllers.

6.5 Summary

This chapter discussed the integration of three and four active chassis control systems developed in the previous chapter to enhance vehicle handling performance. It started with the integration of three controllers with two methods and assessed by comparing with passive, subsystems and combined control system and analyzed their control authorities on vehicle handling dynamics. Then, integration of four subsystems was developed by a fuzzy approach and evaluated by comparing with a passive and combined control system for various maneuvers in order to demonstrate the effectiveness of the proposed integrated scheme.

Chapter 7

Conclusion

7.1 Conclusions

The results and the achievements of the presented research will be summarized in this chapter. It begins with a short review of the contents of the thesis and the contribution to the proposed solution. Then, the met objectives of the thesis will be confirmed. Finally, the chapter demonstrates recommendations for future work.

It was proved that active vehicle dynamics control has a significant impact on the enhancement of vehicle stability, performance, and handling. A detailed review of literature according to several standalone control systems has been carried out for the investigation of the current development of vehicle dynamics control related to handling section. Aims of these controllers are to control the longitudinal, lateral and vertical forces. Although all the aforementioned standalone chassis control systems enhance the lateral vehicle dynamics, each standalone chassis control system has its strong side and weak side. Therefore, different subsystems are integrated to comprise for each other's drawbacks. However, the integration of standalone chassis control systems is not a simple task. The conflicting and overlapping of the objectives can occur due to the integration. Besides, The more increase the number of standalone vehicle dynamics control systems, the more increase the complexity, undesirable interactions and performance deterioration in vehicle control system. Consequently, a precise and careful work is needed to integrate different standalone chassis vehicle systems. Recently, different approaches have been made by the researchers in order to enhance vehicle performance. After a detailed review of literature according to integrated control systems, weak points of previous research are pointed out as follows:

- Improper utilize of the necessary range of detailed of linear and

nonlinear vehicle models;

- Improper range of realistic test situations to evaluate the proposed vehicle control systems over a characteristic range of vehicle handling conditions;
- Improper definitions of the controlling aim according to different handling regime of interest;
- Deficiency of clarification of interactions among systems and approaches to vehicle control system integration.

To meet these objectives, a 2-DOF linear vehicle model and a 14-DOF nonlinear vehicle model have been utilized to design, analyze and evaluate lateral vehicle dynamics. The nonlinear vehicle model utilizes 6-DOF to describe the motion of car-body and other 8-DOF are used for wheels displacement and rotation. In order to model the nonlinear tire model, the Pacejka tire model has been utilized for both pure and combined slip conditions. VI-Grade utilizes nonlinear Pacejka tire model and 14-DOF of vehicle model which was used in this thesis to analyze and evaluate the effect of control systems on the vehicle. The different features of lateral dynamics according to the range of lateral acceleration has been determined through steady-state and transient handling aspects of the vehicle. Four distinct control goals, safety, performance and comfort of vehicle handling have been determined. The decent active subsystems are selected according to the corresponding control tasks in order to enhance vehicle safety, performance and safety through the relationship between standalone chassis control systems which cover the entire range of vehicle handling. In order to optimize the control objectives, the standalone chassis control systems have been developed in a way that the subsystems are working independently. In particular, the tasks of ARS, TV, and AAC are to control lateral force, longitudinal force, and normal forces of tires, respectively. In the design of subsystems, subsystems are robust to any variations such as vehicle forward speed and road surface coefficient of friction. To evaluate the standalone chassis control systems, various maneuvers have been done under different conditions to test the subsystems over the entire range of vehicle handling.

Results of standalone chassis control systems have been presented over a range of different handling regime. It turns out that ARS is very effective in enhancing vehicle steering response till the handling limit while it is not able to limit the sideslip motion of the vehicle at the handling limit because of the limitation of the control system. Moreover, the proposed ARS controller has been verified to be robust

to parameter variations and external disturbances. Torque Vectoring system has been developed in order to enhance performance and safety of the vehicle and has been evaluated through critical handling maneuvers. Results related to various maneuvers to assess TV have been presented. It has been notified that TV has a capability of improving safety and performance margin in the entire range of handling even at handling limit by transferring the drive torque between left and right wheel with respect to the situation of the vehicle.

Active Aerodynamic Control (AAC) has been developed for improving the performance and safety of the vehicle at high speeds. The simulation results of the AAC illustrates that Significant improvement of vehicle performance and safety margin especially at high speeds but the capability of the AAC decreases when the vehicle is traveling at low speeds.

Hydraulically Interconnected Suspension (HIS) has been developed in order to decrease the roll motion of the vehicle in roll induced maneuvers. Results of transient and steady-state maneuvers show that HIS has a significant impact on reducing roll motion of the vehicle.

Combined control of the four aforementioned standalone chassis control systems, ARS, TV, AAC and HIS has been analyzed and noticed that it is not possible to obtain overall vehicle performance improvement over the corresponding standalone chassis control systems. This study has demonstrated that the conflict in controlling objectives can occur by the combination of subsystems.

For optimizing the overall performance of the vehicle over a wide range of handling regimes, a novel control strategy for ARS, TV, and AAC has been proposed. Note that, even though the Hydraulic Interconnected Suspension (HIS) is implemented, the behavior of HIS is not integrated. The integrated schemes based on optimal control and fuzzy logic system have been developed to coordinate the control actions of the three standalone chassis control system. The proposed integrated control systems have been evaluated in the 14 DOF vehicle model by comparing them to each standalone subsystems and corresponding combined control under critical driving situations. Simulation results demonstrated that the proposed integrated control systems remarkably improve lateral vehicle dynamics in the wide range of vehicle handling regarding performance, safety, and comfort. It is interesting to point out that novel integrated scheme provides two options for a driver (safe and sport) according to the interest of a driver by utilizing the fuzzy logic method.

In particular, according to the aims and objectives of the thesis, the following has been obtained:

- Seven classifications of active subsystems have been developed for analyzing the lateral vehicle dynamics over the entire range of vehicle handling. This consists of the separation of vehicle handling into three distinct features: safety, performance, and comfort. This characterization leads to utilize in the proposal of the new integration system.
- After analyzing and investigation, four standalone chassis control system have been chosen involving ARS, TV, AAC and HIS. The reasons for choosing these active subsystems were to maintain the vehicle stability close to and at the limit of handling, enhance the performance of the vehicle on cornering maneuvers, improve the performance and safety of the vehicle at high speeds, enhance the steerability of the vehicle and reduce trade-off between road holding and comfort of passengers.
- The proposed integration system covers the wide range of vehicle handling regime by coordinating ARS, TV, and AAC. Simulation results demonstrated the significant improvement of vehicle handling regarding safety, performance, and comfort under different maneuvers and road conditions.

7.2 Recommendations for Further Work

This thesis has suggested a novel approach to integrated vehicle dynamics control for vehicle handling. The aim of the thesis has been obtained. However, some possible areas are considered to require further investigation in future research. Some of which are:

- Test the model using a real-time hardware to verify its correct response timing.
- Examine the system on a Hardware-in-the-Loop (HIL) systems to evaluate the whole system as a vehicle-driver closed loop maneuver. Therefore, the controller can be assessed in the existence of unpredictable driver reactions.
- Develop Hydraulically Interconnected Suspension to four wheels to control pitch, roll and heave motion as well. Moreover, converting passive HIS to active one by utilizing motor for the change of pressure in accumulators.
- Develop the logic of Torque Vectoring System in order to control the ratio of transferred driving torque.

- Develop the logic of Electronic Stability Control by utilizing the fuzzy logic method.

Bibliography

[1] Ira Herbert Abbott and Albert Edward Von Doenhoff. *Theory of Wing Sections: Including a Summary Of Aerofoil Data*. Dover, 1959.

[2] Masato Abe, Yoshio Kano, Kazuasa Suzuki, Yasuji Shibahata, and Yoshimi Furukawa. Side-slip control to stabilize vehicle lateral motion by direct yaw moment. *JSAE review*, 22(4):413–419, 2001.

[3] Jrgen Ackermann and Tilman Bünte. Yaw disturbance attenuation by robust decoupling of car steering. *Control Engineering Practice*, 5(8):1131–1136, 1997.

[4] Juergen Ackermann. Robust control prevents car skidding. *IEEE Control Systems*, 17(3):23–31, 1997.

[5] Jürgen Ackermann. Robust car steering by yaw rate control. In *Decision and Control, 1990., Proceedings of the 29th IEEE Conference on*, pages 2033–2034. IEEE, 1990.

[6] Jürgen Ackermann. Yaw rate and lateral acceleration feedback for four-wheel steering. *JSAE Review*, 2(16):214, 1995.

[7] Jürgen Ackermann, Tilman Bünte, Wolfgang Sienel, Holger Jeebe, and Karl Naab. Driving safety by robust steering control. In *in Proc. Int. Symposium on Advanced Vehicle Control*. Citeseer, 1996.

[8] Jürgen Ackermann and Wolfgang Sienel. Robust yaw damping of cars with front and rear wheel steering. *IEEE Transactions on Control Systems Technology*, 1(1):15–20, 1993.

[9] Masami Aga, Hideki Kusunoki, Yukiharu Satoh, Ryouzou Saitoh, and Masami Ito. Design of 2-degree-of-freedom control system for active front-and-rear-wheel steering. Technical report, SAE Technical Paper, 1990.

[10] Amos Albert. Comparison of event-triggered and time-triggered concepts with regard to distributed control systems. *Embedded world*, 2004:235–252, 2004.

[11] Andrew Alleyne. Improved vehicle performance using combined suspension and braking forces. *Vehicle System Dynamics*, 27(4):235–265, 1997.

[12] Audi. *Audi SQ7 TDI: Driving Innovation, Audi MediaCenter.*, 2017. https://www.audi-mediacenter.com/en/press-releases/audi-sq7-tdi-driving-innovation-5730.

[13] MS Bang, SH Lee, Chang-Soo Han, DB Maciuca, and JK Hedrick. Performance enhancement of a sliding mode wheel slip controller by the yaw moment control. *Proceedings of the Institution of Mechanical Engineers, Part D: Journal of Automobile Engineering*, 215(4):455–468, 2001.

[14] Ahmad Barari, Fereydoon Diba, and Ebrahim Esmailzadeh. Down force control of the low velocity racing car using active aerodynamic inverse wings. In *ASME 2011 International Design Engineering Technical Conferences and Computers and Information in Engineering Conference*, pages 739–745. American Society of Mechanical Engineers, 2011.

[15] Richard Harry Barnard. *Road vehicle aerodynamic design-an introduction*. 2009.

[16] Edward J Bedner and Hsien H Chen. A supervisory control to manage brakes and four-wheel-steer systems. Technical report, SAE Technical Paper, 2004.

[17] Bently. *Bently Bentayga Diesel: Effortless Driving With Peerless Luxury, Bentley Newsroom.*, 2017. https://www.bentleymedia.com/en/newsitem/697.

[18] SY Bhave. Effect of connecting the front and rear air suspensions of a vehicle on the transmissibility of road undulation inputs. *Vehicle System Dynamics*, 21(1):225–245, 1992.

[19] BL Boada, MJL Boada, and V Diaz. Fuzzy-logic applied to yaw moment control for vehicle stability. *Vehicle System Dynamics*, 43(10):753–770, 2005.

[20] MJL Boada, BL Boada, A Munoz, and V Diaz. Integrated control of front-wheel steering and front braking forces on the basis

of fuzzy logic. *Proceedings of the Institution of Mechanical Engineers, Part D: Journal of Automobile Engineering*, 220(3):253–267, 2006.

[21] R Bosch. Gmbh, automotive handbook, troy, mi. *Society of Automotive Engineers*, 2000.

[22] A Brunn, E Wassen, D Sperber, W Nitsche, and F Thiele. Active drag control for a generic car model. In *Active Flow Control*, pages 247–259. Springer, 2007.

[23] John P Brzustowicz, Todd H Lounsberry, and Jean-Michel Esclafer de La Rode. Experimental & computational simulations utilized during the aerodynamic development of the dodge intrepid r/t race car. Technical report, SAE Technical Paper, 2002.

[24] Kenneth R Buckholtz. Use of fuzzy logic in wheel slip assignment-part i: yaw rate control. Technical report, SAE Technical Paper, 2002.

[25] Josep Fontdecaba I Buj. Integral suspension system for motor vehicles based on passive components. Technical report, SAE Technical Paper, 2002.

[26] G Burgio and P Zegelaar. Integrated vehicle control using steering and brakes. *International Journal of Control*, 79(05):534–541, 2006.

[27] D Cao, S Rakheja, and CY Su. Pitch plane analysis of a twin-gas-chamber strut suspension. *Proceedings of the Institution of Mechanical Engineers, Part D: Journal of Automobile Engineering*, 222(8):1313–1335, 2008.

[28] Dongpu Cao, Subhash Rakheja, and Chun-Yi Su. Pitch attitude control and braking performance analysis of heavy vehicle with interconnected suspensions. Technical report, SAE Technical Paper, 2007.

[29] Dongpu Cao, Subhash Rakheja, and Chun-Yi Su. Dynamic analyses of roll plane interconnected hydro-pneumatic suspension systems. *International journal of vehicle design*, 47(1-4):51–80, 2008.

[30] I Cech. Anti-roll and active roll suspensions. *Vehicle system dynamics*, 33(2):91–106, 2000.

[31] Federico Cheli, Michele Giaramita, Marco Pedrinelli, Germano Sandoni, and Gian Claudio Travaglio. A new control strategy

for a semi-active differential (part i). *IFAC Proceedings Volumes*, 38(1):140–145, 2005.

[32] B-C Chen and C-C Kuo. Electronic stability control for electric vehicle with four in-wheel motors. *International Journal of Automotive Technology*, 15(4):573–580, 2014.

[33] Junghui Chen and Tien-Chih Huang. Applying neural networks to on-line updated pid controllers for nonlinear process control. *Journal of process control*, 14(2):211–230, 2004.

[34] Wu-wei Chen, Yan-min Wang, Qi-dong Wang, Qi-rui WANG, and Jun LIU. Study on multi-variable adaptive integrated control of automobile electric power steering and active suspension systems. *Journal of vibration engineering*, 3:019, 2005.

[35] Wuwei Chen, Hansong Xiao, Liqiang Liu, and Jean W Zu. Integrated control of automotive electrical power steering and active suspension systems based on random sub-optimal control. *International journal of vehicle design*, 42(3-4):370–391, 2006.

[36] Wuwei Chen, Hansong Xiao, Qidong Wang, Linfeng Zhao, and Maofei Zhu. *Integrated vehicle dynamics and control*. John Wiley & Sons, 2016.

[37] H Cherouat, M Lakehal-Ayat, and S Diop. An integrated braking and steering control for a cornering vehicle. In *Proc. AVEC*, volume 4, pages 341–346, 2004.

[38] T Chu and R Jones. Integrated four-wheel-steering and direct yaw moment control via robust eigenstructure assignment techniques. *Proc. AVEC06*, 2006.

[39] Chatchai Chumjun, Chak Chantalakhana, and Saiprasit Koetniyom. A compromise of comfort and handling in automotive vertical dynamics. In *The 20th Conference of Mechanical Engineering Network of Thailand Nakhon Ratchasima, Thailand*, 2006.

[40] Se-Kyo Chung and Hwi-Beom Shin. High-voltage power supply for semi-active suspension system with er-fluid damper. *IEEE transactions on vehicular technology*, 53(1):206–214, 2004.

[41] Nicholas Cooper, David Crolla, Martin Levesley, and Warren Manning. Integration of active suspension and active driveline to ensure stability while improving vehicle dynamics. Technical report, SAE Technical Paper, 2005.

[42] Matteo Corno, Stefano Bottelli, Mara Tanelli, Cristiano Spelta, and Sergio M Savaresi. Active control of aerodynamic surfaces for ride control in sport vehicles. *IFAC Proceedings Volumes*, 47(3):7553–7558, 2014.

[43] Toyota Motor Corporation. *Deep Dive: Bentley Dynamic Ride Explained", Blog.caranddriver.com.*, 2017.

[44] DA Crolla, G Firth, and D Horton. *An introduction to vehicle dynamics*. University of Leeds, Department of Mechanical Engineerin, 1992.

[45] Paul Hendrik Cronje and Pieter Schalk Els. Improving off-road vehicle handling using an active anti-roll bar. *Journal of Terramechanics*, 47(3):179–189, 2010.

[46] S Diasinos and A Gatto. Experimental investigation into wing span and angle-of-attack effects on sub-scale race car wing/wheel interaction aerodynamics. *Experiments in Fluids*, 45(3):537, 2008.

[47] Fereydoon Diba, Ahmad Barari, and Ebrahim Esmailzadeh. Active aerodynamic system to improve the safety and handling of race cars in lane change and wet road maneuvers. In *ASME 2012 International Design Engineering Technical Conferences and Computers and Information in Engineering Conference*, pages 417–423. American Society of Mechanical Engineers, 2012.

[48] Ioannis Dimitriou and Kevin P Garry. Use of a narrow belt for moving ground simulation and its effects on the aerodynamic forces generated on a formula-1 car. Technical report, SAE Technical Paper, 2002.

[49] John C Dixon. Tires, suspension and handling. *Warrendale, PA: Society of Automotive Engineers, 1996. 636*, 1996.

[50] Carlo Doniselli, Giampiero Mastinu, and Massimiliano Gobbi. Aerodynamic effects on ride comfort and road holding of automobiles. *Vehicle System Dynamics*, 25(S1):99–125, 1996.

[51] Christof Ebert and Capers Jones. Embedded software: Facts, figures, and future. *Computer*, 42(4), 2009.

[52] Keyanoush Efatpenah, Joseph H Beno, and Steven P Nichols. Energy requirements of a passive and an electromechanical ac-

tive suspension system. *Vehicle System Dynamics*, 34(6):437–458, 2000.

[53] M Ersoy and A Hartmann. Aktives fahrwerk zum integrierten aufbaustabilisierung und variabler raddämpfung—asca. 15. In *Aachener Kolloquium. Aachen*, 2006.

[54] Rana Raouf Hasan Farag. *Active neuro-fuzzy integrated vehicle dynamics controller to improve the vehicle handling adn stability at complicated maneuvers*. PhD thesis, Universidad Carlos III de Madrid, 2013.

[55] Hermann Fasel, Albert Hack, Ralf Rossmanith, Jörg Russow, Volker Schwarz, and Rainer Tiefenbacher. Motor vehicle with flow-influencing devices to reduce air resistance, April 30 2002. US Patent 6,378,932.

[56] J Feng, F Yu, and J Li. An investigation on integrated control of vehicle anti-lock braking system and active suspension. *Transactions of the Chinese Society of Agricultural Machinery*, 33(2):15–19, 2002.

[57] Ian J Fialho and Gary J Balas. Design of nonlinear controllers for active vehicle suspensions using parameter-varying control synthesis. *Vehicle System Dynamics*, 33(5):351–370, 2000.

[58] Michael Fodor, John Yester, and Davor Hrovat. Active control of vehicle dynamics. In *Digital Avionics Systems Conference, 1998. Proceedings., 17th DASC. The AIAA/IEEE/SAE*, volume 2, pages I14–1. IEEE, 1998.

[59] International Organization for Standardization. *Mechanical vibration and shock-Evaluation of human exposure to whole-body vibration-Part 1: General requirements*. The Organization, 1997.

[60] Katsuhiko Fukui, Kazuo Miki, Yasutaka Hayashi, and Junzo Hasegawa. Analysis of driver and a "four wheel steering vehicle" system using a driving simulator issn0148-7191. Technical report, SAE Technical Paper, 1988.

[61] GS Gao and SP Yang. Semi-active control performance of railway vehicle suspension featuring magnetorheological dampers. In *Industrial Electronics and Applications, 2006 1ST IEEE Conference on*, pages 1–5. IEEE, 2006.

[62] Thomas Kenneth Garrett, Kenneth Newton, and William Steeds. *Motor vehicle*. Butterworth-Heinemann, 2000.

[63] Giancarlo Genta. *Motor vehicle dynamics: modeling and simulation*, volume 43. World Scientific, 1997.

[64] L Gianone, László Palkovics, and József Bokor. Design of an active 4ws system with physical uncertainties. *Control Engineering Practice*, 3(8):1075–1083, 1995.

[65] T.D. Gillespie. *Fundamentals of Vehicle Dynamics*. Premiere Series Bks. Society of Automotive Engineers, 1992.

[66] Thomas D Gillespie. Vehicle dynamics. *Warren dale*, 1997.

[67] Avesta Goodarzi and Mohsen Alirezaie. A new fuzzy-optimal integrated afs/dyc control strategy. In *Proc. AVEC*, pages 20–24, 2006.

[68] Tim Gordon, Mark Howell, and Felipe Brandao. Integrated control methodologies for road vehicles. *Vehicle System Dynamics*, 40(1-3):157–190, 2003.

[69] S Gosselin-Brisson, M Bouazara, and MJ Richard. Design of an active anti-roll bar for off-road vehicles. *Shock and Vibration*, 16(2):155–174, 2009.

[70] Kynan E Graves, Pio G Iovenitti, and Dario Toncich. Electromagnetic regenerative damping in vehicle suspension systems. *International Journal of Vehicle Design*, 24(2-3):182–197, 2000.

[71] BMW Group. *The new BMW 7 Series.*, 2017. https://www.press.bmwgroup.com/global/article/detail/T0221224EN/the-new-bmw-7-series.

[72] Emanuele Guglielmino, Tudor Sireteanu, Charles W Stammers, Gheorghe Ghita, and Marius Giuclea. *Semi-active suspension control: improved vehicle ride and road friendliness*. Springer Science & Business Media, 2008.

[73] Bilin Aksun Guvenc, Tilman Bunte, Dirk Odenthal, and Levent Guvenc. Robust two degree-of-freedom vehicle steering controller design. *IEEE Transactions on Control Systems Technology*, 12(4):627–636, 2004.

[74] Aleksander Hac and Mark O Bodie. Improvements in vehicle handling through integrated control of chassis systems. *International journal of vehicle autonomous systems*, 1(1):83–110, 2002.

[75] Yoshikazu Hattori, Ken Koibuchi, and Tatsuaki Yokoyama. Force and moment control with nonlinear optimum distribution for vehicle dynamics. In *Proc. of the 6th International symposium on advanced vehicle control*, pages 595–600, 2002.

[76] Junjie He. *Integrated vehicle dynamics control using active steering, driveline and braking*. PhD thesis, University of Leeds, 2005.

[77] Bernd Heißing, Metin Ersoy, and Stefan Gies. Fahrwerkhandbuch. *Vieweg+ Teubner Verlag, Wiesbaden*, 2007.

[78] Christian Hilgers, Jens Brandes, Heike Ilias, Holger Oldenettel, Alexander Stiller, and Christian Treder. Aktives luftfederfahrwerk für eine größere bandbreite zwischen komfort-und dynamikabstimmung. *ATZ-Automobiltechnische Zeitschrift*, 111(9):600–609, 2009.

[79] Yutaka Hirano and Katsumi Fukatani. Development of robust active rear steering control for automobile. *JSME International Journal Series C Mechanical Systems, Machine Elements and Manufacturing*, 40(2):231–238, 1997.

[80] Shinichiro Horiuchi, Naohiro Yuhara, and Akihiko Takei. Two degree of freedom/ h_∞ controller synthesis for active four wheel steering vehicles. *Vehicle System Dynamics*, 25(S1):275–292, 1996.

[81] Davor Hrovat. Survey of advanced suspension developments and related optimal control applications. *Automatica*, 33(10):1781–1817, 1997.

[82] Guoliang Hu, Fengshuo Liu, Zheng Xie, and Ming Xu. Design, analysis, and experimental evaluation of a double coil magnetorheological fluid damper. *Shock and Vibration*, 2016, 2016.

[83] Kunsoo Huh, Chanwon Seo, Joonyoung Kim, and Daegun Hong. Active steering control based on the estimated tire forces. In *American Control Conference, 1999. Proceedings of the 1999*, volume 1, pages 729–733. IEEE, 1999.

[84] Shoji Inagaki, Ikuo Kushiro, and Masaki Yamamoto. Analysis on vehicle stability in critical cornering using phase-plane method. *Jsae Review*, 2(16):216, 1995.

[85] Bengt Jacobson. Vehicle dynamics compendium for course mmf062. Technical report, Chalmers University of Technology, 2015.

[86] Kiumars Jalali, Thomas Uchida, Steve Lambert, and John McPhee. Development of an advanced torque vectoring control system for an electric vehicle with in-wheel motors using soft computing techniques. 2013.

[87] Fangjun Jiang and Zhiqiang Gao. An application of nonlinear pid control to a class of truck abs problems. In *Decision and Control, 2001. Proceedings of the 40th IEEE Conference on*, volume 1, pages 516–521. IEEE, 2001.

[88] WD Jones. Easy ride: Bose corp. uses speaker technology to give cars adaptive suspension. *IEEE Spectrum*, 42(5):12–14, 2005.

[89] Dean Karnopp. Theoretical limitations in active vehicle suspensions. *Vehicle System Dynamics*, 15(1):41–54, 1986.

[90] Dean Karnopp, Michael J Crosby, and RA Harwood. Vibration control using semi-active force generators. *Journal of engineering for industry*, 96(2):619–626, 1974.

[91] Cor-Jacques Kat and Pieter Schalk Els. Interconnected air spring model. *Mathematical and Computer Modelling of Dynamical Systems*, 15(4):353–370, 2009.

[92] Joseph Katz. Aerodynamics of race cars. *Annu. Rev. Fluid Mech.*, 38:27–63, 2006.

[93] Joseph Katz. *Race car aerodynamics: designing for speed*. R. Bentley, 2006.

[94] Mehrdad N Khajavi, Vahid Hemmati, and Sh_Aliyari Shouredeli. A novel approach to enhance roll stability of suvs by a fuzzy logic controller. *Proc World Acad Sci Engng Technol*, 37:1070–1075, 2009.

[95] Uwe Kiencke and Lars Nielsen. Automotive control systems: for engine, driveline, and vehicle, 2000.

[96] Chul Kim and Paul I Ro. An accurate full car ride model using model reducing techniques. *TRANSACTIONS-AMERICAN SOCIETY OF MECHANICAL ENGINEERS JOURNAL OF MECHANICAL DESIGN*, 124(4):697–705, 2002.

[97] HJ Kim and CR Lee. Hybrid roll control using electric arc system considering limited bandwidth of actuating module. *Int. J. Automotive Technology*, 3(3):123–128, 2002.

[98] S Kim, K Park, HJ Song, YK Hwang, SJ Moon, HS Ahn, and M Tomizuka. Development of control logic for hydraulic active roll control system. *International Journal of Automotive Technology*, 13(1):87–95, 2012.

[99] Ryohei Kizu, H Harada, and H Minabe. Electronic control of car chassis: Present status and future perspective. In *INTERNATIONAL CONGRESS ON TRANSPORTATION*, 1988.

[100] Guido Koch, Oliver Fritsch, and Boris Lohmann. Potential of low bandwidth active suspension control with continuously variable damper. *Control Engineering Practice*, 18(11):1251–1262, 2010.

[101] Youseok Kou, Wanil Kim, SangHo Yoon, JeongWoo Lee, and Dongshin Kim. Integration chassis control (icc) systems of mando. Technical report, SAE Technical Paper, 2004.

[102] Allan Y Lee. Coordinated control of steering and anti-roll bars to alter vehicle rollover tendencies. *TRANSACTIONS-AMERICAN SOCIETY OF MECHANICAL ENGINEERS JOURNAL OF DYNAMIC SYSTEMS MEASUREMENT AND CONTROL*, 124(1):127–132, 2002.

[103] William S Levine. *The control handbook*. CRC press, 1996.

[104] D Li, X Shen, and F Yu. Integrated vehicle chassis control with a main/servo-loop structure. *International journal of automotive technology*, 7(7):803–812, 2006.

[105] Daofei Li and Fan Yu. A novel integrated vehicle chassis controller coordinating direct yaw moment control and active steering. Technical report, SAE Technical Paper, 2007.

[106] Y Lin. Improving vehicle handling performance by a closed-loop 4ws driving controller. Technical report, SAE Technical Paper, 1992.

[107] PJ Liu, S Rakheja, and AKW Ahmed. Properties of an interconnected hydro-pneumatic suspension system. *Transactions of the Canadian Society for Mechanical Engineering*, 19(4):383–396, 1995.

[108] Nicholas Mace. *Analysis and synthesis of passive interconnected vehicle suspensions.* PhD thesis, University of Cambridge, 2004.

[109] Said Mammar and VB Baghdassarian. Two-degree-of-freedom formulation of vehicle handling improvement by active steering.

In *American Control Conference, 2000. Proceedings of the 2000*, volume 1, pages 105–109. IEEE, 2000.

[110] Said Mammar and Damien Koenig. Vehicle handling improvement by active steering. *Vehicle system dynamics*, 38(3):211–242, 2002.

[111] C March and T Shim. Integrated control of suspension and front steering to enhance vehicle handling. *Proceedings of the Institution of Mechanical Engineers, Part D: Journal of Automobile Engineering*, 221(4):377–391, 2007.

[112] Ismenio Martins, Jorge Esteves, Gil D Marques, and F Pina Da Silva. Permanent-magnets linear actuators applicability in automobile active suspensions. *IEEE Transactions on vehicular technology*, 55(1):86–94, 2006.

[113] Isménio Martins, M Esteves, F Pina Da Silva, and Pedro Verdelho. Electromagnetic hybrid active-passive vehicle suspension system. In *Vehicular Technology Conference, 1999 IEEE 49th*, volume 3, pages 2273–2277. IEEE, 1999.

[114] Naoki Matsumoto and Masayoshi Tomizuka. Vehicle lateral velocity and yaw rate control with two independent control inputs. In *American Control Conference, 1990*, pages 1868–1875. IEEE, 1990.

[115] JP Meijaard, AR Savkoor, and G Lodewijks. Potential for vehicle ride improvement using both suspension and aerodynamic actuators. In *Industrial Electronics, 2005. ISIE 2005. Proceedings of the IEEE International Symposium on*, volume 1, pages 385–390. IEEE, 2005.

[116] William F Milliken, Douglas L Milliken, et al. *Race car vehicle dynamics*, volume 400. Society of Automotive Engineers Warrendale, 1995.

[117] Rakuzou Mitamura, Masanori Tani, Tadao Tanaka, and Miroo Yuasa. System integration for new mobility. Technical report, SAE Technical Paper, 1988.

[118] Manfred Mitschke and Henning Wallentowitz. *Dynamik der kraftfahrzeuge*, volume 4. Springer, 1972.

[119] JA Mohrfeld-Halterman and M Uddin. High fidelity quasi steady-state aerodynamic model effects on race vehicle performance pre-

dictions using multi-body simulation. *Vehicle System Dynamics*, 54(7):963–981, 2016.

[120] JA Mohrfeld-Halterman and M Uddin. Quasi steady-state aerodynamic model development for race vehicle simulations. *Vehicle System Dynamics*, 54(1):124–136, 2016.

[121] Ossama Mokhiamar and Masato Abe. Simultaneous optimal distribution of lateral and longitudinal tire forces for the model following control. *Journal of dynamic systems, measurement, and control*, 126(4):753–763, 2004.

[122] Sumio Motoyama, H Uki, K ISODA Manager, and H YUASA Manager. Effect of traction force distribution control on vehicle dynamics. *Vehicle System Dynamics*, 22(5-6):455–464, 1993.

[123] Aua Müller, W Achenbach, E Schindler, Th Wohland, and G-W MOHN. Das neue fahrsicherheitssystem electronic stability program von mercedes-benz. *ATZ. Automobiltechnische Zeitschrift*, 96(11):656–670, 1994.

[124] Martin Münster, Ulrich Mair, Heinz-Joachim Gilsdorf, Achim Thomä, Christian Müller, Marko Hippe, and Jürgen Hoffmann. Elektromechanische aktive aufbaukontrolle. *ATZ-Automobiltechnische Zeitschrift*, 111(9):644–649, 2009.

[125] Masao Nagai. Active four-wheel-steering system by model following control. In *11th IAVSD Symposium, Kingston*, pages 428–439, 1989.

[126] Masao Nagai. Integrated control law of active rear wheel steering and direct yaw moment control. *Proc. of AVEC'96, Aachen University of Technology*, 1996.

[127] Masao Nagai, Motoki Shino, and Feng Gao. Study on integrated control of active front steer angle and direct yaw moment. *JSAE review*, 23(3):309–315, 2002.

[128] Andrzej G Nalecz and Alan C Bindemann. Handling properties of four wheel steering vehicles. Technical report, SAE Technical Paper, 1989.

[129] Y Nau. Yaw-control enhancement for buses by active front-wheel steering, doctoral theses. *Pennsylvania: The Pennsylvania State University*, 2007.

[130] C Nouillant, F Assadian, X Moreau, and A Oustaloup. A cooperative control for car suspension and brake systems. *International journal of automotive technology*, 3(4):147–155, 2002.

[131] Katsuhiko Ogata and Yanjuan Yang. Modern control engineering. 1970.

[132] E Ono, S Hosoe, S Doi, K Asano, and Y Hayashi. Theoretical approach for improving the vehicle robust stability and maneuverability by active front wheel steering control. *Vehicle system dynamics*, 29(S1):748–753, 1998.

[133] Eiichi Ono, Shigeyuki Hosoe, Hoang D Tuan, and Shun'ichi Doi. Robust stabilization of vehicle dynamics by active front wheel steering control. In *Decision and Control, 1996., Proceedings of the 35th IEEE Conference on*, volume 2, pages 1777–1782. IEEE, 1996.

[134] Eiichi Ono, Kaoru Takanami, Norio Iwama, Yasutaka Hayashi, Yutaka Hirano, and Yukiharu Satoh. Vehicle integrated control for steering and traction systems by μ-synthesis. *Automatica*, 30(11):1639–1647, 1994.

[135] M Ortiz. Principles of interconnected suspensions. *RaceCar Engineering*, 7(7-8), 1997.

[136] Hans Pacejka. *Tire and vehicle dynamics*. Elsevier, 2005.

[137] DA Panke, NH Ambhore, and RN Marathe. Review on handling characteristics of road vehicles. *Journal of Engineering Research and Applications (Int J Eng Res Appl)*, 4(7):178–182, 2014.

[138] IH Park and KH Park. A study on integrated control of afs and esp for the improvement of vehicle handling performance. In *Spring Conf. Korean Society of precision Engineering*, volume 5, pages 511–514, 2005.

[139] Kihong Park, Seung-Jin Heo, and Inho Baek. Controller design for improving lateral vehicle dynamic stability. *JSAE review*, 22(4):481–486, 2001.

[140] Johannes JH Paulides, Laurentiu Encica, Elena A Lomonova, and Andre JA Vandenput. Design considerations for a semi-active electromagnetic suspension system. *IEEE Transactions on magnetics*, 42(10):3446–3448, 2006.

[141] JM Pevsner. Equalizing types of suspension. *Automobile Engineer*, 1:10–16, 1957.

[142] Porsche. *Dynamic Chassis Control Sport (PDCC Sport) including Porsche Torque Vectoring Plus (PTV Plus).*, 2017. http://www.porsche.com/international/models/panamera/panamera/drive-chassis/porsche-dynamic-chassis-control-sport-pdcc-sport/.

[143] Charles Poussot-Vassal, Olivier Sename, Luc Dugard, and SM Savaresi. Vehicle dynamic stability improvements through gain-scheduled steering and braking control. *Vehicle System Dynamics*, 49(10):1597–1621, 2011.

[144] M Pyper, W Schiffer, and W Schneider. Abc-active body control. *Verlag Moderne Industrie, Augsburg*, 2003.

[145] Rajesh Rajamani. *Vehicle dynamics and control*. Springer Science & Business Media, 2011.

[146] Chandrasekaran Rengaraj, Adam Adgar, Chris Cox, and Dave Crolla. Integration of yaw control, active suspension and anti-lock brake system to improve ride and handling. 2006.

[147] Ferruccio Resta, Gerald Teuschl, Mauro Zanchetta, and Andrea Zorzutti. A new control strategy for a semi-active differential (part ii). *IFAC Proceedings Volumes*, 38(1):146–151, 2005.

[148] Peter E Rieth and Ralf Schwarz. Esc ii-esc with active steering intervention. Technical report, SAE Technical Paper, 2004.

[149] Günter Roppenecker and Henning Wallentowitz. Integration of chassis and traction control systems what is possible–what makes sense–what is under development. *Vehicle System Dynamics*, 22(5-6):283–298, 1993.

[150] Edoardo Sabbioni, Federico Cheli, Michele Vignati, and Stefano Melzi. Comparison of torque vectoring control strategies for a iwm vehicle. *SAE International Journal of Passenger Cars-Electronic and Electrical Systems*, 7(2014-01-0860):565–572, 2014.

[151] Mutasim Salman, Zhihong Zhang, and Nader Boustany. Coordinated control of four wheel braking and rear steering. In *American Control Conference, 1992*, pages 6–10. IEEE, 1992.

[152] Shoichi Sano, Yoshimi Furukawa, Takashi Nihei, Masaru Abe, and Mitsuya Serizawa. Handling characteristics of steer angle

dependent four wheel steering system. Technical report, SAE Technical Paper, 1988.

[153] Shoichi Sano, Yoshimi Furukawa, and Shuji Shiraishi. Four wheel steering system with rear wheel steer angle controlled as a function of steering wheel angle. Technical report, SAE Technical Paper, 1986.

[154] H Sato, A Hirota, H Yanagisawa, and T Fukushima. Dynamic characteristics of a whole wheel steering vehicle with yaw velocity feedback rear wheel steering. In *Road Vehicle Handling, I Mech E Conference Publications 1983-5. Sponsored by Automobile Division of the Institution of Mechanical Engineers under patronage of Federation Internationale des Societies d'Ingenieurs des Techniques de l'Automobile (FISITA) he*, number C124/83, 1983.

[155] Hiroki Sato, Hiroyuki Kawai, Masaru Isikawa, Hitosi Iwata, and Shin Koike. Development of four wheel steering system using yaw rate feedback control. Technical report, SAE Technical Paper, 1991.

[156] Shinsuke Sato, Hideo Inoue, Masaaki Tabata, and Shoji Inagaki. Integrated chassis control system for improved vehicle dynamics. In *SAE Conference Proceedings p*, pages 413–413. SOC AUTOMATIVE ENGINEERS INC, 1993.

[157] Sergio M Savaresi, Charles Poussot-Vassal, Cristiano Spelta, Olivier Sename, and Luc Dugard. *Semi-active suspension control design for vehicles*. Elsevier, 2010.

[158] A Savkoor and H Happel. Aerodynamic vehicle ride control with active spoilers. In *Proceedings of International Symposium on Advanced Vehicle Control*, pages 647–682, 1996.

[159] Arvin Savkoor, Sanne Manders, and Paolo Riva. Design of actively controlled aerodynamic devices for reducing pitch and heave of truck cabins. *JSAE review*, 22(4):421–434, 2001.

[160] Arvin R Savkoor and CT Chou. Application of aerodynamic actuators to improve vehicle handling. *Vehicle System Dynamics*, 32(4-5):345–374, 1999.

[161] K Sawase and K Inoue. Classification and characteristic analysis of right-and-left torque vectoring mechanisms based on velocity diagram. *VDI BERICHTE*, 2014:121, 2007.

[162] Kaoru Sawase, Yuichi Ushiroda, and Takami Miura. Left-right torque vectoring technology as the core of super all wheel control (s-awc). *Mitsubishi Motors Technical Review*, 18:16–23, 2006.

[163] Franz K Schenkel. The origins of drag and lift reductions on automobiles with front and rear spoilers. Technical report, SAE Technical Paper, 1977.

[164] Adam Julius Scibor-Rylski. *Road vehicle aerodynamics*. Number Monograph. 1984.

[165] Mark Albert Selby. *Intelligent vehicle motion control*. PhD thesis, University of Leeds, 2003.

[166] K-H Senger and W Schwartz. The influence of a four wheel steering system on the stability behaviour of a vehicle-driver system. *Vehicle System Dynamics*, 17(sup1):388–402, 1988.

[167] K Senthilkumar and Ramesh Ramadoss. Designing multicore ecu architecture in vehicle networks using autosar. In *Advanced Computing (ICoAC), 2011 Third International Conference on*, pages 270–275. IEEE, 2011.

[168] RS Sharp and SA Hassan. On the performance capabilities of active automobile suspension systems of limited bandwidth. *Vehicle System Dynamics*, 16(4):213–225, 1987.

[169] Xiao-Ming Shen and Fan Yu. Study on vehicle chassis control integration based on vehicle dynamics and separate loop design approach. *International Journal of Vehicle Autonomous Systems*, 5(1-2):95–118, 2007.

[170] Xiaoming Shen, Huei Peng, and M Abe. Analysis of active suspension systems with hydraulic actuators. In *The Dynamics of Vehicles on Roads and on Tracks Supplement to Vehicle System Dynamics: Proceedings Of The 18th Iavsd Symposium Held In Kanagawa, Japan August*, pages 24–30, 2003.

[171] Xiaoming Shen and Fan Yu. Study on vehicle chassis control integration based on a main-loop-inner-loop design approach. *Proceedings of the Institution of Mechanical Engineers, Part D: Journal of Automobile Engineering*, 220(11):1491–1502, 2006.

[172] Yasuji Shibahata, Namio Irie, Hideo Itoh, and Kenji Nakamura. The development of an experimental four-wheel-steering vehicle. Technical report, SAE Technical Paper, 1986.

[173] Yasuji Shibahata, K Shimada, and T Tomari. Improvement of vehicle maneuverability by direct yaw moment control. *Vehicle System Dynamics*, 22(5-6):465–481, 1993.

[174] Kazuhiko Shimada and Yasuji Shibahata. Comparison of three active chassis control methods for stabilizing yaw moments. Technical report, SAE Technical Paper, 1994.

[175] Motoki Shino and Masao Nagai. Independent wheel torque control of small-scale electric vehicle for handling and stability improvement. *JsAE Review*, 24(4):449–456, 2003.

[176] BUMA Shuuichi, Yasuhiro Ookuma, Akiya Taneda, Katsumi Suzuki, CHO Jae-Sung, and Masaru Kobayashi. Design and development of electric active stabilizer suspension system. *Journal of System Design and Dynamics*, 4(1):61–76, 2010.

[177] Wolfgang Sienel. Estimation of the tire cornering stiffness and its application to active car steering. In *Decision and Control, 1997., Proceedings of the 36th IEEE Conference on*, volume 5, pages 4744–4749. IEEE, 1997.

[178] Henk Smakman et al. Functional integration of active suspension with slip control for improved lateral vehicle dynamics. In *Proc. AVEC*, volume 397404, 2000.

[179] MC Smith and GW Walker. Interconnected vehicle suspension. *Proceedings of the Institution of Mechanical Engineers, Part D: Journal of Automobile Engineering*, 219(3):295–307, 2005.

[180] Wade A Smith, Nong Zhang, and William Hu. Hydraulically interconnected vehicle suspension: handling performance. *Vehicle System Dynamics*, 49(1-2):87–106, 2011.

[181] Michael Strassberger and Jurgen Guldner. Bmw's dynamic drive: an active stabilizer bar system. *IEEE control systems*, 24(4):28–29, 2004.

[182] Ralph Streiter. Abc pre-scan im f700. *ATZ-Automobiltechnische Zeitschrift*, 110(5):388–397, 2008.

[183] Ralph H Streiter. *Entwicklung und Realisierung eines analytischen Regelkonzeptes für eine aktive Federung.* na, 1996.

[184] Shuaishuai Sun, Huaxia Deng, Haiping Du, Weihua Li, Jian Yang, Guiping Liu, Gursel Alici, and Tianhong Yan. A compact

variable stiffness and damping shock absorber for vehicle suspension. *IEEE/ASME Transactions on Mechatronics*, 20(5):2621–2629, 2015.

[185] A Szosland. Fuzzy logic approach to four-wheel steering of motor vehicle. *International Journal of Vehicle Design*, 24(4):350–359, 2000.

[186] Y Tagawa, H Ogata, K Morita, M Nagai, and H Mori. Robust active steering system taking account of nonlinear dynamics. *Vehicle system dynamics*, 25(S1):668–681, 1996.

[187] Saied Taheri and E Harry Law. Investigation of a combined slip control braking and closed loop four wheel steering system for an automobile during combined hard braking and severe steering. In *American Control Conference, 1990*, pages 1862–1867. IEEE, 1990.

[188] Tadahiko Takiguchi, Noritaka Yasuda, Shigeki Furutani, Hirotaka Kanazawa, and Hitoshi Inoue. Improvement of vehicle dynamics by vehicle-speed-sensing four-wheel steering system. Technical report, SAE Technical Paper, 1986.

[189] H Tanaka, H Inoue, and H Iwata. Development of a vehicle integrated control system. In *XXIV FISITA CONGRESS. 7-11 JUNE 1992, LONDON. HELD AT THE AUTOMOTIVE TECHNOLOGY SERVING SOCIETY. TECHNICAL PAPERS. TOTAL VEHICLE DYNAMICS. VOLUME 1.(IMECHE NO. C389/220 AND FISITA NO. 925049)*, 1992.

[190] Kaidong Tian, Bangji Zhang, Nong Zhang, Xuhui Liu, and Jinchen Ji. A piecewise hysteresis model for a damper of his system. *Shock and Vibration*, 2016, 2016.

[191] E Tingwall. *Deep Dive: Bentley Dynamic Ride Explained", Blog.caranddriver.com.*, 2017. http://blog.caranddriver.com/deep-dive-bentley-dynamic-ride-explained/.

[192] Tomokazu Tokuda. Cars in the'90s as a humanware. Technical report, SAE Technical Paper, 1988.

[193] P Tondel and TA Johansen. Control allocation for yaw stabilization in automotive vehicles using multiparametric nonlinear programming. In *American Control Conference, 2005. Proceedings of the 2005*, pages 453–458. IEEE, 2005.

[194] H Eric Tseng and Davor Hrovat. State of the art survey: active and semi-active suspension control. *Vehicle system dynamics*, 53(7):1034–1062, 2015.

[195] Hongtei Eric Tseng, Behrouz Ashrafi, Dinu Madau, T Allen Brown, and Darrel Recker. The development of vehicle stability control at ford. *IEEE/ASME transactions on mechatronics*, 4(3):223–234, 1999.

[196] Michael Valasek, Ondrej Vaculin, and Jaromir Kejval. Global chassis control: integration synergy of brake and suspension control for active safety. In *Proceedings AVEC 04, 7th International Symposium on Advanced Vehicle Control*, pages 495–500. KIVI-NIRIA, 2004.

[197] Anton T Van Zanten. Evolution of electronic control systems for improving the vehicle dynamic behavior. In *Proceedings of the 6th International Symposium on Advanced Vehicle Control*, volume 2, page 9, 2002.

[198] MICHELE VIGNATI. Torque vectoring control per veicoli elettrici con quattro motoruote. 2013.

[199] John Voelcker. The soul of a new mercedes. *IEEE Spectrum*, 45(12), 2008.

[200] K Wakamatsu, Y Akuta, M Ikegaya, and N Asanuma. Adaptive yaw rate feedback 4ws with friction coefficient estimator between tire and road surface. In *Proceedings of AVEC*, volume 96, 1996.

[201] Long Wang and J Ackermann. Robustly stabilizing pid controllers for car steering systems. In *American Control Conference, 1998. Proceedings of the 1998*, volume 1, pages 41–42. IEEE, 1998.

[202] Y Wang and M Nagai. Intelligent vehicle motion control by adaptive front steering system. In *International Symposium on Advanced Vehicle Control, 1992, Yokohama, Japan*, 1992.

[203] Mohamed Watany. Performance of a road vehicle with hydraulic brake systems using slip control strategy. *American Journal of Vehicle Design*, 2(1):7–18, 2014.

[204] Jonathan C Wheals, Hanna Baker, Keith Ramsey, and Will Turner. Torque vectoring awd driveline: design, simulation, capabilities and control. Technical report, SAE Technical Paper, 2004.

[205] John C Whitehead. Four wheel steering-maneuverability and high speed stabilization. 1988.

[206] RA Williams. Automotive active suspensions part 2: practical considerations. *Proceedings of the Institution of Mechanical Engineers, Part D: Journal of Automobile Engineering*, 211(6):427–444, 1997.

[207] RA Williams and A Best. Control of a low frequency active suspension. In *Control, 1994. Control'94. International Conference on*, volume 1, pages 338–343. IET, 1994.

[208] Jo Yung Wong. *Theory of ground vehicles*. John Wiley & Sons, 2008.

[209] X Xia and EH Law. Nonlinear analysis of closed loop driver/automobile performance with four wheel steering control. Technical report, SAE Technical Paper, 1992.

[210] Masaki Yamamoto. A study on active controlled chassis system for vehicle dynamics. In *Proceedings of 11th IAVSD Symposium, 1989*, 1989.

[211] Yoshiyuki Yasui, Hiroyuki Kodama, Minekazu Momiyama, Hiroaki Kato, Wataru Tanaka, Eiichi Ono, and Yuji Muragishi. Electronic stability control (esc) coordinated with electric power steering (eps). In *FISITA Congress*, volume 2006, 2006.

[212] F Yu, J-Z Feng, and J Li. A fuzzy logic controller design for vehicle abs with a on-line optimized target wheel slip ratio. *International Journal of Automotive Technology*, 3(4):165–170, 2002.

[213] Fan Yu, Dao-Fei Li, and DA Crolla. Integrated vehicle dynamics control—state-of-the art review. In *Vehicle Power and Propulsion Conference, 2008. VPPC'08. IEEE*, pages 1–6. IEEE, 2008.

[214] Jianlong Zhang, Deling Chen, and Chengliang Yin. Adaptive fuzzy controller for hybrid traction control system based on automatic road identification. In *Automation Science and Engineering, 2006. CASE'06. IEEE International Conference on*, pages 524–529. IEEE, 2006.

[215] Nong Zhang, Wade A Smith, and Jeku Jeyakumaran. Hydraulically interconnected vehicle suspension: background and modelling. *Vehicle System Dynamics*, 48(1):17–40, 2010.

[216] Xin Zhang and Jonathan Zerihan. Aerodynamics of a double-element wing in ground effect. *AIAA journal*, 41(6):1007–1016, 2003.

[217] Chen Zhenfu. Status and tendency of the vehicle chasses control technology. *Automotive Engineering*, 28(2):105–113, 2006.